THE PROCEEDINGS OF
THE PHYSICAL SOCIETY

Section A

VOL. 65, PART 4 1 April 1952 No. 388 A

The Relative Ionization Produced by Low Energy Protons, Deuterons and Alpha-Particles in Various Gases

BY P. R. TUNNICLIFFE* AND A. G. WARD*
Atomic Energy Research Establishment, Harwell, Didcot, Berks.

MS. received 8th May 1951, and in amended form 22nd October 1951

ABSTRACT. Mono-energetic neutrons have been used to produce recoil protons, deuterons and α-particles in a proportional counter. The maximum pulse sizes produced by the different recoil particles are compared with the accurately known ratios of maximum recoil energies. From the results for protons and deuterons it can be inferred that, for protons between 200 and 550 kev energy, the ionization is proportional to the energy with a deviation of less than 1%. The total ionization in argon produced by a proton is about 8% greater than that of an α-particle of equal energy, for energies between 200 and 400 kev.

§ 1. INTRODUCTION

THE experiments reported in this paper were carried out as part of a programme to establish a method of fast neutron flux measurement using proportional counter techniques. In measurements of this kind, using recoil protons produced in the gas volume of a proportional counter or ionization chamber (Rossi and Staub 1949) it has been customary to assume that the value of *W*, the mean energy expended in producing an ion pair, is nearly independent of the proton energy. A review article by Gray (1944) summarizes most of the experimental data on which this assumption is based. In view of the meagre experimental data available for low energy protons (100–500 kev) it cannot be considered proven that *W* is energy independent, and these experiments were designed to investigate the variation of *W* with proton energy in this region.

Recent experiments of Jesse, Forstat and Sadauskis (1950) and of Franzen, Halpern and Stephens (1950) appear to indicate the essential constancy of *W* in pure argon over an extended range of α-particle energies, and suggest that *W* is the same for protons and ^{7}Li ions as well to a relatively high order of accuracy. A discussion of these measurements and their effect on the range–energy relationship for protons is given by Bethe (1950). The above evidence for the constancy of *W* for protons and α-particles is in disagreement with experimental results of Hanna (1950) as well as with earlier measurements of Cranshaw and Harvey (1948). Data have been taken for very low energy α-particles, produced by neutron recoil, in an attempt to provide further useful information.

---

* Now at the Atomic Energy Project, National Research Council, Chalk River, Ontario, Canada.

§ 2. EXPERIMENTAL METHOD

Mono-energetic neutrons were used to produce nuclear recoils in the gas of a proportional counter. Hydrogen and deuterium, or hydrogen and helium, were included as constituents of the gas in the counter. Pulse size distributions were obtained showing two steps corresponding to the maximum recoil energies of the two nuclei, and the ratio of these steps could be measured to an accuracy within about 1%.

The maximum recoil energy E_m given to a nucleus of mass M (in units of neutron mass) by a neutron of energy E is $E_m = qE$ where $q = 4M/(M+1)^2$. The coefficients q for hydrogen, deuterium and helium respectively are $q_p = 1{\cdot}000$, $q_d = 0{\cdot}890$, $q_\alpha = 0{\cdot}643$, within the accuracy required.

In a counter containing both hydrogen and deuterium the energy distributions of recoiling protons and deuterons will have upper limits E and $q_d E$ respectively. Since the pulse size is proportional to the ionization, the ratio of the upper limits of the pulse size distributions P_p and P_d will be given by

$$\frac{P_p}{P_d} = \frac{W_d(q_d E)}{W_p(E)} \frac{1}{q_d}$$

where $W_p(E)$ is the average energy expended per ion pair by a proton of initial energy E while being stopped in a gas.

It can be expected that protons and deuterons of equal velocity will lose equal amounts of energy per ion pair produced. It follows that $W_d(q_d E) = W_p(\frac{1}{2} q_d E)$. Substituting in the preceding equation we find

$$\frac{W_p(\frac{4}{9}E)}{W_p(E)} = \frac{8P_p}{9P_d}. \qquad \ldots\ldots(1)$$

Equation (1) was used to establish the relationship between W_p and E.

Similarly in a counter containing hydrogen and helium

$$\frac{W_\alpha(q_\alpha E)}{W_p(E)} = q_\alpha \frac{P_p}{P_\alpha}. \qquad \ldots\ldots(2)$$

Equation (2) together with the data concerning W_p was used to investigate the ratio of W_α / W_p and possible variation of W with E.

§ 3. EXPERIMENTAL APPARATUS

The neutrons were obtained from the ^{7}Li(p, n)^{7}Be reaction. An analysed proton beam of energy up to 2·5 MeV from the Harwell Van de Graaff machine (Fortescue and Hall 1949) was used, with beam currents up to 5 μA. Normally the energy spread of the beam was about ± 5 kev, and target thicknesses of 6 to 20 kev were used. Machine voltages were measured with a generating voltmeter, calibrated using the ^{7}Li(p, n)^{7}Be threshold, and neutron energies were calculated from the known proton voltage. An accurate knowledge of the neutron energy is not required for these experiments. Measurements were all made at 0° to the direction of the proton beam. One set of measurements was taken using 2·5 MeV neutrons from the reaction D(d, n)^{3}He, in this case using a low voltage (200 kev) accelerating equipment and a thick heavy ice target. For these measurements the counter was placed at an angle of approximately 90° to the direction of the deuteron beam.

The proportional counter used for these experiments is shown in fig. 1. It is made of thin-walled soda glass with an external cathode (Maze 1946), lead glass being used where indicated to provide better insulation for the counter wire. It is somewhat unusual in design in that glass 'field tubes' (Cockroft and Curran 1951) are used, and maintained at a suitable potential by applying a voltage to external graphite coatings as indicated. This produces a well-defined collecting volume in the counter and insures a uniform field gradient along the central wire over the full length of the collecting space. This design of counter results in a simple construction and has proved satisfactory. The counter was operated with the central wire near ground potential and was mounted in a thin-walled (30 gauge) aluminium box to provide electrical shielding. Cellotape 'slings' were used to support the counter and provide insulation for the cathode.

The gases used for filling the counter were of high purity. The argon was obtained from cylinders of stated purity 99·7%, and then further purified by circulation over heated calcium and magnesium turnings. The helium was spectroscopically pure. Methane purified by fractional distillation was used.* Deuterium was prepared by electrolysis from water containing approximately 97% deuterium, and introduced into the counter through a palladium leak.

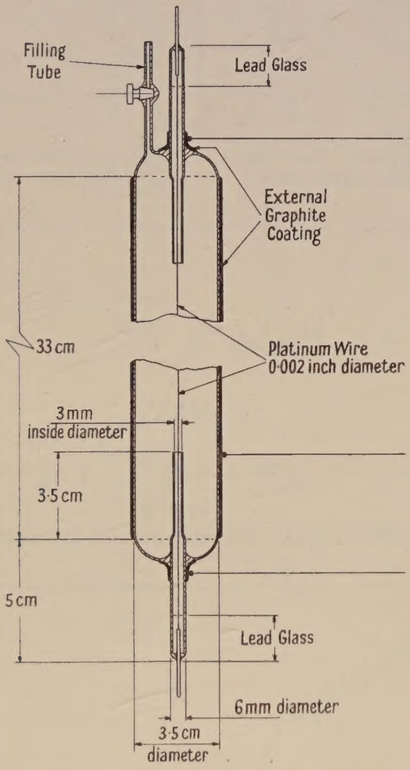

Fig. 1. Counter construction.

For most of the measurements the counter was located with its centre approximately 18 inches from the target. Pulses from the counter were amplified using the 1008-type head amplifier and main amplifier, the head amplifier being mounted directly on the counter assembly. They were then transmitted to a 30-channel pulse analyser via a relay unit and amplifier. In some measurements, in order to select and expand a part of the pulse-size distribution, a non-linear amplifier was used before pulses were fed to the relay unit. Frequent calibrations of the amplifiers and pulse analyser were made using an accurate pulsed signal generator, the pulses being introduced by capacity coupling to the grid of the first valve of the head amplifier. In all cases the pulse size ratios quoted are based on the overall calibrations.

---

* The authors are indebted to Dr. H. London of the Atomic Energy Research Establishment for the methane used in these experiments.

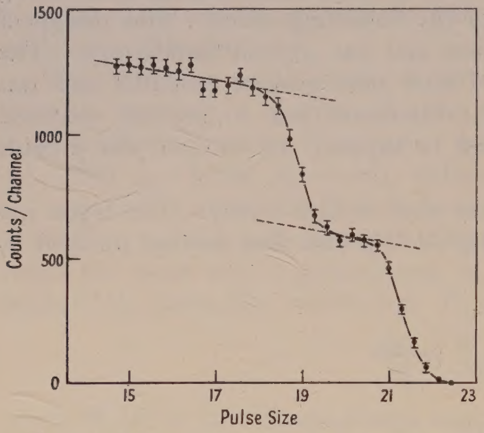

Fig. 2. Pulse size distribution. See table 1 row 4 for experimental conditions.

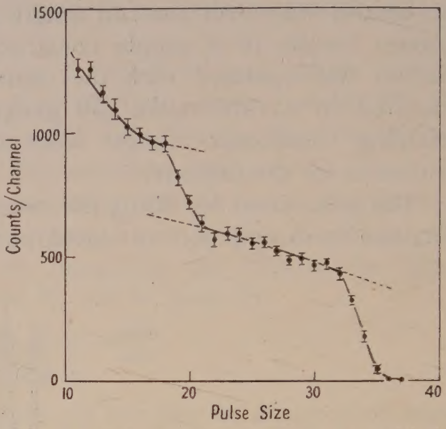

Fig. 3. Pulse size distribution. See table 3 row 4 for experimental conditions.

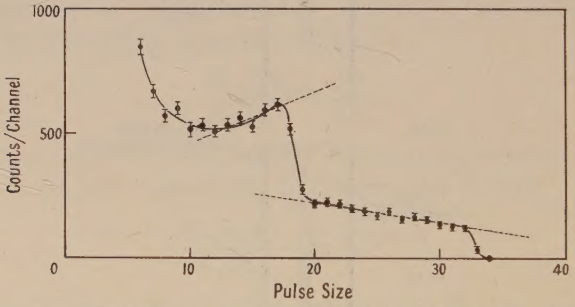

Fig. 4. Pulse size distribution. See table 2 row 2 for experimental conditions.

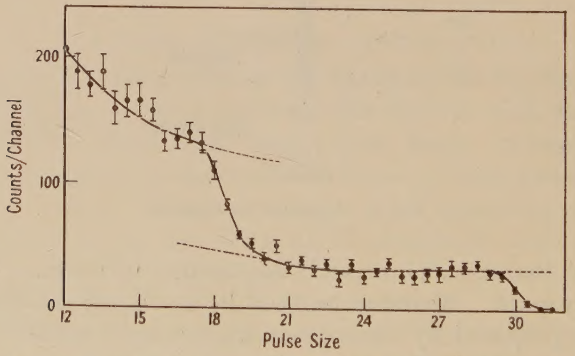

Fig. 5. Pulse size distribution. See table 4 row 1 for experimental conditions.

§ 4. EXPERIMENTAL RESULTS

Figures 2, 3, 4 and 5 show representative data obtained in these measurements. The data have been analysed to obtain the ratio of pulse sizes in a relatively simple and straightforward manner. Data taken from the pulse analyser were plotted on a large scale and the best fitting curve, as judged by visual inspection, drawn through the points. An assumed curve, shown dotted, for the shape of

Table 1

E(kev)	Counter Filling	Stopping Power (%)	Gain	P_p/P_d	$W_p(\frac{4}{9}E)/W_p(E)$
54_3	A 24·2 cm D_2 10·1 cm CH_4 2·0 cm	82 10 8	23	$1\cdot13_1\pm0\cdot005$	$1\cdot00_6\pm0\cdot005$
54_3	same	same	28	$1\cdot13_1\pm0\cdot01$	$1\cdot00_6\pm0\cdot01$
41_6	same	same	23	$1\cdot13_4\pm0\cdot02$	$1\cdot00_9\pm0\cdot02$
54_3	D_2 25·8 cm CH_4 14·8 cm	31 69	8	$1\cdot13_1\pm0\cdot005$	$1\cdot00_6\pm0\cdot005$

Table 2

E(kev)	Counter Filling	Stopping Power (%)	Gain	P_p/P_α	$W_\alpha(q_\alpha E)/W_p(E)$
68_9	He 44·3 cm CH_4 10·4 cm	50 50	24	$1\cdot72_8\pm0\cdot012$	$1\cdot11_1\pm0\cdot008$
59_2	same	same	18	$1\cdot74_4\pm0\cdot019$	$1\cdot12_2\pm0\cdot012$
59_2	same	same	6	$1\cdot73_5\pm0\cdot015$	$1\cdot11_6\pm0\cdot010$
49_1	same	same	21	$1\cdot73_1\pm0\cdot012$	$1\cdot11_3\pm0\cdot008$
37_2	same	same	23	$1\cdot77_3\pm0\cdot03$	$1\cdot14_4\pm0\cdot02$

Table 3

E(kev)	Counter Filling	Stopping Power (%)	Gain	P_p/P_α	$W_\alpha(q_\alpha E)/W_p(E)$
64_1	A 27·3 cm He 27·8 cm CH_4 7·0 cm	63 18 19	20	$1\cdot68_5\pm0\cdot015$	$1\cdot08_4\pm0\cdot01$
54_3	same	same	12	$1\cdot71_3\pm0\cdot012$	$1\cdot10_2\pm0\cdot008$
44_3	same	same	19	$1\cdot65_8\pm0\cdot03$	$1\cdot06_6\pm0\cdot02$
36_5	A 15 cm He 15·3 cm CH_4 3·9 cm	63 18 19	15	$1\cdot71_0\pm0\cdot018$	$1\cdot10_0\pm0\cdot012$

Table 4

E(kev)	Counter Filling	Stopping Power (%)	Gain	P_p/P_α	$W_\alpha(q_\alpha E)/W_p(E)$
2500	A 116 cm He 30·7 cm CH_4 9·0 cm	85 7 8	6	$1\cdot63_2\pm0\cdot012$	$1\cdot05_0\pm0\cdot008$
83_4	same	same	36	$1\cdot66_5\pm0\cdot016$	$1\cdot07_1\pm0\cdot010$
83_4	same	same	16	$1\cdot62_0\pm0\cdot023$	$1\cdot04_2\pm0\cdot015$
83_4	same	same	5	$1\cdot69_3\pm0\cdot013$	$1\cdot09_0\pm0\cdot008$
73_8	same	same	19	$1\cdot69_9\pm0\cdot023$	$1\cdot09_3\pm0\cdot015$
59_2	same	same	6	$1\cdot68_2\pm0\cdot017$	$1\cdot08_2\pm0\cdot011$
59_2	same	same	25	$1\cdot67_8\pm0\cdot008$	$1\cdot08_0\pm0\cdot005$

Gain = proportional gain.

the distribution due to proton recoils was then drawn in, and 'end-points' for the distributions were taken to be the value at which the curve fell to 50% of the extrapolated height (shown dotted) of the plateau. Previous experience of the shape of the curves obtained with counters containing a pure methane filling was of some use in the assessment of the contribution due to proton recoils, but the results depend relatively little upon the exact shape of the contribution assumed.

In view of the fact that usually one or more pulse analyser channels gave readings on the steeply sloping portions of these curves, this method of analysing the data permitted the 50% point to be located with an error small compared with one channel width. Separate analysis of the data by two independent observers gave measured values of the ratio of pulse sizes usually agreeing to within $\frac{1}{2}$%, and a more detailed analysis was not considered justifiable.

Since the scattering of neutrons by helium is markedly asymmetrical (Hall and Koontz 1947) particularly at the higher neutron energies used in these experiments, it is not obvious that the above method of analysing the experimental data to obtain an end-point for recoil α-particles is legitimate. However, a detailed investigation of this point has shown that, under the conditions of the experiment, an error of less than 1% is introduced in the assessment of the α-particle end-point. In view of the smallness of this correction, and the lack of knowledge of the asymmetry of scattering at the neutron energies used in the experiment, no correction to the results has been made.

Results of all the useful experimental data are summarized in tables 1, 2, 3 and 4. The errors given are an attempt to assess reasonable limits of error, and have been assigned in a somewhat arbitrary manner based on the consistency of the data for different runs under the same conditions. The proportional gain was measured by introducing a known signal to the input grid of the head amplifier through a small condenser, the condenser and signal generator having previously been calibrated by comparison with ^{234}U α-particle pulses from a grid type ionization chamber filled with purified argon.

The following deductions can be drawn from the results of tables 1, 2, and 3. (*a*) The value of $W_p(E)$ for protons of energy 200–550 kev appears constant to within 1%, both for a gas mixture where 82% of the stopping power is contributed by argon, and a mixture where 69% is contributed by methane. (*b*) The value of $W_\alpha(E)$ for α-energies between 250–400 kev is higher by about 10% than the (constant) value of $W_p(E)$ for protons of comparable energy. (*c*) There is no definite evidence for a variation of the ratio W_α/W_p within this rather restricted energy range.

The results given in tables 2 and 3 indicate that there is a definite variation of the ratio W_α/W_p depending on the nature of the gas filling in the counter. For this reason a further series of measurements were taken and the results are given in table 4. The results confirm the fact that the ratio W_α/W_p is nearer unity when argon contributes most of the stopping power. In addition a point taken using 2·5 Mev neutrons provides some evidence that there is a change in the ratio W_α/W_p as a function of neutron energy, the value of this ratio being nearer to unity at the higher energies. This evidence is not entirely convincing, however, since the change involved (3%) is only three times the estimated experimental error of the measurements.

§5. DISCUSSION OF RESULTS

Possible sources of error in these experiments exist in the multiplication mechanism of the proportional counter or in the loss of free electrons in the relatively weak collecting field of the counters.

There was no evidence of space-charge limitation of the proportional multiplication. This is shown in table 3 where the ratio W_α/W_p is not affected by a change of a factor of two in stopping power and in tables 3 and 4 where measurements have been taken at values of proportional gain varying by as much as seven times. The measured ratio is constant within the experimental error.

Initial recombination, volume recombination and negative ion formation are unlikely to cause an appreciable loss of electrons at the field strengths and pressures prevailing in these experiments. The shape of the pulse distribution near the end-point, which agreed with that calculated from the known energy spread of the neutrons, clearly showed that such effects are unimportant.

The information on columnar recombination available in the literature (Wilkinson 1950) suggests that it will be negligible in the present experiments, and this is also supported by the results in table 3.

Since the method requires the presence of hydrogen and deuterium, or hydrogen and helium in the counter filling, it is not possible to measure directly the ratios $W_p(\frac{4}{9}E)/W_p(E)$ and $W_\alpha(q_\alpha E)/W_p(E)$ (hereafter referred to as W_α/W_p for brevity) for pure gases. This limitation of the method is not serious, as far as investigating the behaviour of pure gases is concerned, for previous measurements (Gray 1944) indicate that the variation of W with energy for α-particles is similar in hydrogen and the rare gases.

An estimate can be made of the value of the ratio W_α/W_p in pure argon from the results of tables 2, 3 and 4. This has been done in the following way. The results in table 2 show no significant variation over the range of neutron energies used, and the results of the first four rows have been averaged, giving $W_\alpha/W_p = 1{\cdot}114 \pm 0{\cdot}005$ for a neutron energy of about 600 kev. This refers to a counter filling where the stopping power is equally divided between helium and methane. Similarly, the results in table 3 give $W_\alpha/W_p = 1{\cdot}092 \pm 0{\cdot}006$, the stopping power in this case being 63% in argon and 37% in helium and methane. Again from table 4 we obtain a value $W_\alpha/W_p = 1{\cdot}081 \pm 0{\cdot}005$ for a neutron energy of about 600 kev, with stopping power 85% in argon and 15% in helium and methane. Extrapolating from the above data we obtain a value of $W_\alpha/W_p = 1{\cdot}077 \pm 0{\cdot}006$ for 600 kev neutrons and a pure argon filling. Since the correction to the results in table 4 necessary to obtain the value of pure argon is so small (0·4%) we shall neglect this correction in the further discussion of these results.

From their measurements on α-particles in argon Cranshaw and Harvey (1948) have proposed the formula $W = 27{\cdot}5 + 1{\cdot}9/\sqrt{E}$ where W is in electron volts and E in Mev. This formula is empirical and follows the form proposed by Gerbes (1935) to fit measurements of W in air for electrons from 300 to 60 000 ev. This form was subsequently used by Gray (1944) for an analysis of the variation of W for α-particles in air. It is of interest to see how well the results of the experiments described here can be fitted by a similar formula, with the additional assumption that protons, deuterons and α-particles all have the same value of W when travelling at the same velocity.

Thus we assume

$$W_{\mathrm{p}}=A(1+a/\sqrt{E_{\mathrm{p}}}),\ W_{\mathrm{d}}=A(1+\sqrt{2}a/\sqrt{E_{\mathrm{d}}}),\ W=A(1+2a/\sqrt{E_{\alpha}}).$$

Using the values (table 4) 1·050, 1·076 and 1·081 for $W_{\alpha}/W_{\mathrm{p}}$ measured for 2·5, 0·834 and 0·592 Mev neutrons, the values of a derived from the above formulae are $0{\cdot}55_5$, $0{\cdot}04_9$ and $0{\cdot}04_4$ respectively. Since a change of $\frac{1}{2}\%$ in $W_{\alpha}/W_{\mathrm{p}}$ will change the value of a by about 10%, this agreement may be considered good. It should be noted that this value of a is lower than that suggested by Cranshaw and Harvey (1948), viz. $a=0{\cdot}069$.

If, however, we use an average value of $a=0{\cdot}05$ to calculate the ratio $W_{\mathrm{d}}/W_{\mathrm{p}}$ for 500 kev neutrons we get the value 1·032, which is well outside the estimated experimental error for the results given in table 1. It is apparent that such a simple variation of W with velocity, independent of the nature of the ionizing particle, cannot give a good interpretation of the experiments described in this paper.

Bethe (1950) has summarized recent evidence of the constancy of the value of W in argon as follows: "Barring very strange accidental compensations, we must agree with the authors mentioned, that the ionization in argon is strictly proportional to the energy, independently of the energy and also of the kind of particle used (H, ^{3}H, ^{4}He, ^{7}Li, ^{14}C)". The experimental results of this paper favour the occurrence of 'strange accidental compensations'. In addition, there is a rather direct conflict of experimental measurements as discussed by G. C. Hanna (1950).

§ 6. CONCLUSIONS

The experiments described in this paper provide strong evidence that the value of W in argon depends on the nature of the ionizing particle. The range of particle energies investigated is not large enough to prove conclusively that the value of W is also a function of particle energy, although the results favour this interpretation.

ACKNOWLEDGMENTS

It is a pleasure to acknowledge our indebtedness to Mr. C. D. Florida of the Atomic Energy Research Establishment, Harwell, who designed and supplied much of the special electronic equipment used for this experiment, including the 30-channel pulse analyser. We are indebted also to Mr. A. E. Pyrah for the efficient operation of the electrostatic generator, and to Dr. M. J. Poole and Mr. D. Allen for permission to use their 200 kev accelerating set. We wish to thank the Director, Atomic Energy Research Establishment, for permission to publish this paper.

REFERENCES

Bethe, H. A., 1950, *Rev. Mod. Phys.*, **22**, 213.
Cockroft, A. L., and Curran, S. C., 1951, *Rev. Sci. Instrum.*, **22**, 37.
Cranshaw, T. E., and Harvey, J. A., 1948, *Canad. J. Res.* A, **26**, 243.
Fortescue, R. L., and Hall, P. D., 1949, *Proc. Instn. Elect. Engrs.*, **96**, 77.
Franzen, W., Halpern, J., and Stephens, W. E., 1950, *Phys. Rev.*, **77**, 641.
Gerbes, W., 1935, *Ann. Phys., Lpz.*, **23**, 648.
Gray, L. H., 1944, *Proc. Camb. Phil. Soc.*, **40**, 72.
Hall, T. A., and Koontz, P. G., 1947, *Phys. Rev.*, **72**, 196.
Hanna, G. C., 1950, *Phys. Rev.*, **80**, 530.
Jesse, W. P., Forstat, H., and Sadauskis, J., 1950, *Phys. Rev.*, **77**, 782.
Maze, R., 1946, *J. Phys. Radium*, **7**, 164.
Rossi, B., and Staub, H., 1949, *Ionization Chambers and Counters* N.N.E.S. Vol. V-2. (New York : McGraw-Hill).
Wilkinson, D. H., 1950, *Ionization Chambers and Counters* (Cambridge : University Press).

The Inelastic Scattering of Very Slow Neutrons by Iron

By R. LATHAM* and J. M. CASSELS†
Cavendish Laboratory, Cambridge

MS. received 27th November 1951

ABSTRACT. The increase with temperature of the total cross section of iron for very slow neutrons has been measured with the help of a cyclotron and a neutron velocity selector. Part at least of this increase is caused by the inelastic scattering associated with lattice vibrations, but the observed rise in cross section is much greater than is predicted by the theory of this effect. It is suggested that a ferromagnetic scattering process may be responsible for the discrepancy.

§1. INTRODUCTION

Cassels and Latham gave in 1948 a preliminary account of an experimental study of the neutron total cross section of iron. The neutrons concerned were moving so slowly that their associated wavelengths were longer than twice the maximum Bragg spacing in the iron crystal structure. It is well known that under these conditions most of the elastic scattering of a polycrystalline material disappears because of destructive interference. Some elastic scattering does remain, however, if there are differences in the scattering properties of isotopes, or if the scattering depends on the relative orientation of neutron and nuclear spins. Another part of the total cross section is due to inelastic scattering processes in which the neutron exchanges energy with the scatterer. A third contribution to the total cross section arises from nuclear absorption. For very slow neutrons the absorption cross section of iron is proportional to the neutron wavelength, and its magnitude can be found from the results of other experiments.

The relative amounts of elastic and inelastic scattering can be estimated by measuring the total cross section as a function of the temperature of the scatterer. The elastic cross section decreases only very slightly as the temperature is raised, while the inelastic term increases rapidly. In the experiment under discussion the total cross section was measured at 77, 290, 630 and 800° K. Although the results have poor statistical accuracy, there is clear evidence that the inelastic scattering is much greater than predicted by the theory of Weinstock (1944). The process considered by Weinstock involves an exchange of energy between the neutron and the thermal vibrations of the crystal lattice.

Hughes, Burgy and Woolf (1950) have examined the inelastic scattering of iron by a rather different method, and also come to the conclusion that there is too much to be accounted for by the lattice vibration theory.

The conclusion to be drawn is either that the theory is inaccurate, or that there is some other process contributing to the observed total cross section. The object of the present paper is to discuss these alternatives.

---

[*] Now at Imperial College of Science, London.
[†] Now at Atomic Energy Research Establishment, Harwell, Berks.

§2. THEORETICAL TOTAL CROSS SECTIONS

If the scattering is assumed to be entirely nuclear, then the theoretical cross sections at long neutron wavelengths ($\lambda > 4{\cdot}04$ Å) can be evaluated from the relation (Cassels 1951)

$$\sigma_{\mathrm{t}} = \sigma_{\mathrm{a}} + E_{\mathrm{el}}(s) + E_{\mathrm{in}}(S) + E_{\mathrm{in}}(s),$$

where σ_{a} is the absorption cross section and $E_{\mathrm{el}}(s)$, $E_{\mathrm{in}}(S)$, $E_{\mathrm{in}}(s)$ are respectively the disordered elastic, the ordered inelastic and the disordered inelastic scattering cross sections. The last three terms in the equation are functions of the temperature of the iron, and their theoretical values in terms of the constants S and s have already been published (Cassels and Latham 1948, Cassels 1950).

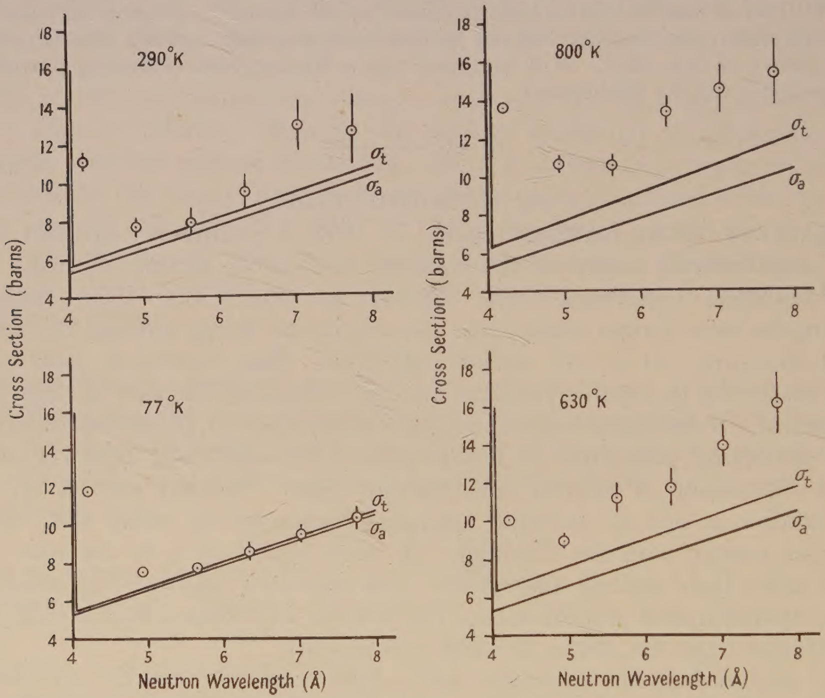

Fig. 1. Comparison of experimental and theoretical total cross sections at four temperatures. The theoretical cross sections are labelled σ_{t}, and the contribution of the absorption cross section σ_{a} is also indicated.

It only remains to adopt numerical values for σ_{a}, S and s. The best value of σ_{a} (Colmer and Littler 1950, Pomerance 1951) appears to be 1·33 barns/Å, or 2·4 barns at the standard neutron speed of 2200 m/sec. The possible values of S and s are restricted by the fact that their sum is equal to the scattering cross section at short wavelengths, namely 11·0 barns (Havens, Rainwater, Wu and Dunning 1948). The fraction contributed by s can be estimated by adjusting the theoretical cross section to fit the experimental results at 77° K (fig. 1). It has been found that s must be reduced to zero in order to secure agreement.

If in fact σ_{a} is smaller than the value adopted, and it can hardly be larger, then a finite value for s would be needed. The theoretical cross sections at all temperatures would hardly be affected because the rate of increase of σ_{t} with temperature depends almost entirely on the magnitude of the sum of S and s.

§ 3. EXPERIMENTAL METHOD

The general arrangement of the experimental apparatus need not be described in detail here, since it was very similar to that used later to study the inelastic scattering of very slow neutrons by aluminium (Cassels 1951). The techniques used in the iron experiment were cruder in the following respects: (*a*) The iron scatterer was not extremely pure. It was in fact a sheet of mild steel 9·88 g/cm^2 thick, but the presence of about 0·1% by weight of carbon could not have significantly altered the results. (*b*) For the high temperature measurements the scatterer was heated by a gas flame, rather than by an electric furnace. The heating was judged to be adequately uniform by inspection at dull red heat. (*c*) The flight path of the neutrons was 4½ metres, instead of 3, and the 'gate open' times were 810 microseconds, instead of 270. The neutron velocity resolution was thus rather poorer than that used in the later work, but this does not greatly matter because the total cross sections vary slowly and smoothly with neutron wavelength. In spite of the longer flight path, the geometry was 'bad' in the sense that neutrons scattered through angles up to 1° were still counted. A small angle-scattering effect discovered by Hughes, Burgy, Heller and Wallace (1949) could not therefore have affected the measurements.

§ 4. RESULTS

In fig. 1 the experimental results at the four temperatures are compared with the theoretical cross sections. It is clear that the increase of the cross section with temperature is at a rate between two and three times greater than that predicted.

§ 5. DISCUSSION

There are now two strong reasons for believing that this discrepancy is not due to a fault in the lattice vibration theory.

First, the results of other work with aluminium (Cassels 1951) and magnesium (Squires, private communication) have shown very good agreement between experiment and theory, and there is no reason to suppose that the vibrations of iron crystals are in any way abnormal.

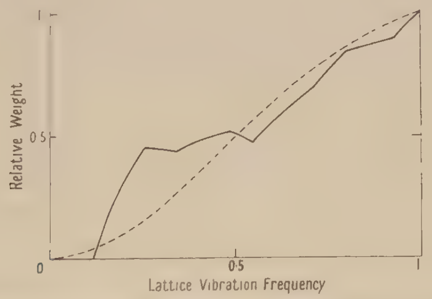

Fig. 2. The relative contributions made by lattice vibrations of various frequencies to the specific heat at 130° K (broken line) and the ordered inelastic scattering at 6 Å and 500° K (full line). The lattice vibration frequency is expressed as a fraction of the cut-off frequency.

Secondly, the most dubious step in the theory is the derivation of the frequency spectrum of the thermal vibrations by means of the Debye approximation. The earlier suggestion (Cassels and Latham 1948) that this approximation might be the cause of the trouble must now be regarded as unlikely to be correct. In fig. 2 the broken line shows the relative contributions made by thermal vibrations of various frequencies to the specific heat of iron at 130° K. These were computed by means of the Debye theory. The full curve shows the relative contributions to the ordered inelastic scattering at 6 Å and 500° K. The kinks in this curve are caused by reciprocal lattice vectors cutting in and out according to certain selection rules. The two curves evidently have much the same shape. Since the Debye temperature was adjusted to suit the specific heat, it is very probable that the inelastic scattering has been quite accurately predicted.

If some other scattering process is to be invoked, as seems necessary, then it is most likely to be connected with the magnetic properties of the atomic electrons in iron. Indeed, it may be thought that ferromagnetic effects should have been expected from the first, in view of the well-known experiments (for references see Burgy *et al.* 1950) in which a large change in the total cross section of iron for thermal neutrons is induced by an external magnetic field. However, this effect depends on an interference term between the nuclear and magnetic scattering amplitudes. In the absence of an external field this term is as often positive as negative, and so cancels out. All other magnetic effects are of second order in the magnetic scattering amplitude, and were thought to be small on that account.

One of these second-order terms has the effect of increasing the value of S, but it seems quite impossible for S to be more than doubled, as would be necessary to explain the observations. At wavelengths just below 4·04 Å, moreover, there does not seem to be an unexpectedly large amount of ordered inelastic scattering, which is also proportional to S.

The possibility of other second-order magnetic effects becomes apparent when it is remembered that the atomic spins are thrown out of alignment by thermal agitation. There is some elastic scattering even at long neutron wavelengths because the various scattering centres are no longer identical, and some inelastic scattering because the iron is not in its ground state magnetically.

The second of these processes has been examined theoretically by Moorhouse (1951), who has found surprisingly large differential cross sections in certain directions. The cross section integrated over all angles has not been evaluated, but it seems at least possible that it might be large enough to account for the experimental results.

If this explanation turns out to be correct, then it is clear that much can be learnt about ferromagnetism (and anti-ferromagnetism also) by more refined neutron scattering experiments. In particular, measurements of the neutron energy before and after scattering should yield information about the magnetic energy levels. A step in this direction has already been taken by Egelstaff (1951).

ACKNOWLEDGMENTS

We should like to thank Mr. G. L. Squires for help with the measurements at 77° K. Most of the apparatus was made in the workshops by Mr. J. Banham, and the cyclotron was operated by Mr. E. Morley.

One of us (J. M. C.) gratefully acknowledges a grant from the Department of Scientific and Industrial Research.

REFERENCES

Burgy, M., Hughes, D. J., Wallace, J. R., Heller, R. B., and Woolf, W. E., 1950, *Phys. Rev.*, **80**, 953.
Cassels, J. M., 1950, *Progress in Nuclear Physics*, I (London : Butterworth–Springer); 1951, *Proc. Roy. Soc.* A, **208**, 527.
Cassels, J. M., and Latham, R., 1948, *Phys. Rev.*, **74**, 103.
Colmer, F. C. W., and Littler, D. J., 1950, *Proc. Phys. Soc.* A, **63**, 1175.
Egelstaff, P. A., 1951, *Nature, Lond.*, **168**, 290.
Havens, Jr., W. W., Rainwater, L. J., Wu, C. S., and Dunning, J. R., 1948, *Phys. Rev.*, **73**, 963.
Hughes, D. J., Burgy, M. T., Heller, R. B., and Wallace, J., 1949, *Phys. Rev.*, **75**, 565.
Hughes, D. J., Burgy, M. T., and Woolf, W. E., 1950, *Phys. Rev.*, **80**, 481.
Moorhouse, R. G., 1951, *Proc. Phys. Soc.* A, **64**, 1097.
Pomerance, H., 1951, *Phys. Rev.*, **83**, 641.
Weinstock, R., 1944, *Phys. Rev.*, **65**, 1.

The Angular Distribution of Scattered Nucleons in High Energy Nuclear Collisions

By H. MESSEL and H. S. GREEN
University of Adelaide, South Australia

MS. received 25*th October* 1951

ABSTRACT. The theory of the mean square angle of emission of nucleons resulting from a high energy nucleon–nucleus collision is developed. Graphical results are given both for light and for heavy nuclei.

§1. INTRODUCTION

The amount of experimental data on nuclear collisions, derived by the photographic-plate and cloud-chamber techniques, is steadily increasing. It is true that data on nucleon–nucleon collisions must remain scanty for some time, and the information concerning the lateral structure of air showers is so much averaged that the finer detail of the processes involved is obscured. The photographic-plate technique, however, is providing much information on the scattered particles which result from collisions between nucleons and nuclei. The amount of data for high energy collisions is small at present but will undoubtedly increase. From the statistical analysis of this data one may hope to obtain information on nuclear cross sections at energies unattainable under laboratory conditions.

The mean square angle of scatter in nucleon–nucleon collisions has been derived in a previous paper by Green and Messel (1951); the object of the present paper is to extend this work to collisions between a nucleon and a nucleus. In the course of the work use will be made of the differential cross section derived in the previous paper.

The fundamental diffusion equation is first set up with reference to the energy and direction of motion of a particle within the target nucleus, regarded as a sphere of homogeneous nuclear matter. Using our solution of this diffusion equation, we have determined the mean square angle of emission of high energy nucleons, in a nucleon–nucleus collision, for both light and heavy nuclei. The result represents the second and obviously essential step towards our final objective, which is to derive theoretical information on the lateral spread of the nucleon component in air showers.

§2. THE DIFFUSION EQUATION AND ITS SOLUTION

Let $n(U, C, z)\,dU\,dC$ be the probability of finding a nucleon at depth z in homogeneous nuclear matter, with energy in the interval U, $U+dU$, and with direction of motion making an angle with the vertical whose cosine lies in the interval C, $C+dC$. Further, let $W(U', U, c)\,dU\,dc$ be the differential probability of finding a scattered nucleon with energy in the interval U, $U+dU$ and making with the direction of motion of the direct ancestor, of energy U', an angle whose cosine is in the range c, $c+dc$.

Denote by ω the angle between the plane containing the vertical and the direction of motion of the scattered nucleon, and the plane passing through the directions of motion of the scattered nucleon and its direct ancestor. Let c_0 be the cosine of the maximum angle which the scattered nucleon of energy U can make with the direction of its ancestor of energy U'. Also, write $S=(1-C^2)^{1/2}$ and $s=(1-c^2)^{1/2}$.

Now, consider a nucleon arriving at depth z with energy U, $U+dU$, and making an angle with the axis of the cascade within the nucleus whose cosine is C, $C+dC$. The probability that such a nucleon has passed through a layer of depth $z-\zeta$ is $\exp\{-(z-\zeta)/C\}$, if the depth is measured in nuclear cascade units. The probability that, in addition, there was a nucleon–nucleon collision between the depths ζ, $\zeta+d\zeta$, which generated the nucleon considered, is equal to the path length $d\zeta/C$ within the layer $d\zeta$. Furthermore, the probability that the direct ancestor had an energy in the range U', $U'+dU'$ and a direction of motion whose polar angles were $\cos^{-1}c$ and ω with respect to the direction of motion of its descendant is $n(U', Cc+Ss\cos\omega, \zeta)\,W(U', U, c)\,dU'\,dc\,d\omega/2\pi$; hence one may write

$$n(U, C, z)=2\left[\int_0^z e^{-(z-\zeta)/C}\,d\zeta/C\right]\int_U^\infty\int_{C_0}^1\int_0^{2\pi} n(U', Cc+Ss\cos\omega, \zeta)W(U', U, c)$$
$$\times\, dU'\,dc\,d\omega/2\pi+n(U, C, 0)\,e^{-z/C}. \qquad \ldots\ldots(1)$$

On differentiation the above reduces to

$$C\frac{\partial}{\partial z}n(U, C, z)+n(U, C, z)$$
$$=2\int_U^\infty\int_{C_0}^1\int_0^{2\pi} n(U', Cc+Ss\cos\omega, z)W(U', U, c)\,dU'\,dc\,d\omega/2\pi. \qquad \ldots\ldots(2)$$

In order to obtain the solution of (2), $n(U, C, z)$ is expanded in a series of Legendre polynomials, thus:

$$n(U, C, z)=\sum_{k=0}^{\infty}\tfrac{1}{2}(2k+1)V_k(U, z)P_k(C). \qquad \ldots\ldots(3)$$

The boundary condition $n(U, C, z)=\delta(U-U_0)\delta(C-1)$ at $z=0$ gives

$$\delta(U-U_0)\delta(C-1)=\sum_{k=0}^{\infty}\tfrac{1}{2}(2k+1)V_k(U, 0)P_k(C). \qquad \ldots\ldots(4)$$

So one must have
$$V_k(U,0)=\delta(U-U_0) \qquad \ldots\ldots(5)$$
for all k.

Substituting (3) into (2), one makes use of the addition theorem
$$P_k(Cc+Ss\cos\omega)=P_k(C)P_k(c)+2\sum_{l=1}^{k}\frac{(k-l)!}{(k+l)!}P_k^l(C)P_k^l(c)\cos(l\omega)$$
and also the relation $(2k+1)CP_k(c)=kP_{k-1}(C)+(k+1)P_{k+1}(C)$. Then the diffusion equation reduces to
$$\frac{\partial}{\partial z}\left\{\frac{k+1}{2k+1}V_{k+1}(U,z)+\frac{k}{2k+1}V_{k-1}(U,z)\right\}+V_k(U,z)$$
$$=2\int_U^\infty\int_{C_0}^1 V_k(U',z)P_k(c)W(U',U,c)\,dU'\,dc. \qquad \ldots\ldots(6)$$

Now the value of $V_0(U,z)$ is known; for, by multiplying (3) by $P_0(C)=1$ and integrating, one obtains
$$N(U,z)=\int_{-1}^{1}n(U,C,z)\,dC=V_0(U,z), \qquad \ldots\ldots(7)$$

where $N(U,z)$ is simply the average number function (Messel 1951). The values of V_1, V_2 . . . can therefore be obtained by setting $k=0$, 1 . . . and solving the resultant equations by the well-known method of Mellin transforms. For a homogeneous type of cross section like that adopted in our previous paper we find*
$$V_1(U,z)=V_0(U,z)=\frac{1}{2\pi i}\frac{1}{U_0}\int_{S_0-i\infty}^{S_0+i\infty}\left(\frac{U}{U_0}\right)^{-(s+1)}e^{-\alpha(s)z}\,ds \qquad \ldots\ldots(8)$$
and
$$V_2(U,z)=\frac{1}{2\pi i}\frac{1}{U_0}\int_{S_0-i\infty}^{S_0+i\infty}\left(\frac{U}{U_0}\right)^{-(s+1)}\left\{e^{-\alpha(s)z}-\frac{3}{4U}\frac{\alpha(s+1)+\alpha(s)-2}{\alpha(s)}(e^{-\alpha(s)z}-1)\right\}ds$$
$$\ldots\ldots(9)$$
where
$$\alpha(s)=1-2\int_0^\infty\left(\frac{U}{U'}\right)^s w\left(\frac{U}{U'}\right)\frac{dU}{U'} \qquad \ldots\ldots(10)$$
and $w(U/U')$ is simply the total cross section given by
$$w(U/U')=\int_{C_0}^{1}W(U',U,c)\,dc. \qquad \ldots\ldots(11)$$
We have determined V_3 and V_4 in a similar manner; however, for the evaluation of the mean square angle of emission only V_0 and V_2 are required, as we shall show in the following section.

§ 3. THE MEAN SQUARE ANGLE OF EMISSION

The expression for the mean square angle as a function of the energies and depth z is given by
$$\langle\theta^2(U',U,z)\rangle=\left\{\int_{-1}^{1}n(U,\ \cos\theta,\ z)\sin^2\theta\,d(\cos\theta)\right\}$$
$$\times\left\{\int_{-1}^{1}n(U,\cos\theta,z)\,d(\cos\theta)\right\}^{-1}, \qquad \ldots\ldots(12)$$
if one neglects the difference between $\sin^2\theta$ and θ^2 for the small angles with which we are concerned.

---

* Higher approximations to V_1 and V_2 are being evaluated in a subsequent paper.

Making use of the fact that $\sin^2\theta = 1 - C^2 = \frac{2}{3}\{P_0(C) - P_2(C)\}$ and substituting from (3) into (12), we find

$$\langle\theta^2(U', U, z)\rangle = \frac{2}{3}\left\{\frac{V_0(U, z) - V_2(U, z)}{V_0(U, z)}\right\}. \qquad \ldots\ldots(13)$$

The physically interesting quantity is for integral spectra, that is, for particles with energies greater than some given energy U. This is obtained from (13) by integrating both numerator and denominator with respect to U from U to U_0, the energy of the primary nucleon. Furthermore to obtain the mean square angle of emission of nucleons from a nucleus we apply the averaging operator $\int_0^{D_A} 2z\,dz/D_A{}^2$ to the numerator and denominator which results. Here D_A represents the average number of collisions suffered by a nucleon in making a diametrical passage through a nucleus of atomic weight A. For the light nuclei oxygen and nitrogen we use $D_A = 3{\cdot}7$, and for the heavy nuclei silver and bromine $D_A = 6{\cdot}8$. This yields the mean square angle of emission of nucleons with energies greater than U, from a nucleus of atomic weight A:

$$\langle\theta^2(U_0, U)\rangle = I_1/I_2, \qquad \ldots\ldots(14)$$

where $$I_1 = \frac{1}{2\pi i}\,\frac{1}{2U}\int_{S_0-i\infty}^{S_0+i\infty}\left(\frac{U}{U_0}\right)^{-s} f\{D_A\alpha(s)\}\,\frac{2-\alpha(s)-\alpha(s+1)}{\alpha(s)}\,\frac{ds}{s+1} \qquad \ldots\ldots(15)$$

and $$I_2 = \frac{1}{2\pi i}\int_{S_0-i\infty}^{S_0+i\infty}\left(\frac{U}{U_0}\right)^{-s}\frac{1-f\{D_A\alpha(s)\}}{s}\,ds. \qquad \ldots\ldots(16)$$

Both the primary energy U_0 and the secondary energy U are measured in proton mass units. Also

$$f(x) = 1 - 2\,\frac{1-(1+x)\,\mathrm{e}^{-x}}{x^2} \qquad \ldots\ldots(17)$$

and $$\alpha(s) = 1 - 240\{(s+2)(s+3)(s+4)(s+5)\}^{-1} \qquad \ldots\ldots(18)$$

for the special choice of cross section:

$$w\left(\frac{U}{U_0}\right) = \frac{20}{U_0{}^4}\,U(U_0 - U)^3. \qquad \ldots\ldots(19)$$

The integrals I_1 and I_2 were evaluated by the method of steepest descent, the integrands both showing a maximum on the real axis which becomes progressively sharp as the ratio U/U_0 decreases. This method is therefore trustworthy for all energies except for secondary energies approaching the energy of the primary. The results for light and heavy nuclei are shown graphically in the figure.

§ 4. DISCUSSION

It will be seen from the figure that the mean square angular deviation of high energy (greater than a few thousand MEV) nucleons of a given energy U has a maximum for a specific value of the primary energy U_0. This maximum occurs where $U \sim \frac{1}{3}U_0$, which is approximately the average energy loss in a nucleon–nucleon collision. The height of the maximum is greater for lower energies, which is what one would expect qualitatively from our previous work. Another significant feature of the results is the difference in the value of $\langle\theta^2\rangle$ for heavy and light nuclei for given values of the primary and secondary energies. This again is what one would expect, since the number of collisions which can take place in a heavy nucleus will be greater than in a light nucleus.

For comparison of these conclusions with experiment we are indebted to Dr. D. H. Perkins who supplied data on the angular distribution of particles resulting from high energy nucleon–nuclei collisions in photographic plates. The number of measurable high energy events so far recorded is, unfortunately, too small for a quantitative comparison, but the following qualitative conclusions can be drawn.

The fact that the mean square angular deviation of the particles increases with the number of heavy prongs observed in photographic plate stars is in agreement with the difference which we have noted for heavy and light nuclei. The increase in the backward fraction of emitted particles as one passes from light to heavy nuclei is also readily understood from our results.

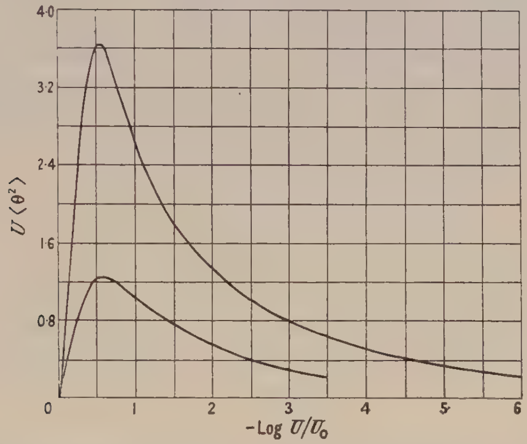

A plot of $U\langle\theta^2\rangle$ against the logarithm of the ratio of the energy U *above* which nucleons are emitted from a nucleus to the primary energy U_0. The energies are measured in proton mass units. $\langle\theta^2\rangle$ gives the mean square angle of emission in radians squared of nucleons with energies greater than U, resulting from a high energy nucleon–nucleus collision. The upper curve is for the heavy nuclei bromine and silver, the lower curve for the light nuclei nitrogen and oxygen.

Quantitative experimental verification of our results would afford valuable confirmation of the differential cross section for high energy nucleon–nucleon collisions which we have adopted. Assuming the validity of these results, they provide a valuable method for the determination of the primary energies in high energy nucleon–nucleus collisions, for the mean square angular deviation of the emitted particles is a good measure of the primary energy.

REFERENCES

Green, H. S., and Messel, H., 1951, *Proc. Phys. Soc.* A, **64**, 1083.
Messel, H., 1951, *Proc. R. Irish Acad.* A, **54**, 125.

The Nuclear Magnetic Moment of $^{197}_{79}$Au

By F. M. KELLY*
Clarendon Laboratory, Oxford

Communicated by H. Kuhn; *MS. received* 19*th November* 1951

ABSTRACT. The hyperfine structure of the 6s and 7s levels of Au I have been measured. The values of the nuclear magnetic moments calculated from the structure of these two levels using the Goudsmit–Fermi–Segrè formula agree. Since the Fermi–Segrè factor is very large (1·424) for the 6s level and small (1·038) for the 7s level, this affords a good check on the validity of the method introduced by Crawford and Schawlow for the evaluation of this factor. When the corrections for the finite size of the nucleus are included, the spectroscopic value of the nuclear magnetic moment of ^{197}Au is $+0{\cdot}136$ n.m.

§ 1. INTRODUCTION

A SPECTROSCOPIC determination of the nuclear magnetic moment of ^{197}Au has been made by Elliott and Wulf (1939) from the hyperfine structure of the 6s level of Au I. Their calculations, however, neglected the important Fermi–Segrè factor (Fermi and Segrè 1933) and the correction for the finite size of the nucleus (Rosenthal and Breit 1932). A numerical calculation shows that the Fermi–Segrè factor, $1-d\sigma/dn$, has the value 1·424 for the 6s level of Au I. This factor is considerably larger than those occurring in previous comparisons between moments determined spectroscopically and by nuclear induction methods (Crawford and Schawlow 1949, Schawlow, Hume and Crawford 1949, Kelly, Richmond and Crawford 1950). The value of $1-d\sigma/dn$ decreases rapidly with increasing n, and in Au I is 1·038 for the 7s level. At the present time no measurement of the nuclear magnetic moment of gold by the induction method is available, so that a comparison of the spectroscopic values obtained from the 6s and 7s levels of Au I can provide valuable information.

§ 2. EXPERIMENTAL

The light source was a hollow-cathode discharge tube cooled with liquid oxygen and similar to that used by Kuhn and Woodgate (1951). It was made from a copper–glass seal. The cathode was a conical-shaped aluminium block which was pulled tightly by a screw into a copper block and had a cavity at its upper end 0·45 cm in diameter and 1·5 cm deep. Gold was evaporated into the cathode cavity so that it would be in good thermal contact with the aluminium.

A side arm containing a few pellets of charcoal which could be cooled with liquid oxygen and a discharge tube with magnesium electrodes were connected to the source. The charcoal was used to clean neon while the magnesium discharge was used with argon and krypton. No attempt was made to circulate the gas.

The resonance lines of Au I ($6s\,^2S_{1/2}-6p\,^2P_{1/2,\,3/2}$; 2676 Å and 2428 Å) were photographed with a quartz spectrograph having achromatic triplet lenses of quartz and rock salt with focal lengths of 150 cm and an aperture ratio f/30. The

---

* Postdoctorate Fellow from the National Research Council of Canada.

Fabry–Perot interferometer plates were of fused quartz and were coated with aluminium. The interferometer was mounted between the collimator and the prism. Neon at a pressure of 0·9 mm Hg was the carrier gas for the discharge in the hollow cathode. Ilford Zenith plates were used to record the patterns.

The transitions $6p\,^2P_{1/2,\,3/2}-7s\,^2S_{1/2}$ (5837 Å and 7511 Å) were first photographed with an auto-collimating spectrograph with a focal length of 3 metres and an aperture ratio f/45. To increase the speed of the spectrograph it was later modified by the use of a lens with a focal length 103 cm, making the aperture ratio f/15. The interferometer plates were coated with silver having a transmission of 12% in the red and were mounted externally to the spectrograph. Both neon and argon were used as carrier gas for exciting 5837 Å. Neon was found to be the most satisfactory for 7511 Å. 5837 Å was photographed on Ilford HP3 plates, while 7511 Å was recorded on plates specially prepared for this research by the Ilford Research Laboratory and hypersensitized with triethanolamine.

§ 3. RESULTS

The two resonance lines ($6s\,^2P_{1/2}-6p\,^2P_{1/2,\,3/2}$, 2676 Å and 2428 Å) were photographed using currents in the hollow cathode varying from 50 to 3 milliamperes. Since these lines have been studied previously (Elliott and Wulf 1939) only one etalon spacer, 0·7476 cm in length, was used.

With a current of 50 mA a single flat-topped interference fringe was observed. When the current was reduced to 40 mA two components appeared. As the current was further reduced the width of the components decreased and the resolution improved. With a current of 10 mA a slight intensity difference between the two components could be seen, while currents of 5 and 3 mA gave patterns with the lower frequency components clearly stronger than the other. This confirms the positive sign of the nuclear magnetic moment. Visual estimates of the intensity ratio were consistent with that to be expected with the value $I=3/2$ of the nuclear spin, indicating that the effect of self-absorption in the source was small.

The structure observed in the line 2676 Å was measured in three exposures taken at 3 mA and six at 5 mA. The patterns had five orders on the average and each was measured five times. There was no difference between the results from the 3 and 5 mA exposures. The separation of the two components was found to be $0{\cdot}212 \pm 0{\cdot}003$ cm^{-1}. Two exposures taken with a 10 mA current were measured and the separation of the components was found to be $0{\cdot}225 \pm 0{\cdot}004$ cm^{-1}.

For 2428 Å three exposures at 5 mA and one at 3 mA were measured. The separation of the two components is $0{\cdot}204 \pm 0{\cdot}002$ cm^{-1}. Again the 10 mA exposures resulted in a slightly larger value of the splitting, $0{\cdot}213 \pm 0{\cdot}003$ cm^{-1}.

The separations obtained by Elliott and Wulf are 0·218 and 0·214 cm^{-1} for 2676 Å and 2428 Å respectively. These results agree fairly well with our measurements of the 10 mA exposures but are larger than our results obtained with 3 and 5 mA currents. Since Elliott and Wulf cooled their source with carbon dioxide and acetone and used considerably higher currents, it appears that self-absorption had a slight effect on their results.

The transition $6p\,^2P_{1/2}-7s\,^2S_{1/2}$ (5837 Å) was studied with 3 and 5 cm etalons with currents of 15, 10 and 5 mA. Three components were observed in the patterns obtained with both neon and argon as carrier gas. The three components appeared equally intense and almost equally spaced. The separations from the central component are $-0{\cdot}0208 \pm 0{\cdot}0004$ cm^{-1} and $+0{\cdot}0227 \pm 0{\cdot}0009$ cm^{-1}.

The predicted hyperfine structure for 5 837 Å using $I=3/2$ is drawn to scale in the figure. Four components are expected. However, the weakest component lies close to the central component and since the intensity ratio is 1 : 5 the effect of it on the position of the observed central component is less than the experimental error and may be neglected. Thus the splitting of the 7s level is $0{\cdot}0208 \pm 0{\cdot}0004$ cm^{-1} and the splitting of the 6p $^2P_{1/2}$ level $0{\cdot}0227 \pm 0{\cdot}0009$ cm^{-1}.

The photographic plates were not sufficiently sensitive to record the transition $6p\,^2P_{3/2}-7s\,^2S_{1/2}$ (7511 Å) with the 3-metre spectrograph. With the shorter focal length it was necessary to use a narrow slit (0·15 mm) to separate 7511 Å from neighbouring stronger lines of neon. With a discharge current of 10 mA the over-exposed neon lines partly obscured the pattern of 7511 Å. With a current of 15 mA and a 5 cm etalon some poorly resolved structure was observed about a strong central component. From rough measurements the interval factor for the $p_{3/2}$ electron was estimated to be 0·003 cm^{-1}. No accurate measurement of a_{7s} could be obtained from this line.

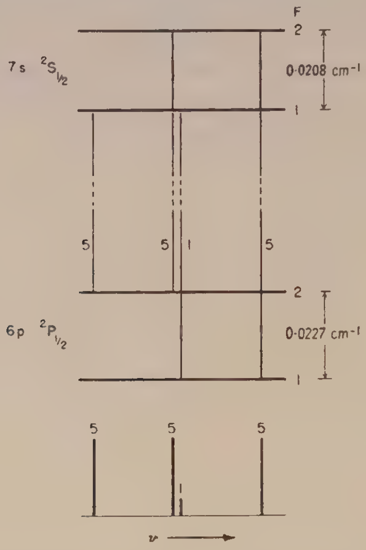

The theoretical pattern of 5 837 Å fitted to the observed components.

The observed structures are summarized in table 1. The theoretical intensities of the components are given in brackets. Experimental errors are given in the text and are the average deviations from the mean.

Table 1

Wavelength (Å)	Transition	Observed components (cm^{-1})
2428	$6s\,^2S_{1/2}-6p\,^2P_{3/2}$	0(5)+0·204(3)
2676	$6s\,^2S_{1/2}-6p\,^2P_{1/2}$	0(5)+0·212(3)
5837	$6p\,^2P_{1/2}-7s\,^2S_{1/2}$	−0·0208(5) 0(5)+0·0227(5)

An allowance must be made for the influence of the unresolved structure of the ^2P levels before the interval factor a_{6s} can be calculated from the observed structure of the resonance lines. This can be done from the theoretical patterns for the lines and using the a_{6p} interval factors obtained from the structures of 5 837 Å and 7511 Å. Thus from 2426 Å, $a_{6s}=0{\cdot}107$ cm^{-1}, while from 2676 Å, $a_{6s}=0{\cdot}102$.

The gyromagnetic ratio can be calculated from the observed interval factor using the Goudsmit (1933) Fermi and Segrè (1933) formula

$$g(I)=\frac{1838\;3n_0^3\,a_{ns}}{8R\alpha^2Z_iZ_0^2\kappa(\tfrac{1}{2},Z_i)(1-d\sigma/dn)}.$$

The value of κ is taken from Goudsmit's paper. The Fermi–Segrè factor $(1-d\sigma/dn)$ is evaluated by the method of Crawford and Schawlow (1949) from the term values given by Platt and Sawyer (1941). A plot of the quantum defect σ against term values indicates that the 6s and 7s levels are not perturbed. Substituting numerical values, we obtain $a_{6s}=1{\cdot}17\,g(I)$, $a_{7s}=0{\cdot}118\,g(I)$. The nuclear magnetic moments (μ^0) evaluated from the observed structure of the 6s and 7s levels are given in table 2.

Table 2

Level	Interval factor	$1-\dfrac{d\sigma}{dn}$	μ^0
6s	0·105	1·424	0·134
7s	0·0105	1·038	0·133
		Average	0·134

The good agreement of the values from the two levels with widely different Fermi–Segrè factors justifies the use of this factor when evaluated by the method of Crawford and Schawlow (1949). It follows that the spectroscopic value of the nuclear magnetic moment is sufficiently accurate to provide information on nuclear structure by comparison with the value from nuclear induction experiments. For elements like gold, which have only one stable isotope, it is not possible to obtain this information from isotope shifts or by comparing ratios of magnetic moments with ratios of hyperfine structure splittings.

The corrections which we shall here apply for the nuclear structure are for the finite size of the nucleus (Rosenthal and Breit 1932) and for the volume distribution of magnetic moment (Bohr and Weisskopf 1950). The corrected moment is given by $\mu=\mu^0\,(1-\delta)(1-\epsilon)$. For an s-electron in gold the charge correction is $1-\delta=0{\cdot}888$ and the magnetic correction $1-\epsilon=1{\cdot}11$ (in the formula of Bohr and Weisskopf, we have used $g_L=1$). Thus the final value of the magnetic moment of gold is $\mu=$ *0·136 nuclear magnetons*.

This result is expected to be accurate to about 6%. In this case the two corrections nearly cancel. It would be interesting to compare this result with a value obtained by the induction method.

The nuclear magnetic moment can also be calculated from the observed structure of the $6p_{1/2}$ level. From the Goudsmit formula, $g(I)=11{\cdot}4\,a_{p_{1/2}}$ and $\mu^0=0{\cdot}195$. This result cannot be expected to be accurate since the 6p levels are probably perturbed. An indication that the 6p levels are perturbed is given by the fact that Z_i calculated from the fine structure doublet separation using the Landé formula is greater than Z. A further indication of perturbation is that the Goudsmit formula predicts a value 9·6 for the ratio $a_{p_{1/2}}/a_{p_{3/2}}$, while the observed ratio 3·6 is much smaller.

Throughout this paper the nuclear spin of ^{197}Au has been assumed to be 3/2 as found by Elliott and Wulf (1939). The observations made during this research are consistent with this value, but no effort was made to confirm it as it appears to be well established.

ACKNOWLEDGMENTS

The author acknowledges the help of Dr. H. Kuhn, under whose direction the research was carried out. Thanks are due to Professor Lord Cherwell for providing the facilities of the Clarendon Laboratory during the tenure of a Postdoctorate Overseas Fellowship awarded by the National Research Council of Canada.

REFERENCES

Bohr, A., and Weisskopf, V. F., 1950, *Phys. Rev.*, **77,** 94.
Crawford, M. F., and Schawlow, A. L., 1949, *Phys. Rev.*, **76,** 1310.
Elliott, R. M., and Wulf, J., 1939, *Phys. Rev.*, **55,** 170.
Fermi, E., and Segrè, E., 1933, *Z. Phys.*, **82,** 729.
Goudsmit, S., 1933, *Phys. Rev.*, **43,** 636.
Kelly, F. M., Richmond, R., and Crawford, M. F., 1950, *Phys. Rev.*, **80,** 295.
Kuhn, H., and Woodgate, G. K., 1951, *Proc. Phys. Soc.* A, **64,** 1090.
Platt, J. R., and Sawyer, R. A., 1941, *Phys. Rev.*, **60,** 866.
Rosenthal, J. E., and Breit, G., 1932, *Phys. Rev.*, **41,** 459.
Schawlow, A. L., Hume, J. N. P., and Crawford, M. F., 1949, *Phys. Rev.*, **76,** 1876.

A Radioactive Isomer of ^{166}Ho

By F. D. S. BUTEMENT
Atomic Energy Research Establishment, Harwell, Berks.

MS. received 20th August 1951, *and in final form 3rd December* 1951

ABSTRACT. Irradiation of holmium with pile neutrons produces, in addition to 27-hour ^{166}Ho, a new long-lived holmium isotope with a half-life greater than 30 years. It is shown that it cannot be ^{167}Ho produced by neutron capture in ^{166}Ho, nor ^{164}Ho produced by a (n, 2n) reaction. It is therefore probably an isomer of the 27-hour ^{166}Ho.

It decays with emission of β-particle groups of energies 0·18, 0·28 and 1·1 MeV, γ-rays of energies 0·830, 0·725, 0·280, 0·212 and (weak) 0·095 MeV, and weak erbium K x-rays.

β–γ and γ–γ coincidence measurements have been made and a decay scheme suggested.

§ 1. INTRODUCTION

Holmium has only one stable isotope of mass-number 165. Its cross section for the thermal (n, γ) reaction is 60 barns, and the product, ^{166}Ho, has a half-life of 27 hours.

If ^{167}Ho has a half-life appreciably greater than that of ^{166}Ho, it should be possible to make it by the process ^{166}Ho (n, γ) ^{167}Ho if holmium is subjected to a long irradiation in a high neutron flux, and the ^{166}Ho activity is then given time to die out. When this experiment was tried, a new long-lived holmium activity was found, although more detailed study showed that it was not ^{167}Ho, but could be an isomer of ^{166}Ho.

§ 2. PREPARATION

A sample of 32 mg of very pure holmium oxide, prepared by the ion-exchange method (Ketelle and Boyd 1947), was irradiated for 20 days in a pile in a neutron flux of 10^{12} cm^{-2} sec^{-1}, and the holmium isolated from slight traces of other rare earth activities by the ion-exchange method.

The elutriant containing the holmium was collected in four fractions, and the decay of the recovered holmium oxide samples followed for one year.

After disappearance of the 27-hour activity there remained a weak long-lived activity which in each sample was accurately proportional to the 27-hour activity at a given time. The long activity was consequently due to holmium, and not a possible contamination, which would not separate in a 'peak' coincident with the holmium (see table 1).

Table 1. Activity of Samples (counts per minute)

	I	II	III	IV
a. After 23 days (total activity)	3806	10174	8010	3062
b. After 150 days (long activity)	651	1682	1350	526
c. Short activity $=a-b$	3155	8492	6660	2536
Ratio c/b	4·85	5·05	4·93	4·82

The long activity obtained was about 2000 beta-disintegrations per minute per milligram of oxide.

It showed no measurable decay in one year: since a decay of 2% could have been detected, it is deduced that the half-life is greater than 30 years.

§ 3. MASS ASSIGNMENT

The possibility that the long activity was ^{167}Ho produced by successive capture of two neutrons by ^{165}Ho was investigated by irradiating samples of holmium oxide in the same experimental hole in the pile, at constant pile power, for different periods t hours. If $\lambda=0{\cdot}0257\,\mathrm{hr}^{-1}$ is the decay constant of 27-hour ^{166}Ho, then the specific activity of ^{167}Ho will be proportional to $\lambda t+\exp(-\lambda t)-1$. If, however, the long activity is produced by single neutron capture (i.e. a ^{166}Ho isomer) or by a fast (n, 2n) reaction (i.e. ^{164}Ho), then the specific activity will be simply proportional to t.

Three small samples of holmium oxide, about one milligram each, were irradiated for periods of 7, 17 and 34·5 hours, the irradiations ending simultaneously.

Table 2

	Sample		
	I	II	III
a. Irradiation time, t hours	7	17	34·5
b. 27-hr. activity (counts per minute)	8091	17250	40688
c. $\lambda t/\{1-\exp(-\lambda t)\}$	1·092	1·234	1·508
d. Corrected 27-hr. activity $=bc$	8835	21287	61358
e. Long activity (counts per minute)	156	353	1009
f. Long activity/27-hr. activity $=e/d$	0·0177	0·0166	0·0164
Relative f (sample I $=1{\cdot}00$)	1·00	0·94	0·93
g. $\{\lambda t+\exp(-\lambda t)-1\}/t$	0·00217	0·00488	0·00866
Relative g (sample I $=1{\cdot}00$)	1·00	2·25	3·99

The holmium was chemically purified with hold-back carriers, and the activities of the 27-hour period determined 19 days later, when its intensity was convenient for counting. These activities, multiplied by $\lambda t/\{1-\exp(-\lambda t)\}$ to correct for decay during irradiation, give the relative amounts of holmium in the samples. The residual long activities were subsequently measured. The results are given in table 2. The ratio of long to short activities is independent of t, so that the long activity cannot be ^{167}Ho or the ratio would vary as $\{\lambda t+\exp(-\lambda t)-1\}/t$.

The method does not require a uniform distribution of samples on the counting discs, provided that, as in this case, thin samples are used, or any knowledge of the weight of holmium, the neutron flux or the geometrical counting efficiency.

To investigate the possibility that the long activity was an isomer of the known 35-minute ^{164}Ho, produced by a fast (n, 2n) reaction, one sample of holmium oxide was irradiated for 5 days in a normal experimental hole in the pile, and another sample, screened with sufficient boron to cut off virtually all slow neutrons, was simultaneously irradiated inside a hollow uranium slug, thus receiving a much higher flux of fast neutrons than the first sample, and a lower flux of slow neutrons. The ratio of 27-hour to long activities was, however, the same, within 10%, so that the long activity cannot be ^{164}Ho.

Leland (1950) has shown that, apart from ^{165}Ho, there is no stable holmium isotope of abundance greater than 0·04%, so that, unless the long activity is due to neutron capture by a very scarce undiscovered isotope, it is, presumably, an isomer of the 27-hour ^{166}Ho. The 27-hour activity decays with the emission of γ-rays of energies 80 kev and 1·2 Mev (Grant and Hill 1949). Coincidence absorption measurements were made which showed that both γ-rays were in coincidence with β-particles, so that the long isomer is not produced by a branching decay by γ-ray emission from the 27-hour isomer.

§ 4. RADIATION EMITTED

The long activity decayed with emission of β-particles, the negative sign being checked by magnetic deflection. Absorption measurements in aluminium (fig. 1) showed, in addition to γ-rays, a hard β-component (1·1 Mev by the Feather method) accounting for about 8% of the disintegrations, and one or more soft β-particles, of limiting range around 70 mg cm^{-2}, accounting for the remaining 92% of the disintegrations. Correction was made for absorption in the counter window.

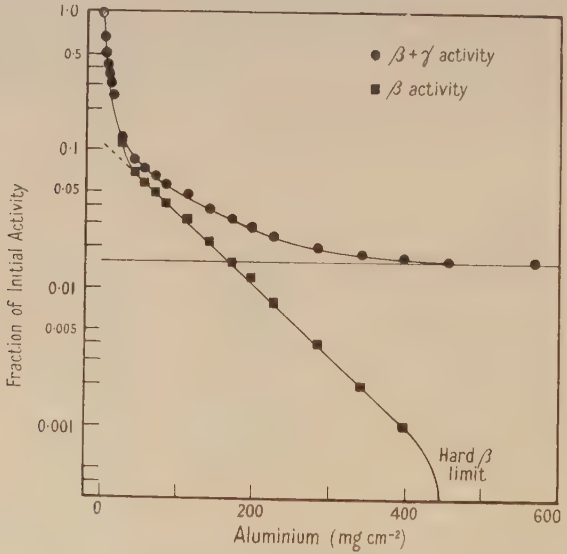

Fig. 1. Absorption of radiation from ^{166}Ho isomer.

The γ-radiation was studied by absorption measurements in copper and lead, using a scintillation counter. It showed two components of energies 0·2 and 0·8 Mev, and no detectable softer radiation.

More detailed measurements were made by Mr. R. B. Owen by measurement of the photo-electron peaks on a γ-scintillation spectrometer, and showed γ-energies of 0·830, 0·725, 0·280, 0·212, 0·095 (very weak) and approximately 0·057 (very weak) Mev. The last component is explicable as the K x-rays of erbium, produced as a consequence of a very small degree of internal conversion.

§ 5. COINCIDENCE MEASUREMENTS

β–γ coincidence measurements were made, using a scintillation counter and a Geiger counter. For γ–γ coincidences the latter was used as a low efficiency γ-counter.

(i) *β-coincidences with* 0·83 *and* 0·725 *Mev γ-rays.* The γ-radiation was filtered through 10·6 g cm^{-2} of lead, which virtually transmits only the 0·83 and 0·725 Mev components. The β–γ coincidence rate was measured with varying thicknesses of aluminium absorber on the β side. After subtraction of a small γ–γ coincidence background the graph of coincidence rate against absorber thickness showed that the limiting β-energy was 0·28 Mev (71 mg cm^{-2} Al) and the shape of the graph clearly indicated that about half the total β-particles were due to another group of limiting energy about 0·18 Mev. The ratio of β-coincidences to γ-counts was almost exactly equal to the known geometrical efficiency of the β-counter, so that the ratio of total hard γ-rays (0·83 + 0·725 Mev) to total soft β-particles (0·18 + 0·28 Mev) is unity.

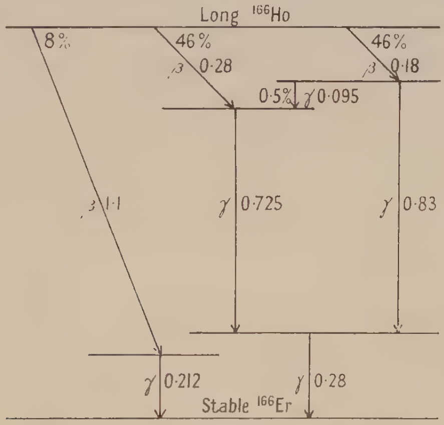

Fig. 2. Decay scheme of ^{166}Ho isomer. Energies in Mev.

(ii) *γ coincidences with* 1·1 *Mev β-particles.* The β-radiation was filtered through 71 mg cm^{-2} of aluminium so as to transmit only β-particles of energy above 0·28 Mev. The coincidence rate was measured with varying thicknesses of lead on the γ side. Since part of the coincidences are γ–γ, a similar run was made with 0·5 gm cm^{-2} of aluminium on the β side, to cut out all β-particles but transmit virtually all γ-rays. The differences between the two sets of results gave the true hard β–γ coincidences, which showed that the 1·1 Mev β was in coincidence with a γ-ray of 0·21 Mev, with a β/γ ratio of about unity.

(iii) *γ–γ coincidences.* The Geiger counter was screened with 10·6 g cm^{-2} of lead, so that it counted only the 0·83 and 0·725 MeV γ-rays. Varying thicknesses of lead were interposed on the scintillation counter side, and the γ–γ coincidence rates measured. The results showed that the hard γ group is in coincidence with a 0·28 MeV γ-ray. The ratio of coincidences to total hard γ-rays (0·83 + 0·725 MeV) was almost exactly equal to the known efficiency of the scintillation counter for 0·28 MeV γ-rays. The spectrometer measurements had shown that the 0·83 and 0·725 MeV γ-rays were of about equal intensity, consequently each is in coincidence with a 0·28 MeV γ-quantum. The 0·095 and 0·057 MeV electromagnetic radiations, and the presumed conversion electrons, were all of such low intensity as not to interfere significantly with the above measurements.

A suggested decay scheme which is consistent with the measured energies and intensities of the radiations is given in fig. 2. The small discrepancies between the total energies of the various decay routes are within the limits of experimental error.

0·18 MeV β followed by 0·83 and 0·28 MeV gammas.	Total 1·29 MeV.
0·28 MeV β followed by 0·725 and 0·28 MeV gammas.	Total 1·29 MeV.
1·1 MeV β followed by 0·212 MeV gamma.	Total 1·31 MeV.

ACKNOWLEDGMENTS

Acknowledgment is made to Mr. R. B. Owen for carrying out measurements of γ-ray energies, and to the Director, Atomic Energy Research Establishment, for permission to publish these results.

This paper was read at the XIIth International Congress of Pure and Applied Chemistry, New York, 10th–13th September 1951.

REFERENCES

Grant, P. J., and Hill, J. M., 1949, *Nature, Lond.*, **163**, 524.
Ketelle, B. H., and Boyd, G. E., 1947, *J. Amer. Chem. Soc.*, **69**, 2800.
Leland, W. T., 1950, *Phys. Rev.*, **77**, 634.

The Structure of Extensive Showers

By I. D. CAMPBELL* and J. R. PRESCOTT†
Physics Department, Melbourne University, Australia

MS. received 15*th October* 1951

ABSTRACT. The form of the structure function of extensive showers at small distances from the core has been investigated by observations of coincidences between ionization chambers at sea level.

The observations considered are the decoherence curve and the burst-ratio distribution. Both sets of results indicate a structure function that varies as $1/r^{0 \cdot 8}$ for small r (less than 0·04 lateral shower units at sea level) as opposed to the well-known Moliere function which behaves as $1/r$ for small r. A modified structure function is given in tabular form. The advantages of the burst-ratio distribution method of studying the structure function are discussed.

---

[*] Now with the Commonwealth of Australia Department of Supply, at the Physics Department, Imperial College, London.

[†] Now at the Clarendon Laboratory, Oxford.

§ 1. INTRODUCTION

The study of the lateral structure of extensive showers is one that has received some attention since their discovery. Initially the interest centred in the information that could be derived about multiple scattering processes of electrons and photons at high energies, but more recently it has shifted to questions of the origin of the showers and the way in which the nature of the initiating process will be reflected in the structure of the shower (see, for example, Cocconi, Tongiorgi and Greisen 1949). In the most favoured current theory of the origin of extensive showers, they are produced in high energy nuclear interactions through the intermediary of one or more short-lived neutral mesons. Recent experiments (Williams 1948, Blatt 1949, Cocconi, Tongiorgi and Greisen 1949, Singer 1951) have looked for a multiple core structure in showers, which would be expected to give information about the angular distribution at the point of production of the neutral mesons, but the experiments indicate a shower with a unique core. A knowledge of the form of the structure function is necessary for the interpretation of Geiger counter observations.

Moliere (1946) has calculated the form of the structure function of extensive showers assuming that there is a single core and that the lateral distribution of particles is governed by multiple coulomb scattering of electrons. The form of the structure function for large distances from the core has also been calculated by Eyges (1948) and by Eyges and Fernbach (1951) down to moderate distances. A convenient analytic approximation to the Moliere function has been worked out by Bethe (1948). The form of the Moliere function has been verified experimentally by Williams (1948) whose observations cover the range from about 3 to 20 m from the core, and by Cocconi, Tongiorgi and Greisen (1949) who find good agreement with Moliere at distances from 5 to 200 m. The Moliere structure function is widely used in interpreting experimental results on extensive showers.

The present experiments were designed to give information on shower structure, particularly at small distances, and were performed between December 1947 and May 1950. They were interrupted by the destruction of the apparatus by fire in October 1948, and advantage was taken of this to publish some preliminary results (Prescott and Mohr 1949 a, b; these papers will be jointly referred to as 'PM'). The present paper contains some of the results of these papers together with much new material.

§ 2. APPARATUS

The apparatus consisted of two ionization chambers in coincidence and a system of Geiger counters.

The ionization chambers (PM, b) were steel cylinders of wall thickness 0·175 cm and contained commercial nitrogen at a pressure of 39 atmospheres. The effective length of the chamber was 57·6 cm and the effective diameter 8·8 cm. Positive ion collection was employed, the collection time being 0·6 sec. Recording was by means of magic eye tuning indicators (Montgomery and Montgomery 1939) driven by d.c. amplifiers. Images of the shadow edge of the magic eyes were thrown in juxtaposition on 35 mm film moving at 2mm/min behind a slit of width 0·00075 in. Resolving time for coincidences was 0·6 sec.

During the second half of the experiments, a system of Geiger counters was employed in conjunction with the ionization chambers. A vertical triangular arrangement of Geiger counters either in three- or four-fold coincidence was carried on a light aluminium framework immediately over one of the ionization chambers (known as chamber A). This system worked as a 'Master Group' (known as M). When it was discharged, the discharge or otherwise of four 'analysing counters' spaced at intervals up to 5 m from M was recorded on the 35-mm film. All counters were 30 cm long and 2·7 cm in diameter.

Bridge *et al.* (1948) showed that the greater part of the bursts in an ionization chamber are due to fragments from nuclear disintegrations taking place in the walls. A burst in the present chamber A, produced by a shower, could be distinguished from such a disintegration burst by the fact that M was discharged simultaneously. The efficiency of M for detecting showers of the minimum density used in the analysis of the records (600 particles per m^2) was 99%. Where the chambers were shielded with lead, a correction was necessary for the loss of efficiency of the master group, for the addition of lead increases the effective density of the shower, so that showers of smaller density are now detected. The efficiency of M falls off as the particle density decreases and a correction is therefore necessary for coincidences in which the burst size is small. This correction was made by assuming most shower particles to have an energy of about 100 Mev (of the order of the critical energy for air) and finding the expected multiplication in lead of such particles from the theoretical data of Bhabha and Chakrabarty (1948). The maximum correction necessary to the integral rates was about 10%.

The ionization chambers were calibrated by making small changes in the high tension voltage. In order to correlate burst size with shower density, it is necessary to assume a value of specific ionization for the shower particles. The value adopted was 71 ion pairs cm^{-1} atm^{-1} regardless of recombination and including secondary ionization (Prescott 1949), and 63% saturation (Lea 1934, Cox 1934) giving an effective specific ionization of 45 ion pairs cm^{-1}. A burst of $4{\cdot}2 \times 10^5$ ion pairs in an unshielded chamber corresponded to a shower density of 600 particles per m^2 and this was the minimum burst size used in the analysis, although in most cases measurements were carried to smaller burst sizes.

The apparatus was located beneath the roof of a hut in the grounds of the University of Melbourne (altitude 50 m). Apart from a few trees the site was clear from about 10° above the horizon. The roof of the hut consisted of 2·5 g cm^{-2} of asbestos. Corrections were applied for multiplication, both in this roof and in the wall of the chamber. For extensive shower particles of energy 100 Mev, the combined multiplication of roof and chamber walls was 1·19 (Williams 1948). All shower densities given in this paper are equivalent shower densities in the open air.

§ 3. RESULTS

3.1. *Decoherence Curves and the Structure Function*

Because of the density gradient across a shower, the coincidence rate between two Geiger counters or two ionization chambers increases as the separation between them is decreased. The function, coincidence rate against separation, is generally known as a decoherence curve and can be related more or less directly to the structure function. Blatt (1949) has pointed out the advantages over Geiger counters of using ionization chambers for the study of the structure of extensive showers. An ionization chamber decoherence curve gives the coincidence rate for bursts greater than a given size in *both* chambers, as a function of separation.

In table 1 ionization chamber data are collected. In columns 5–9 are given the rates per hour of coincidences between the two ionization chambers in which burst size was greater than $4{\cdot}2 \times 10^5$ ion pairs in both; the error limits (as elsewhere in the table) are calculated on the number of events recorded in each instance. Accidental coincidences have been allowed for where necessary. Readings were obtained at five chamber separations with shielding consisting of 0, 0·6 and 1·2 cm effective thickness of lead. This shielding was in the form of hemicylindrical caps 0·5 cm thick, fitting over and extending one inch beyond the end of the chamber and one inch below the centre on either side.

In column 2 are given the integral single chamber rates for all bursts; this includes a large contribution from disintegrations*. In column 3 are given data for coincidences between the Geiger counter system and the ionization chambers, i.e. the rate of bursts greater than $4{\cdot}2 \times 10^5$ ion pairs in a *single* ionization chamber (chamber A) accompanied by a discharge of M (cf. §2). This certainly includes all the single chamber bursts due to extensive showers but may also include some due to other agencies, such as narrow showers. In order to eliminate the latter an additional requirement was imposed, viz. that *at least one* of the analysing counters at 3 and 5 m should also be discharged. On the surface this does not seem a reliable criterion, since the total efficiency of a counter at 5 m for showers of all densities which also discharge the master group is only about 45%. However, if we impose the additional condition that the shower must have a density greater than 600 particles per m² at chamber A then the efficiency of detection of the 5 m counter becomes 89% and of the counter at 3 m 92·5%. The probability that *both* counters will be missed is therefore only 0·009. Thus we can identify over 99% of the bursts due to extensive showers. The above figures were obtained numerically in the usual way, by a double integration over the plane and the number distribution of the showers (Ise and Fretter 1949). Instead of integrating from zero to infinity in both cases, however, the requirement that the particle density at A must exceed 600 particles per m² is introduced by making A the origin and integrating for r only within the circle of radius r_0 given by $600 = Nf(r_0)$, where $f(r)$ is the shower structure function. The rates for extensive shower bursts identified in the above manner are given in column 4 of table 1.

Table 1. Coincidence Data—Rates per hour

(Bursts greater than $4{\cdot}2 \times 10^5$ ion pairs)

1	2	3	4	5	6	7	8	9
	Single chamber bursts			Chamber coincidences—Separation (metres)				
ielding n Pb)	All bursts	A+Master	Extensive showers	0·16 m	0·32 m	1·0 m	3·0 m	5·0 m
Nil	7·5±0·2	0·155±0·01	0·105±0·01	0·10±0·02	0·07±0·02			0·056±0·01
0·61	16·4±0·2	0·49 ±0·04	0·21 ±0·03		0·16±0·03			0·10 ±0·02
1·2	27±0·1	0·58 ±0·07	0·27 ±0·05		0·26±0·04	0·21±0·05	0·24±0·05	0·20 ±0·03

---

* These are higher than the corresponding rates given in PM. In the first part of the observations, single chamber measurements were made only down to burst sizes corresponding to densities of 600 particles per m². The new apparatus was run at greater sensitivity and measurement of burst sizes pushed to smaller shower densities. It appears that, in the first series of observations, an appreciable fraction of the single chamber bursts was being lost in the statistical background of general cosmic-ray ionization. Coincident bursts were, however, much easier to identify and it is considered that none of these could have been missed.

The data of table 1 are shown in fig. 1 in the form of decoherence curves corresponding to 0, 0·6 and 1·2 cm of lead shielding. A logarithmic scale is used for the ordinate, and a square root scale for the abscissa. Points at zero separation are the rates for extensive shower bursts in a single chamber. This can be validly interpreted as the chamber coincidence rate at zero separation, for if we imagine one chamber to coincide exactly with the other, both will record the same burst rate and the coincidence rate will be that for one chamber alone.

The curves for each lead thickness have been drawn geometrically similar to show that there is no significant variation with the amount of shielding material. In the following discussion therefore, the data for all lead thicknesses have been lumped together to improve the statistics.

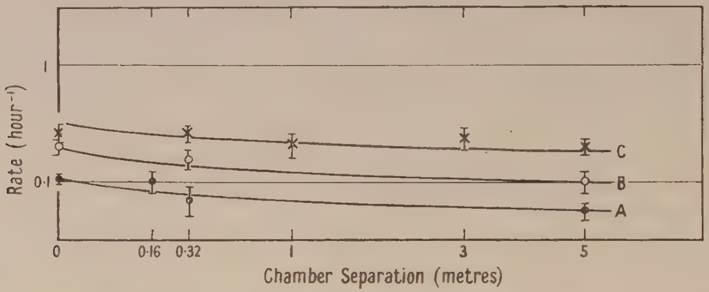

Fig. 1. Ionization chamber decoherence curves for unshielded chambers (A), for chambers shielded with 0·6 cm of lead (B) and 1·2 cm of lead (C).

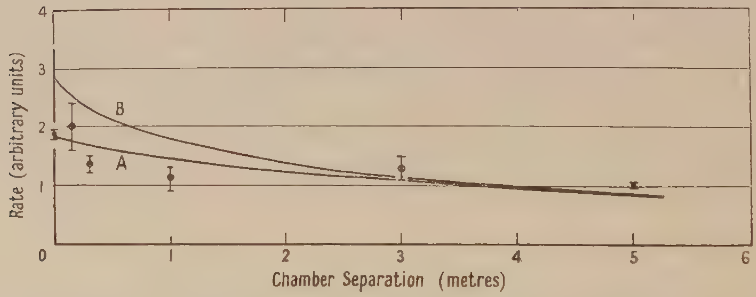

Fig. 2. Comparison of experimental results with theoretical decoherence curves. Curve B assumes the Moliere shower structure function, curve A the modified structure function discussed in the text.

Early theoretical attempts to determine the form of the ion chamber decoherence curve were made by Euler (1940) and Wolfenstein (1945). The best calculation of the decoherence curve is that of Blatt (1949) who assumed the Moliere structure function. His calculations were set up to interpret the data of Williams (1948) and he was not concerned with predicting an absolute rate. They predict a sharp increase in the coincidence rate at small chamber separations.

In fig. 2 the data of the present experiment are compared with a theoretical curve (B) of Blatt (1949, fig. 5). No details of the theoretical treatment will be given here as it is fully described by Blatt (§ 5). Blatt's figures have been reduced to sea level by taking the appropriate value (74 m) for the characteristic lateral shower unit of length, in which chamber separations must be measured.

Blatt's curve includes a correction for the finite size of the chambers used by Williams (1948). The chambers used in the present experiments were almost the same geometrically, so that much the same correction will apply. It is clear that Blatt's curve is too steep. This would result from the use of a structure function that varies too steeply near the origin. Now, the Moliere function for describing the shower structure, which predicts a density dependence as $1/r$ near the origin, applies strictly only to showers at maximum development. For showers past maximum development (which will include the majority of showers at sea level) the structure function varies as $1/r^{2-s}$ near the origin (Blatt 1949), where s is greater than unity and increases as the shower becomes older. There is, of course, also the further possibility that the Moliere function is actually wrong at small separations as, in fact, suggested by Blatt.

We have therefore repeated Blatt's calculation in detail, the only difference being the use of a structure function varying as $1/r^{0\cdot8}$ near the origin (i.e. $s=1\cdot2$);* the result of the new calculation is compared with the experimental results in fig. 2, curve A. The new calculation follows the form of Blatt's curve at large separations (as it must) but is much flatter at small separations. Agreement between theory and experiment is now much better.

However, as Blatt points out, decoherence curve measurements are not sufficiently sensitive to the form of the structure function to give *detailed* information about it. In addition the form of the decoherence curve is sensitive to other factors, for example, the exponent γ in the shower number–distribution $S(N)=\sigma N^{-\gamma}$, where $S(N)$ is the number of showers containing more than N particles. No attempt was made therefore to obtain a better fit to the experimental results. Probably all that can be concluded from fig. 2 is that the structure function at sea level has an r-dependence at small distances nearer to $1/r^{0\cdot8}$ than $1/r$. A better method of checking the structure function is described in the next section.

3.2. *The Burst-Ratio Distribution and the Structure Function*

Disadvantages of the use of the decoherence curve for the determination of the form of the structure function of an extensive shower have been mentioned in the previous section. Blatt (1949) points out that the structure function is essentially proportional to the second derivative of the decoherence curve. Hence a prohibitively long time is needed to obtain good statistics. Further, the decoherence curve depends on γ, the exponent of the shower-size distribution, which must be known before anything may be deduced about the structure function. Indeed, as Blatt's relation (6.2) shows, the curve is as sensitive to changes in γ as in s. A further difficulty is introduced by the fact that coincidences between chambers at the larger separations, say greater than 0·05 lateral shower units, are due to a shower-size distribution with γ about 1·8 or greater, i.e. to large showers, while for small separations where contributions from small showers predominate γ is about 1·5.

Most of the above difficulties may be avoided, and better information about the structure function deduced, by the use of a burst-ratio distribution. We form the ratios λ of the pairs of coincident bursts observed in two chambers at a fixed separation (taking λ always greater than unity) and construct the integral distribution of these ratios. Such a distribution for 53 coincidences in 946 hours at 5 m separation obtained in the present experiments is plotted in fig. 3 (*a*) on a logarithmic scale. It is seen to be approximately a straight line of slope $2{\cdot}6 \pm 0{\cdot}3$, that is, the distribution follows a power law.

---

* The method of constructing this function and a table of values is given in the Appendix.

We now derive a theoretical expression for the burst-ratio distribution. If a shower is to give a burst-ratio greater than or equal to λ, its core must fall within a region $D(\lambda)$ surrounding one or other of the chambers; since the system is symmetrical, we need consider one chamber only. Assuming similarity of structure function for all showers, $D(\lambda)$ is independent of the shower size N but depends strongly on the form of the structure function (see Williams 1948, fig. 11, for such a set of regions). Consider a chamber A at $\xi = -a$ and another B at $\xi = +a$. If a shower core falls in the right half-plane, then the burst in B must be greater than in A. If both chambers are biased to record a minimum shower density ρ, then, for a coincidence we require: $Nf(r) > \rho$ where N is the shower size, r is the distance in metres of the shower core from A and $f(r)$ is the structure function.

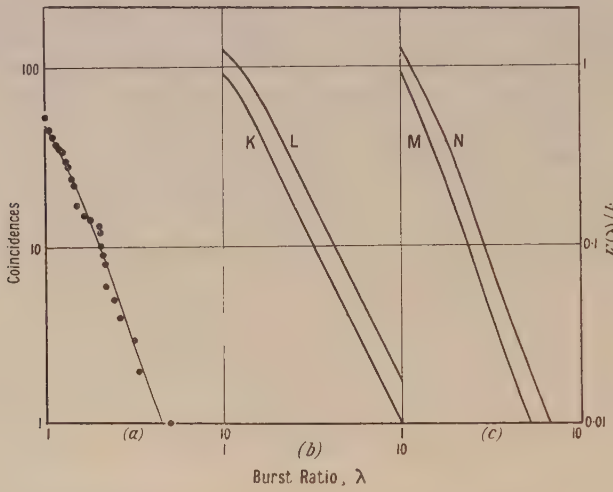

Fig. 3. (*a*) Experimental burst-ratio distribution. (*b*) Theoretical burst-ratio distributions assuming the Moliere structure function; curves K and L correspond to values of γ of 1·5 and 1·8 respectively. (*c*) Theoretical burst-ratio distributions assuming the modified structure function; curves M and N correspond to values of γ of 1·5 and 1·8 respectively.

If $S(N)$ is the number of showers per m² per hour of size greater than N, then the number of showers whose cores fall in a particular region $D(\lambda)$ about B (and hence give a burst-ratio greater than λ) will be:

$$\iint_{D(\lambda)} S[\rho/f(r)]\, d\xi\, d\eta. \qquad \ldots\ldots(3.1)$$

Now let us take $S(N) = \sigma N^{-\gamma}$ where σ and γ are constants. We obtain

$$F(\lambda) = 2\sigma\rho^{-\gamma} \iint_{D(\lambda)} [f(r)]^{\gamma}\, d\xi\, d\eta \qquad \ldots\ldots(3.2)$$

where the factor 2 is introduced to allow for the interchange of the chamber A with chamber B. $F(\lambda)$ is the required burst-ratio distribution.

The form of the above expression for $F(\lambda)$ was evaluated numerically for values of γ of 1·5 and 1·8 using Bethe's analytic approximation to the Moliere structure function. This can be expressed in the form

$$f(r) = (0{\cdot}454/r_1^2)\phi_1(x) \qquad \ldots\ldots(3.3)$$

where x is measured in shower units, i.e. in units of r_1 (74 m at sea level). The function behaves as $1/x$ for small x. Inserting (3.3) in (3.2) we have:

$$F(\lambda)=\frac{k}{r_1^2}\iint_{D(\lambda)}[\phi_1(x)]^\gamma \, d\xi \, d\eta \qquad \ldots\ldots(3.4)$$

where k is a constant that is independent of the form of the structure function. The function $F(\lambda)/k$ is plotted in fig. 3 (*b*), curves K and L, which correspond respectively to values of γ of 1·5 and 1·8.

Two observations are noteworthy: apart from a multiplying constant, the curves are almost identical except for λ near unity, viz. they are both straight lines of slope 2; and the calculated curves do not agree with the experimental results in fig. 3 (*a*).

The first of these facts suggests that the form of $F(\lambda)$ is almost independent of γ, a rather surprising result and one that we have not been able to establish analytically except for the asymptotic case of large λ. For large λ, the regions $D(\lambda)$ become approximately circles about chamber B. Since the distances from B are small we can relate the radius r' of a circle for a particular λ by:

$$\lambda=f(r')/f(r)\simeq(r_1/r')/\phi(2a/r_1) \qquad \ldots\ldots(3.5)$$

where we have used the approximation to the Moliere structure function for small radii. $F(\lambda)$ then becomes

$$F(\lambda)=k\pi[\phi_1(2a/r_1)]^{\gamma-2}\lambda^{-2} \qquad \ldots\ldots(3.6)$$

where k is the same constant as in relation (3.4). The exponent of the distribution is seen to be -2, which is the value obtained, even for quite small λ, by the numerical calculation.

If we consider a structure function that behaves as $1/r^{2-s}$ for small r, we obtain for large λ

$$F(\lambda)\sim\lambda^{2/(s-2)}. \qquad \ldots\ldots(3.7)$$

The importance of the expressions (3.6) and (3.7) is that (at least for large λ) the slope of $F(\lambda)$ depends only on the structure function and not on the shower distribution, i.e. on s but not γ. The numerical calculation strongly suggests that the same applies, at least approximately, for small λ also. We feel that this property of the burst-ratio distribution gives it marked superiority over the decoherence curve method for the interpretation of shower structure.

The fact that the experimental distribution has a slope of about 2·5 leads, from expression (3·7), to consideration of a structure function of the form $1/r^{0\cdot 8}$ for small r, i.e. $s=1\cdot 2$. A structure function of this form was therefore constructed and the calculations repeated. The method of construction of this function and a table of values is given in the Appendix. If we denote the new structure function by

$$f_{1\cdot 2}(r)=(0\cdot 457/r_1^2)\phi_{1\cdot 2}(x) \qquad \ldots\ldots(3.8)$$

then expression (3.4) becomes

$$F_{1\cdot 2}(\lambda)=\frac{k_{1\cdot 2}}{r_1^2}\iint_{D_{1\cdot 2}(\lambda)}[\phi_{1\cdot 2}(x)]^\gamma \, d\xi \, d\eta. \qquad \ldots\ldots(3.9)$$

The values of $F_{1\cdot 2}(\lambda)/k_{1\cdot 2}$ are plotted in fig. 3 (*c*), curves M and N. As before, the curves for the two values of γ are the same shape. Curve N ($\gamma=1\cdot 8$) is fitted to the experimental results in fig. 3 (*a*). It is seen that the modification of the structure function for distances less than 3 or 4 m now gives agreement with experimental results. Despite the poor statistics, it appears that the structure function is in fact flatter than that given by Moliere, being more like $1/r^{0\cdot 8}$

than $1/r$ for small distances, which is the same conclusion reached from the decoherence curve observations.

The finite size of the ionization chamber modifies the function $F(\lambda)$ for large λ. Without this modification, if a shower falls exactly on one chamber, an infinite burst is recorded by that chamber, and hence an infinite burst-ratio obtained. The chambers used can be regarded in plan as rectangles of length $2L=57{\cdot}6$ cm and width $2m=8{\cdot}8$ cm. To find the maximum λ, we must evaluate relation (3.5), averaging the numerator over chamber B:

$$\lambda_{\max}=\frac{1}{Lmf(2a)}\int_0^L\int_0^m f(r')\,d\xi\,d\eta.$$

The Moliere structure function gives $\lambda_{\max}=68$, and the modified structure function $\lambda_{\max}=28$. $F(\lambda)$ approaches the ordinate $\lambda_{\max}$ asymptotically. The correction for finite size is negligible for λ less than about 7 and in any case the correction applies only to about 0·5% of all the burst ratios.

§4. DISCUSSION AND SUMMARY

The arguments of the previous sections can be summarized as follows. The form of the decoherence curve and the burst-ratio distribution are not consistent with the Moliere structure function. In short, the results favour a structure function that varies less steeply than the Moliere function. An identical conclusion has been reached by Blatt (1949) from his analysis of the decoherence curve data collected by Williams (1948). This could be due to flattening of the structure function for older showers, or Moliere's calculation of the structure function itself might be in error. A further alternative, put forward by Blatt, that a flatter structure function results from a multicore structure of the shower has since been shown not to hold (Williams 1948, Cocconi, Tongiorgi and Greisen 1949, Singer 1951).

In the present paper, a structure function is suggested which varies as $1/r^{0{\cdot}8}$ for r less than 0·04 shower units, as opposed to a $1/r$ dependence for the Moliere function, and then follows Bethe's approximation to the Moliere function for larger values of r. This modified function gives better agreement with both the decoherence curve data and the burst-ratio distribution; in fact, the modified decoherence curve also fits the experimental points of Williams (1948) better than the calculated curve based on the Moliere function.

It may be pointed out that the modified structure function actually gives the effective structure function averaged over showers of all ages; and it is not necessarily the *only* structure function that will give agreement with the experimental data; in particular, the present results are very insensitive to the precise form of the structure function for values of r greater than about 0·5 lateral shower unit. In this region, the Moliere function differs from the Bethe approximation and the recent data of Eyges and Fernbach (1951) by as much as a factor of two. It also seems likely that a structure function that is flatter than the Moliere function at small distances will be flatter at larger distances, so that the true structure function will not vary so abruptly in the region of 0·04 lateral shower unit as does the present one. This, however, cannot affect the validity of the arguments presented here and they indicate a $1/r^{0{\cdot}8}$ dependence for small r. It would, in fact, improve the agreement between theory and experiment in the case of the decoherence curves.

The burst-ratio distribution, discussed here for the first time, is very sensitive to the form of the structure function at small distances from the core and has the very great advantage of being almost independent of the precise form of the number-distribution of the extensive showers. (For the same reason, it is fruitless to attempt to make any estimate of the absolute rate of extensive showers from the burst-ratio distribution, unless the form of the number-distribution is known with some precision from other observations.) On the basis of the burst-ratio distribution one can estimate that the form of the structure function given here is valid down to about 0·01 shower units (about 0·75 m at sea level).

ACKNOWLEDGMENTS

The authors are indebted to Professor L. H. Martin and Associate-Professor C. B. O. Mohr for their constant interest in the progress of the work, and to Miss N. G. Digby for assistance in carrying out the observations.

The work described was performed as part of the joint programme of the Nuclear Physics Section of the Commonwealth Scientific and Industrial Research Organization and the Physics Department, University of Melbourne, Australia.

APPENDIX

THE MODIFIED STRUCTURE FUNCTION

The modified structure function is based on Bethe's analytical approximation to the Moliere structure function $f(r)=(0{\cdot}454/r_1^2)\phi_1(x)$ where $f(r)$ is the density in particles per m^2, r_1 is the lateral shower unit in metres and x is measured in shower units. $\phi_1(x)=x^{-1}(1+4x)\exp(-4x^{2/3})$. This behaves as $1/x$ near the origin.

The slope of the burst-ratio distribution, discussed in § (3.2), suggests that the structure function should show a behaviour like $1/x^{0{\cdot}8}$ near the origin. Now the Moliere function has been verified down to about 0·04 shower unit (3 m at sea level) (Williams 1948, Cocconi, Tongiorgi and Greisen 1949) and to 2 shower units by Cocconi, Tongiorgi and Greisen (1949). To obtain the modified structure function, therefore, we assume the validity of the ϕ part of the Moliere function for large distances from the core but join it smoothly between $x=0{\cdot}03$ and 0·07 to the function $\phi(x)=1{\cdot}25/x^{0{\cdot}8}$, giving the required slower variation at small values of x, less than or equal to 0·03.

After renormalization, the complete function is designated $f_{1{\cdot}2}(x)$:

$$f_{1{\cdot}2}(x)=(0{\cdot}457/r_1^2)\phi_{1{\cdot}2}(x).$$

Table 2. Values of the Function $\phi_{1{\cdot}2}(x)$.

x	$\phi_{1{\cdot}2}(x)$	x	$\phi_{1{\cdot}2}(x)$	x	$\phi_{1{\cdot}2}(x)$
0·01	49·4	0·07	9·26	0·50	0·475
0·02	28·6	0·08	7·88	0·70	0·23
0·03	20·7	0·09	6·78	1·0	$9{\cdot}15\times10^{-2}$
0·04	16·1	0·10	5·93	2·0	$7{\cdot}76\times10^{-3}$
0·05	13·4	0·20	2·29	3·0	$1{\cdot}80\times10^{-3}$
0·06	11·2	0·30	1·21	4·0	$5{\cdot}70\times10^{-4}$

REFERENCES

Bethe, H., 1948, quoted by Williams (1948).
Bhabha, H. J., and Chakrabarty, S. K., 1948, *Phys. Rev.*, **74**, 1352.
Blatt, J. M., 1949, *Phys. Rev.*, **75**, 1584.
Bridge, H. S., Hazen, W. E., Rossi, B., and Williams, R., 1948, *Phys. Rev.*, **74**, 1083.
Cocconi, G., Tongiorgi, V. C., and Greisen, K., 1949, *Phys. Rev.*, **76**, 1020.
Cox, E. F., 1934, *Phys. Rev.*, **45**, 503.
Euler, H., 1940, *Z. Phys.*, **116**, 73.
Eyges, L., 1948, *Phys. Rev.*, **74**, 1801.
Eyges, L., and Fernbach, S., 1951, *Phys. Rev.*, **82**, 23.
Ise, J., and Fretter, W. B., 1949, *Phys. Rev.*, **76**, 933.
Lea, D. E., 1934, *Proc. Camb. Phil. Soc.*, **30**, 80.
Moliere, G., 1946, *Cosmic Radiation*, Chap. III, Ed. Heisenberg, W. (New York : Dover Publications).
Montgomery, C. G., and Montgomery, D. D., 1939, *Rev. Sci. Instrum.* **10**, 350.
Prescott, J. R., 1949, *Nature, Lond.*, **164**, 756.
Prescott, J. R. and Mohr, C. B. O., 1949 a, *Nature, Lond.*, **164**, 21; 1949 b, *Aust. J. Sci. Res.* A, **2**, 184.
Singer, S. F., 1951, *Phys. Rev.*, **81**, 579.
Williams, R., 1948, *Phys. Rev.*, **74**, 1689.
Wolfenstein, L., 1945, *Phys. Rev.*, **67**, 238.

Investigations of Atomic and Molecular Absorption Spectra I—General Features. II—Schumann Region Absorption Spectrum of Gallium Vapour

By W. R. S. GARTON
Department of Astrophysics, Imperial College, London

MS. received 31*st October* 1951

ABSTRACT. Previous work on far ultra-violet atomic absorption spectra is summarized and discussed with particular regard to the phenomenon of auto-ionization. Details are given of a current programme of work on line and band absorption spectra of vaporized elements and hydrides, in which special attention is paid to the vacuum ultra-violet. Results for the Schumann region absorption spectrum of Ga vapour are given.

I. GENERAL FEATURES

§1. INTRODUCTION

This paper is presented as the first of a series, reporting the results of investigations in progress in this laboratory on atomic and molecular absorption spectra obtained by use of high temperature furnaces. In this work, though the observational range is not confined to it, the vacuum ultra-violet region above 400 Å is receiving particular attention.

Studies of this kind are of value both to the physical spectroscopist and to the astrophysicist. To the former, observations of line and band absorption spectra have been of significance in assisting identifications of deep-lying electronic states, and in the determination of oscillator strengths of transitions. Enhanced interest in line absorption resulted from the work of Beutler*, described in an important series of papers which appeared between 1933 and 1935, under the general title *On Absorption Spectra from Excitation of Inner Electrons.* In that work, observation of the extreme ultra-violet absorption spectra of the vapours of a number of elements revealed important lines and terms difficult to reach by emission methods. Beutler's work has been reviewed by Shenstone (1939) and Boyce (1941), and the principal results have been given, for instance, by Herzberg (1944, p. 167). To preserve continuity, a brief explanation will, nevertheless, be appropriate here.

---

* A bibliography of Beutler's papers is given by Boyce (1941).

The elements studied by Beutler comprised K, Rb, Cs, Zn, Cd, Hg, Tl, A, Kr, Xe. Leaving aside, for the moment, the inert gases, the absorption lines observed (in some cases forming long series) involve optical excitation of electrons of the most loosely bound closed subshells of the atom, the valence configuration remaining as for the ground state. Beutler's spectra thus constitute a type intermediate between the normal arc spectrum and the X-ray spectra of an element. The case of HgI is illustrative. The ground term being $5d^{10}6s^2\,{}^1S_0$, the normal arc spectrum is formed by terms of the configurations $5d^{10}6sml$ ($l=s, p, d\ldots$), all converging on the $5d^{10}6s\,{}^2S_{1/2}$ ground state of the ion. In speaking of X-ray spectra, we ordinarily refer to excitation of the deep shells. In his work on Hg vapour, Beutler (1933) found forty absorption lines in the range 1 301 to 745 Å attributable to transitions from the ground state to terms of $5d^9 6s^2\, mp(f)$, that is to terms built on the excitated $5d^9 6s^2\,{}^2D$ levels of HgII. Beutler's designation of this spectrum as HgI^b distinguishes it from the normal (I^a) arc spectrum, the notation being readily extended to other cases, e.g. HgII^b, II^c, where the $5d^{10}$ or $5p^6$ subshells of Hg^+ are respectively excited. The majority of the I^b terms found by Beutler are negative, that is, they lie above the lowest ionization potentials of the atoms concerned, and are thus energetically adjacent to the continua of states extending above the normal term series. Subject to certain selection rules, such negative terms may exhibit, in their combinations with normal terms, a diffuseness which is interpreted (Shenstone 1931) as due to the phenomenon of auto-ionization. The diffuseness of lines involving an upper state of high auto-ionization probability is then ascribed to the resulting reduction in the mean life of the state. Even prior to Beutler's work, the existence of terms arising by excitation of the topmost closed subshells of an atom had frequently been recognized during line analysis, and the occurrence of broad lines had been explained as due to auto-ionization in a few cases additional to CuI, originally discussed by Shenstone (1931). Beutler's far ultra-violet spectra provided, however, a large bulk of systematically investigated material. Nevertheless, auto-ionization is a phenomenon which is as yet little understood since, as remarked by Shenstone (1946), its effects are extremely variable and so far theoretically unpredictable. The only general principles available to date lie in selection rules (Shenstone 1931) deduced by analogy with those governing molecular predissociation, viz. that a level above the lowest ionization potential will be affected if it can find a continuum above the normal term series of the same J and parity as itself, and in LS-coupling of the same L and S.

A striking feature, revealed by Beutler's work and so far unexplained, lies in the abnormal intensities of certain absorption lines which involve upper states of negative term values. This is well illustrated by the cases of the heavy inert gases. No I^b spectrum is concerned here, but the lines of the I^a spectrum form two groups, which converge to limits corresponding respectively to the inverted $p^5\,{}^2P^0_{1/2,\,3/2}$ ground levels of the ion; the separation of the limits ranges from 1431 cm^{-1} for argon, to 10541 cm^{-1} for xenon. In the far ultra-violet absorption spectra, the members of a line series converging to the shorter wavelength limit broaden suddenly, as expected, on passing the longer wavelength limit, but also show an accompanying enormous increase in intensity, making them the strongest lines in the absorption spectrum of the gas. This discovery of intense absorption between series limits of the inert gases clarified the results of earlier work (Herzfeld and Wolff 1928), on the dispersion of A, Kr and Xe in the visible and near ultra-violet; such work had indicated surprisingly large *f*-value assignments to regions beyond the series limits. A similar peculiarity in the dispersion of Hg vapour (Beutler 1933, Wolfsohn 1933) is probably explained by the intense $6s^2\,{}^1S_0$–$5d^9\,6s^2\,6p\,{}^3P_1{}^0$ line at 1126·6 Å. Again, as already briefly reported (Garton 1950 a), the Schumann region absorption spectrum of In vapour contains a group of five intense lines in the 1600–1800 Å range. These lines, attributed to $5s^2\,5p\,{}^2P^0$–$5s\,5p^2\,{}^2S, {}^2P$, appear quite strongly at a vapour pressure at which the resonance lines are barely detectable. Cases of sudden jumps in intensity on passing a limit have also been observed by the author in the tin vapour absorption spectrum.

There are no direct measurements of *f*-values for inner electron transitions yet available, but there is no doubt that in some cases, including most of those just mentioned, the values of the Einstein *A*-coefficients considerably exceed those for ordinary strong permitted transitions, e.g. for the resonance lines of the above atoms. At present, the only quantitative indications appear to be those derived from dispersion data for Hg and the rare gases. Thus, Herzfeld and Wolff (1928) fitted a two-member dispersion formula to the values of the refractive index of argon in the visible and near ultra-violet, one member corresponding to the strongest resonance line, and concluded that the latter had $f = 0{\cdot}025$, and a region beyond the series limit $f = 4{\cdot}58$. Presumably the larger part of this residual *f*-value refers to the first of Beutler's lines lying beyond the longer wavelength series limit. In Hg, the lines $\lambda\,2537$ ($6\,{}^1S_0$–$6\,{}^3P_1{}^0$), and $\lambda\,1849$ ($6\,{}^1S_0$–$6\,{}^1P_1{}^0$) have $f = 0{\cdot}0255$ and 1·19 respectively (Wolfsohn 1933), in comparison with which $\lambda\,1127$ ($6\,{}^1S_0$–$d^9\,s^2\,p\,{}^3P_1{}^0$) has an *f*-value probably between 2 and 3. It is plainly desirable that direct measurements of oscillator strengths be made for such cases. Determination by means of the integral of the absorption coefficient over the line would seem to offer the best prospect, since the lines concerned are of great natural breadths. Difficulties of photographic photometry in the vacuum ultra-violet can probably be overcome.

There is a similar lack of quantitative information on probabilities of auto-ionization. The only measurements of line breadths, from which estimates can be made on the reasonable assumption that the total probability of radiative transitions is comparatively small, are those of Allen (1932) for Cu I lines. Although copper was the first element in which auto-ionization was recognized, the observed lines do not represent such extreme cases as some cited above. Thus, Allen's broadest lines had half-breadths of the order of a few cm^{-1}, corresponding to lifetimes of the order of 10^{-12} sec for the excited states. Though no measurements exist, it appears that the half-breadths of some of the inert gas and other lines above mentioned are some hundreds cm^{-1}, corresponding to lifetimes of 10^{-13} to 10^{-14} sec. A further outstanding case is an Ag line at 1516 Å, said by Shenstone (1940) to have a 'breadth' of 500 cm^{-1}. Owing to the mathematical complexities, quantum-mechanical calculations seem at present unable to give even orders of magnitude. Such calculations have been attempted by Wu (1944) and Wu and Qurom (1950) for doubly excited states of He and Be, but the calculated auto-ionization probabilities are in disagreement with experiment by several powers of ten.

It was stated above that I^b spectra are difficult to excite in emission; this calls for a little amplification. In low pressure or low electron density sources, lines having upper levels of high auto-ionization probability are weak or missing. Shenstone (1939) has pointed out that this effect of auto-ionization can be partially overcome by the use of sources at higher pressures and electron densities, such as arcs, in which inverse auto-ionization is favoured; Allen's work (1932) on the broad lines of Cu I showed, for example, that the intensities, as compared with those of sharp lines, grew rapidly with arc current. Emission lines of some hundreds cm^{-1} breadths have been observed by Shenstone in arcs run in nitrogen (e.g. Ag $\lambda 1516$), and the author has similarly obtained the s^2p–sp^2 group of In in emission. There are some indications that the cross sections for inner-electron excitation by electron impact are low, at least for the range of electron velocities favouring the development of arc spectra in laboratory sources. Thus, Beutler (1933) considered that certain so-called 'ultra-ionization potentials' (critical potentials in excess of the ionization potential) observed for Hg vapour showed little correlation with the positions of his highly excited levels. In later work (Lee 1939), on energy losses of 200-volt electrons in Hg vapour—rather fast electrons—two ultra-ionization potentials have in fact been identified with the two levels above ionization found by Beutler to give the strongest combinations with the ground state. It seems likely that, at least in some cases of I^b line emission in arcs, the main mechanism whereby the upper levels are populated is inverse auto-ionization rather than direct excitation from lower levels. This may even be true for levels not subject to strong auto-ionization, as transfer from a heavily broadened level into a nearby relatively sharp one might be achieved by collision processes.

It will be seen from the foregoing that, in seeking I^b terms which combine with the ground state, the absorption method is superior. Even in the elements investigated hitherto, there must be a host of terms, some of them no doubt important ones, which do not so combine. In seeking these, emission methods are important though, even here, study of the absorption by electrically or thermally excited gas may be as fruitful.

In astrophysics, knowledge of the positions and half-breadths of terms of the type discussed, and values of the oscillator strengths of their combinations may be of some importance. It has been noted that transitions involving such terms are often very strong ones and, in view of current attempts at the extension of the solar ultra-violet spectrum (Durand, Oberly and Tousey 1949, Hopfield and Clearman 1948), information of this type may find early application. This would seem to be the case in other fields also. That of optical dispersion has been mentioned. Application to discharge physics can be anticipated, and in particular it is worth drawing attention to the likely relevance of auto-ionization and its inverse process to situations involving photo-ionization and electron recombination respectively, e.g. spark breakdown. The relation between electron recombination and inverse auto-ionization, sometimes called 'dielectronic recombination' (Bates and Massey 1943), is the subject of a separate paper.

Subsequent to Beutler's work, the far ultra-violet absorption spectra of two further elements, Ag and Mn, were observed by Paul (1937). The results seem uncertain, however, as indicated in the case of Paul's Ag lines by Shenstone (1940). So far as it relates to line spectra, the aim of the present programme is the observation of absorption spectra above 400 Å of as many elements as possible, for which profitable results appear likely. As regards molecular spectra, attention is at present confined to bands due to elements, in some cases appearing incidentally, and to hydrides.

§ 2. EXPERIMENTAL

The main obstacle to observation of far ultra-violet absorption spectra lies in absence of satisfactory sources of background continuum covering the whole range of interest. The continuum given by a positive-column discharge in hydrogen is of good intensity to 2 200 Å, and remains usable on a short focus instrument to 1 650 Å; below this wavelength the continuum is replaced by closely packed rotational structure of H_2, which is useful for revealing only intense or broad absorption lines. The Hopfield He_2 continuum in the 600–900 Å range can also be produced in good intensity. The only emission continuum at present known to fill the gap 900–1 650 Å, and to extend below 600 Å, is that discovered by Lyman to be generated under the conditions of extreme current-density prevailing when a large capacity condenser is periodically discharged through a narrow-bore capillary. For the present work, sources of all three types are available.

The vacuum spectrograph, so far employed, is a one-metre normal-incidence grating, arranged so that a rapid succession of plates can be exposed; gratings of 15 000 lines/inch on speculum, and 30 000 lines/inch on glass are available.

The absorption vessel, interposed between background source and spectrograph, at present has the form of an evacuable King-type furnace of simple design. The heating element is a 6-inch long graphite tube of 1 cm bore, the heated zone being up to 4 inches in length and of 0·5–1·5 mm wall; a length of 1 inch at each end is tapered to fit inside split water-cooled copper clamps. The electrode leads running to these clamps, and the outside of the furnace housing, are all well water-cooled. Power is supplied by a 5 kVA 16 volt transformer set, the input to which is controlled by a Variac auto-transformer. Temperatures of the hot zone of the graphite tube are read from an optical pyrometer sighted through a side window on the outer wall of the tube. The reading obtained is somewhat lower than the temperature inside the tube, but is easily corrected thereto by an initial calibration. This furnace operates without trouble at temperatures up to about 2 200° c. For the higher temperatures and longer absorbing paths which the early experiments have shown desirable, there is under construction a furnace which will provide a heated zone of 12 inches or more, fed by a 40 kVA transformer.

If only the Schumann region is being studied (>1 100 Å), windows of LiF separate discharge tube and spectrograph from the furnace. To retard distillation of material out of the graphite tube, and for the maintenance of clean conditions, a slow current of helium, purified over hot copper oxide and charcoal, is passed through the furnace at a pressure of 50–100 times the vapour pressure of the element present. When attempting to observe hydride spectra, hydrogen purified over charcoal replaces helium. In all cases, when a newly turned graphite tube is to be used, it is first baked out, with the pumps on, at a temperature several hundred degrees above that at which it is intended to operate.

For measurement of wavelengths of absorption lines below 2 000 Å, no special devices have been employed hitherto, but use has been made of impurity or other lines present in the spectrum of the background source, or of absorption lines of wavelengths already known from emission spectra. The internal standards accompanying the hydrogen continuum are somewhat widely scattered, and it may be necessary in later more accurate measurements to employ a proper comparison source and shutter.

First results have already been briefly reported for the cases of Al, Ga, In, Sn and of some new bands obtained in absorption in the quartz ultra-violet (Garton 1950 a, b, c, d, 1951 a, b). Fuller details for these cases and for other elements investigated will be presented in later papers.

II. SCHUMANN REGION ABSORPTION SPECTRUM OF GALLIUM VAPOUR

§ 1 INTRODUCTION

Comparison of the available data for the arc spectra of the earth elements (B, Al, Ga, In, Tl) shows that the Ga I spectrum has been rather poorly observed (Bacher and Goudsmit 1932, Garton 1950 c).

The ground term of the Ga atom is $4s^2\,4p\,{}^2P^0_{1/2,\,3/2}$, and the known series terms, forming rather short sequences, as given by Bacher and Goudsmit (1932), are based on measurements of Uhler and Tanch (1922). The I^b spectrum is formed by the configurations 4s4p*ml*, the terms of which are built on the $4s4p\,{}^{1,3}P^0$ levels of the ion. Since the highest of the latter levels (${}^1P_1$) lies some 119 000 cm^{-1} above the ground term of the neutral atom, the whole I^b spectrum will be comprised within this range, i.e. will occur at wavelengths longer than 840 Å. The I^b configurations able to combine optically with the ground term are 4s4p*mp*, each of which yield, in Russell Saunders notation, ${}^4S$, P, D, ${}^2S(2)$, ${}^2P(2)$, ${}^2D(2)$, eighteen levels in all. The extent and way in which these can combine with the two levsls of the ground term to produce lines of reasonable strength depends on the actual coupling conditions.

Table 1. Application of Irregular Doublet Law

Spectrum	$4^2P^0_{1/2}-4s4p^2\,{}^2S_{1/2}$		$4^2P^0_{1/2}-4s4p^2\,{}^2P_{1/2}$	
	ν (cm^{-1})	$\Delta\nu$	ν (cm^{-1})	$\Delta\nu$
Ga I	~64000		~67000	
		~22000		~24000
Ge II	86395		91010	
		21414		24415
As III	107809		115425	
		20981		20707
Se IV	128790		136132	
				22021
Br V	—		158153	

The lowest of the I^b configurations is $4s4p^2$, which gives only ${}^4P$, ${}^2S$, ${}^2P$, ${}^2D$. The only Ga I^b terms previously recognized were ${}^4P$ and ${}^2S$ of this group (Sawyer and Lang 1929). It has been previously remarked (Garton 1950 c) that, while the $sp^2\,{}^4P$ term of Sawyer and Lang was probably correctly identified, the position suggested, on the basis of an emission line-pair at 2 534·83, 2 482·76 Å for the ${}^2S$ term, was in conflict with identifications in isoelectronic spectra. As seen in table 1, the combinations of the ground term with $4p^2\,{}^2S$ and ${}^2P$ can be expected, assuming correctness of identifications in Ge II to Br V to lie in the 1 500–1 600 Å region, that is, beyond the $4\,{}^2P^0_{1/2}$ series limit at 2 066 Å.

For completeness, the $sp^2\,{}^2D$ term calls for remark. In Al, Ga and In, the earlier members of the D-series show anomalous splittings (Paschen 1932, 1938), suggesting the presence of a perturbing term, presumably $sp^2\,{}^2D$, which therefore lies well below ionization, and is probably so well absorbed into the series that separate identification is not possible (Shenstone and Russell 1932).

§ 2. EXPERIMENTAL

With the general arrangement described in Part I, and using the hydrogen tube as background source, a set of graduated exposures was obtained for the range 1 100–2 200 Å at each of four furnace temperatures, 1 100, 1 250, 1 440, 1 610° C. The corresponding vapour pressures of Ga are given by Dushman (1949), as 0·01, 0·1, 1·0 and 5 mm Hg. On each plate the same set of exposures was repeated with the furnace cold. Plates were also obtained showing the visible and near ultra-violet absorption spectrum of Ga vapour at 1 610° C in an atmosphere of hydrogen, using a Hilger Medium-Quartz spectrograph (Garton 1951 b). The commercial Ga metal used initially had a purity of 99·9%; later, a supply of 5 g of exceptionally pure metal was generously supplied by the Chemical Research Laboratory, Teddington.

§ 3. RESULTS AND DISCUSSION

The Schumann region absorption spectra, obtained with five-minute exposures on Ilford Q/2 plates, at the succession of furnace temperatures indicated, are reproduced in the Plate. The increasing strength of the absorption lines marked A to F is plain. The wavelengths, wave-numbers, characters and classifications of the lines are given in table 2, as are the term values of $sp^2\,{}^2S_{1/2}$, ${}^2P_{1/2,\,3/2}$, resulting when the Uhler and Tanch (1922) absolute value of $4p\,{}^2P^0_{1/2} = 48\,380$ cm⁻¹ is assumed. The only other absorption features present were a few high series members at the long wavelength end of a plate. The series-limit continuum was undetectable, even at 5 mm Ga vapour pressure. The intensity figures in table 2 refer only to estimates within the A–F group, with an arbitrary 10 for the strongest line. The intensities were partly judged from the order of appearance

Table 2. Ga Absorption Lines

Line	λ_{vac} (Å)	ν_{vac} (cm⁻¹)	I	Character	Classification
A	1505·6	66419	4	Almost Sharp	$4\,{}^2P^0_{1/2} - 4s4p^2\,{}^2P_{3/2}$
B	1519·8	65796	10	Diffuse	$4\,{}^2P^0_{1/2} - 4s4p^2\,{}^2P_{1/2}$
C	1524·6	65591	10	Diffuse	$4\,{}^2P^0_{3/2} - 4s4p^2\,{}^2P_{3/2}$
D	1539·1	64972	4	Almost Sharp	$4\,{}^2P^0_{3/2} - 4s4p^2\,{}^2P_{1/2}$
E	1610·3	62100	2	Very Diffuse	$4\,{}^2P^0_{1/2} - 4s4p^2\,{}^2S_{1/2}$
F	1632·0	61274	2		$4\,{}^2P^0_{3/2} - 4s4p^2\,{}^2S_{1/2}$

$$4s4p^2 \quad \left.\begin{aligned} {}^2S_{1/2} &= 13720 \\ {}^2P_{1/2} &= 17417 \\ {}^2P_{3/2} &= 18038 \end{aligned}\right\} \begin{aligned} &\text{cm}^{-1}\text{ above} \\ &4s^2\,{}^1S_0 \text{ Ga II} \end{aligned}$$

of the lines with rising vapour pressure. Such visual estimates relate, of course, as much to breadth as to central intensity; the breadths are here widely different. It has also to be remembered that some lines start on the lesser populated $4\,^2P_{3/2}$ level of the ground state, so that the stated intensities are no indication of transition probabilities. In the absorption spectra, the strongest pair (B, C) occurs weakly at 1 100° c; at 1 250° c the whole PP′-group (A–D) is intense and the $sp^2\,^2S$ combinations (E, F) diffuse and weak; at 1 440° c all six lines are intense.

The group attributed now to $4\,^2P^0_{1/2,\,3/2}$–$4s4p^2\,^2P,\,^2S$ falls in the wavelength region expected from table 1. Further, the splitting $4s4p^2$ ($^2P_{3/2}$–$^2P_{1/2}$) fits the regular doublet law, as can be seen from table 3, where the values of the screening constants *s* for the GaI isoelectronic sequence are given. The value of *s* for the above splitting is much the same as for $4(^2P_{3/2}$–$^2P_{1/2})$ of GaI.

Table 3. Screening Constants

Spectrum	$4s4p^2(^2P_{1/2}-{}^2P_{3/2})$ (cm⁻¹)	*s*
Ga I	621	20·2
Ge II	1107	19·5
As III	1487	19·5
Se IV	2220	19·1
Br V	2853	19·2

On the near ultra-violet plates, obtained with the quartz instrument, the group $4\,^2P^0$–$4s4p^2\,^4P$ of Sawyer and Lang (1929) occurred plainly as five sharp absorption lines at a furnace temperature of 1 610° c; this provides final confirmation of the assignment. The line-pair λλ 2535, 2483, taken by Sawyer and Lang to represent combination of the ground doublet with $sp^2\,^2S_{1/2}$, was not present. The only impurity lines seen were a few very feeble lines of Hg, Cu, Al, Sn.

Though none of the absorption lines A to F is sharp, showing that all are probably affected by auto-ionization, the doublet E, F consists of much wider lines than does the PP′ multiplet A–D. This is in accordance with expectations from Shenstone's rules. For auto-ionization, the upper levels have to find a continuum above normal term-series, of even parity and $J=\frac{1}{2}$, $\frac{3}{2}$ respectively. The only $J=\frac{1}{2}$ continuum available is $4s^2\,Es\,^2S_{1/2}$ (where Es denotes a free electron emitted with kinetic energy E). The $J=\frac{3}{2}$ continuum available is $4s^2\,Ed\,^2D_{3/2}$. In *LS*-coupling the auto-ionizing level and the continuum have also to possess the same *L* and *S* values. In this case the $sp^2\,^2S$ level will auto-ionize, and the ^2P levels of the same configuration will not. With departure from *LS*-coupling, the $sp^2\,^2P$ levels will share some characteristics of ^2D and ^2S, and auto-ionization into the S and D continua may take place. The fact that the PP′ lines are much less diffuse than the $4\,^2P^0 \rightarrow 4s4p^2\,^2S$ pair indicates good approach to *LS*-coupling. Also, in the PP′ group, the intensities are such that the pair having $\Delta J=\Delta L$ is strongest. On the other hand, Bacher and Goudsmit's rule (1934) that in *LS*-coupling the interval sp^2 (^4P–^2P) is equal to three-halves the interval $sp(^3P$–$^1P)$ in the next ion, when the intervals are measured from term centroids, is not too well obeyed here. Thus, the ratio

$$[\mathrm{Ga\,I}(sp^2)(^4P-{}^2P)]/[\mathrm{Ga\,II}(sp)(^3P-{}^1P)]=1{\cdot}23.$$

Though no sequence of Ga absorption spectra, at different furnace temperatures, has been obtained in the near ultra-violet, from which it would be possible to compare total intensities of the Schumann region lines with those of the series lines, it appears likely that, as in the cases mentioned in Part I, some of the $sp^2 \rightarrow s^2 p$ transitions have *f*-values as large as or greater than those of the strongest lines of the series spectrum.

It is proposed to seek lines of the type $4\,^2P^0 \rightarrow 4s4pmp$ ($m > 4$), which will lie further into the far ultra-violet, by use of the Lyman continuum.

ACKNOWLEDGMENTS

For constant interest and encouragement, the author's best thanks are due to Dr. R. W. B. Pearse, Reader in Spectroscopy. The gift of several grammes of pure Ga metal, by the Director, Chemical Research Laboratory, acting through Dr. F. M. Reynolds, is gratefully acknowledged. For much assistance in design and construction of apparatus, thanks are also due to Messrs. A. Davis and T. Shand, of the Physics Department Workshop, Imperial College.

REFERENCES

Allen, C. W., 1932, *Phys. Rev.*, **39,** 42, 55.

Bacher, R. F., and Goudsmit, S., 1932, *Atomic Energy States* (New York : McGraw-Hill) ; 1934, *Phys. Rev.*, **46,** 948.

Bates, D. R., and Massey, H. S. W., 1943, *Rep. Prog. Phys.* **9,** 67 (London : Physical Society).

Beutler, H., 1933, *Z. Phys.*, **86,** 710.

Boyce, J. C., 1941, *Rev. Mod. Phys.*, **13,** 1.

Durand, E., Oberly, J. J., and Tousey, R., 1949, *Astrophys. J.*, **109,** 1.

Dushman, S., 1949, *Scientific Foundations of Vacuum Technique* (New York : Wiley).

Garton, W. R. S., 1950 a, *Nature, Lond.*, **166,** 150 ; 1950 b, *Ibid.*, **165,** 322 ; 1950 c, *Ibid.*, **166,** 317 ; 1950 d, *Ibid.*, **166,** 690 ; 1951 a, *Proc. Phys. Soc.* A, **64,** 509 ; 1951 b, *Ibid.*, **64,** 591.

Herzberg, G., 1944, *Atomic Spectra and Atomic Structure* (New York : Dover).

Herzfeld, K. F., and Wolff, K. L., 1928, *Geiger-Scheel Hand. d. Phys.*, **20,** 490.

Hopfield, J. J., and Clearman, H. E., 1948, *Phys. Rev.*, **73,** 877.

Lee, A. H., 1939, *Proc. Roy. Soc.* A, **173,** 569.

Paschen, F., 1932, *Ann. Phys., Lpz.*, **12,** 509 ; 1938, *Ibid.*, **32,** 148.

Paul, F. W., 1937, *Phys. Rev.*, **52,** 923.

Sawyer, R. A., and Lang, R. J., 1929, *Phys. Rev.*, **34,** 712.

Shenstone, A. G., 1931, *Phys. Rev.*, **38,** 873 ; 1939, *Rep., Prog. Phys.*, **5,** 210 (London : Physical Society); 1940, *Phys. Rev.*, **57,** 894 ; 1946, *Physica*, **13,** 581.

Shenstone, A. G., and Russell, H. N., 1932, *Phys. Rev.*, **39,** 415.

Uhler, H. S., and Tanch, J .W., 1922, *Astrophys. J.*, **55,** 291.

Wolfsohn, G., 1933, *Z. Phys.*, **83,** 234.

Wu, T. Y., 1944, *Phys. Rev.*, **66,** 291.

Wu, T. Y., and Ourom, L., 1950, *Canad. J. Res.*, **28A,** 542.

The Ultra-Violet Absorption Spectra of GeO, GeS, GeSe and GeTe

By G. DRUMMOND and R. F. BARROW
Physical Chemistry Laboratory, Oxford University

MS. received 18*th October* 1951

ABSTRACT. The ultra-violet absorption spectra of GeSe and GeTe have been obtained. New band-systems of both molecules have been found, and the vibrational analysis of one of them, the E–X system of GeSe, has been completed. The corresponding system, E–X, of GeS has been considerably extended, and fairly sharp dissociation limits have been found for both GeS and GeSe. A satisfactory spectrogram of GeO in absorption has been obtained. Values of the electronic and vibrational constants for all the known states of the four molecules are derived.

---

§1. INTRODUCTION

Each of these molecules is known to possess one strong band-system in the ultra-violet region, $D-X^1\Sigma^+$. Apart from some preliminary work by Shapiro, Gibbs and Laubengayer (1932) on the absorption spectrum of GeO, only GeS has been studied in absorption. For the latter molecule two systems, D – X and E – X, were found in absorption and analysed by Shapiro, Gibbs and Laubengayer (1932); the D – X system of GeS was later obtained in emission (Barrow 1941). Vibrational analyses of D – X systems of GeSe and GeTe were put forward by Barrow and Jevons (1940) from measurements of the spectra emitted by high-current positive-column discharges. The vibrational and rotational analyses of the D – X system of GeO were also based on the emission spectrum (Shaw 1937, Jevons, Bashford and Briscoe 1937, Sen Gupta 1937, 1939).

On the basis of the general similarity in the spectra of these four molecules it appeared very probable that E – X systems should also exist for GeO, GeSe and GeTe and, indeed, some weak bands in the emission spectrum of GeSe have already been assigned tentatively to such a system.

We began by examining the absorption spectra of GeSe and GeTe. In the former case an extensive system E – X has been discovered, with a long $v''=0$ progression from which quite a sharp dissociation limit has been obtained. In the case of GeTe it has not been possible to secure any very good photographs of the E – X system, and a tentative vibrational analysis is all that can be given. The success with GeSe prompted us to look again at the absorption spectrum of GeS; as a result of the new spectrograms, the system has been greatly extended on the short-wavelength side, and again it has been possible to derive a reliable dissociation limit.

Satisfactory pictures of the D – X system of GeO in absorption have been obtained for the first time: the E – X system, if it exists, evidently lies in the Schumann region. For GeSe and GeTe, new measurements of the absorption spectrograms of the D – X systems necessitate slight alterations to the original vibrational analyses.

The main result of this work is to strengthen the analogy between the spectroscopic properties of the corresponding germanium, silicon and tin compounds.

§ 2. EXPERIMENTAL

The substance to be studied was placed in a boat inside an aluminium oxide tube, 75 cm long, passing through a 'Glo-bar' furnace. The ends of the absorption tube were closed by water-cooled brass end-pieces bearing quartz windows, and the tube was evacuated through a side-arm in one of the end-pieces. Conventional band lamps and hydrogen lamps were used as sources of continua. The spectra were photographed on Hilger Medium and Small Quartz instruments on Ilford Process and Q1 plates. Fe and Cu arc lines were used as standards, their wavelengths being taken from the M.I.T. list (1939).

(i) *GeO.*

Indications of the absorption spectrum of GeO were obtained by Shapiro, Gibbs and Laubengayer (1932), using GeO and a hot window technique. Under these conditions the windows were attacked very rapidly, and observation of the spectrum was found to be almost impossible. With the cold windows used in the present experiments no trouble arose.

GeO_2 was first tried as the starting material, but only poor spectra were obtained, even at a furnace temperature of about 1 200° c. GeO, prepared by the method of Dennis and Hulse (1930), proved much more satisfactory, and good spectrograms were obtained at about 700° c.

(ii) *GeS.*

Preliminary experiments with a mixture of GeO_2, S and Al in the absorption tube were not successful. GeS was therefore prepared, following the directions of Foster (1946). The final plates were taken at temperatures in the range 470–600° c.

(iii) *GeSe.*

About 1 g of an equimolecular mixture of Ge and Se was used for each exposure, and the optimum temperature was found to be about 660° c.

(iv) *GeTe.*

Satisfactory spectrograms of the D – X system were taken with GeO_2, Al and Te mixtures at about 610–670° c, and with Ge and Te mixtures at 750° c. Although a number of plates were taken, no really good spectrograms of the E – X system were obtained.

§ 3. VIBRATIONAL ANALYSES

Reproductions of the spectra are given in figs. 1 and 2 (Plates). All the bands are red-degraded, and all show a largely unresolved vibrational isotope effect (see earlier papers on these molecules).

(i) *GeO.*

The measurements of the D – X system are in somewhat closer agreement with those of Jevons, Bashford and Briscoe (1937) than with those of Sen Gupta (1937). They add a little to our knowledge of the upper vibrational levels of the state D, and the bands with $v' = 6$ to 12 are therefore listed in table 1. A search down to about 2 000 Å for an E – X system gave negative results, but indications of absorption bands which may belong to this system have recently been obtained in the region 1 700–1 900 Å.

(ii) *GeS.*

The D – X system of GeS was the subject of a detailed study by Shapiro, Gibbs and Laubengayer (1932), and no new features of this system have emerged in the present work.

Table 1. Bands of the D–X System of GeO

12					42817 *2334·8*
					562
11	44209 *2261·3*	973	43236 *2312·2*	981	42255 *2365·85*
	556		562		550
10	43653 *2290·1*	979	42673·6 *2342·65*	968·7	41704·9 *2397·07*
	577		573·9		572·7
9	43075·9 *2320·77*	976·2	42099·7 *2374·59*	967·5	41132·2 *2430·45*
	576·1		575·5		578·5
8	42499·8 *2352·23*	975·6	41524·2 *2407·50*	970·5	40553·7 *2465·12*
	587·6		586·4		
7	41912·2 *2385·21*	974·4	40937·8 *2441·99*		
	584·3		588·7		
6	41327·9 *2418·94*	978·8	40349·1 *2477·62*		
↑ v'					
$v'' \rightarrow$	0		1		2

Table 2. Bands of the E–X System of GeS

v', v''	λ_{air}	ν_{vac}	v', v''	λ_{air}	ν_{vac}
0, 4	2740·2	36483	13, 1	83·3	946
1, 4	16·2	805	11, 0	81·4	979
0, 3	2698·9	37041	14, 1	2368·1	42215
1, 3	76·5	351	12, 0	66·4	245
0, 2	58·4	605	13, 0	51·4	515
2, 3	54·6	659	16, 1	38·7	746
1, 2	37·2	908	14, 0	36·5	786
3, 3	33·7	958	15, 0	21·9	43055
0, 1	18·7	38176	16, 0	08·2	310
2, 2	16·0	215	17, 0	2294·3	573
4, 3	13·3	254	18, 0	81·8	811
1, 1	2597·6	486	19, 0	69·7	44045
3, 2	95·7	514	20, 0	57·6	281
2, 1	77·7	783	21, 0	46·5	500
4, 2	74·9	825	22, 0	35·8	713
3, 1	57·5	39089	23, 0	25·9	912
2, 0	39·6	364	24, 0	16·7	45098
4, 1	37·8	392	25, 0	08·2	272
3, 0	20·4	664	26, 0	01·0	420
5, 1	18·6	693	27, 0	2193·5	575
4, 0	01·5	964	28, 0	86·3	725
6, 1	01·0	972	29, 0	80·3	851
5, 0; 7, 1	2483·0	40262	30, 0	74·3	977
6, 0; 8, 1	65·3	551	31, 0	69·1	46088
7, 0; 9, 1	48·0	837	32, 0	64·5	185
8, 0; 10, 1	30·8	41126	33, 0	60·5	271
9, 0; 11, 1	14·0	412	34, 0	55·1	387
12, 1	2398·8	675	35, 0	51·1	495
10, 0	97·3	701	36, 0	46·3	577

Table 3. Deslandres Scheme for the D – X System of GeSe

v′ ↑ / v″ →	0		1		2		3		4		5	
12	33838·1 (0) 2954·39											
	224·4											
11	33613·7 (1) 2974·11	411·9	33201·8 (2) 3011·01									
	237·5		236·5									
10	33376·2 (2) 2995·28	410·9	32965·3 (3) 3032·61									
	251·1		246·2									
9	33125·1 (3) 3019·13	406·0	32719·1 (3) 3055·43									
	256·3		254·9									
8	32868·8 (4) 3041·52	404·6	32464·2 (4) 3079·42									
	252·9		256·9									
7	32615·9 (5) 3065·10	408·6	32207·3 (4) 3103·99									
	258·9		261·8									
6	32357·0 (6) 3089·60	411·5	31945·5 (2) 3129·43									
	257·4											
5	32099·6 (7) 3114·40											
	264·8											
4	31834·8 (8) 3140·31	408·3	31426·5 (5) 3181·11*									
	261·9		259·9									
3	31572·9 (9) 3166·36	406·3	31166·6 (8) 3207·64*									
	264·7		263·0									
2	31308·2 (10) 3193·13*	404·6	30903·6 (10) 3234·94*	403·2	30500·4 (6) 3277·70*	399·8	30100·6 (1) 3321·24*	400·6	29700·0 (0) 3366·04*	395·8	29304·2 (0) 3411·50*	394·6
	266·1		264·9		264·8		264·7		263·7			
1	31042·1 (8) 3220·50	403·4	30638·7 (9) 3262·91*	403·1	30235·6 (7) 3306·41*	399·7	29835·9 (3) 3350·71*	399·6	29436·3 (0) 3396·19*			
	265·7		268·1		268·6		266·6		266·3			
0	30776·4 (3) 3248·31	405·8	30370·6 (6) 3291·71*	403·6	29967·0 (4) 3336·05*	397·7	29569·3 (2) 3380·92*	399·3	29170·0 (2) 3427·20*	394·5	28775·5 (1) 3474·19*	394·3

v′ / v″	6		7
2	28909·6 (0) 3458·07*		
1			28252·4 3538·53†
			269·3
0	28381·2 3522·46†	398·1	27983·1 3572·57†

* Band observed also in emission. † Band observed only in emission.

Bands of the E – X system were measured by these workers as far as $v'=11$. It will be seen from fig. 2 that this system has now been considerably extended, and levels have been found up to $v'=36$, not far from what on one plate appeared to be a convergence limit at about 2 140 Å. Details of the bands are given in table 2; they confirm the original vibrational analysis.

(iii) *GeSe.*

The band-head measurements for this molecule are given in tables 3 and 4. The absorption plates of the D – X system are appreciably better than the emission plates, and about fifteen new bands belonging to this system have been found. The original vibrational analysis has been largely substantiated, but it has been necessary to increase the values of v'' by one unit.

Table 4. Delandres Scheme for the E – X System of GeSe

9	37223·9 (7) *2685·65**	409·7	36814·2 (6) *2715·54**							
	187·5		189·9							
8	37036·4 (8) *2699·25*	412·1	36624·3 (7) *2729·62**							
	205·2		201·7							
7	36831·2 (8) *2714·29*	408·6	36422·6 (9) *2744·74**							
	205·1		199·6							
6	36626·1 (9) *2729·49*	403·1	36223·0 (10) *2759·86**							
	203·9		201·1							
5	36422·2 (9) *2744·77*	400·3	36021·9 (10) *2775·27**	402·7	35619·2 (10) *2806·65**	397·9	35221·3 (6) *2838·36*			
	200·6		206·8		203·7		205·3			
4	36221·6 (10) *2759·97*	406·5	35815·1 (10) *2791·30**	399·6	35415·5 (9) *2822·79**	399·5	35016·0 (6) *2855·00**	400·3	34615·7 (2) *2888·02**	
			211·4		213·2		211·6		207·7	
3			35603·7 (9) *2807·81*	401·4	35202·3 (8) *2839·89**	397·9	34804·4 (6) *2872·36**	396·4	34408·0 (3) *2905·45**	384·5	34023·5 (3) *2938·29*
			212·4		209·3		204·3		207·1	
2			35391·3 (7) *2824·72*	398·3	34993·0 (7) *2856·88*	392·9	34600·1 (6) *2889·32**	399·2	34200·9 (3) *2923·05**	
			212·8		216·7		213·7		212·5	
1			35178·5 (4) *2841·81*	402·2	34776·3 (5) *2874·68*	389·9	34386·4 (5) *2907·28*	398·0	33988·4 (4) *2941·32*	
							219·0		216·3	
0							34167·4 (5) *2925·91*	395·3	33772·1 (4) *2960·16*	395·9	33376·2 (2) *2995·28*
v'										
v''→	0		1		2		3		4		5

* Band observed also in emission.

Table 4 (*cont.*)

v', v''	λ_{air}	ν_{vac}	v', v''	λ_{air}	ν_{vac}
10, 1	2700·49	37019·4	24, 0	05·0	908
12, 1	2672·18	411·5	27, 1	2503·8	39927
10, 0	70·91	429·3	25, 0; 28, 1	2495·5	40060
13, 1	59·53	589·5	26, 0; 29, 1	86·9	199
11, 0	57·19	622·6	30, 1	79·0	327
14, 1	45·58	787·7	27, 0	78·8	330
12, 0	44·05	809·5	31, 1	70·9	459
15, 1	31·89	984·2	28, 0	70·4	467
13, 0	30·83	999·5	32, 1	64·2	569
16, 1	18·9	38173	29, 0	61·9	607
14, 0	17·40	194·5	33, 1	57·4	681
17, 1	06·2	359	30, 0	54·4	731
15, 0	03·71	395·3	34, 1	49·7	809
18, 1	2594·0	539	31, 0	46·9	856
16, 0	90·3	594	35, 1	42·5	929
19, 1	82·3	714	32, 0	39·5	980
17, 0	78·9	765	33, 0	32·3	41101
20, 1	71·5	876	37, 1	29·9	141
18, 0	66·7	949	34, 0	25·1	223
19, 0	55·1	39126	35, 0	17·9	346
20, 0	45·9	267	36, 0	12·4	440
23, 1	41·6	333	37, 0	06·1	548
21, 0	35·2	433	38, 0	00·3	649
22, 0	24·9	594	39, 0	2394·8	744
23, 0	15·1	748	40, 0	90·9	812
26, 1	12·0	797			

The E − X system (table 4) has a very open Condon parabola, bounded by a long $v'' = 0$ progression, similar to those obtaining in other E − X systems of these molecules, for example SiS (Vago and Barrow 1946 a) and SnSe (Vago and Barrow 1946 b). The vibrational isotope effect in the higher members of the $v'' = 0$ progression is so large that the band-head measurements here are of relative rather than of absolute significance. The convergence of the bands in this progression is clearly marked (fig. 2), and on one exposure there was an indication of a dissociation limit at about 2 360 Å.

(iv) *GeTe.*

As for GeSe, the D − X system for GeTe (table 5) has been considerably extended. The new results require that the original values of v' be increased by one unit, but otherwise the analysis is unchanged.

The bands in the position expected for the E − X system were found to present experimental and analytical problems which it has not been possible to solve completely.

It has already been remarked that it was very difficult to obtain spectrograms with adequate contrast on the band-heads. However, measurements of moderate accuracy were made of about 50 bands which could be assigned without much doubt to GeTe. Many of these bands fit into a fragmentary scheme (table 6 (*a*)), with the long $v'' = 0$ progression expected of the E − X system, but there is another group of about fifteen bands (table 6 (*b*)), separated from the first group by about 55 cm^{-1}, whose relation to the bands of the first group is not yet clear. The isotope effect shows that if there are two systems or sub-systems in this region, then their origins must be very close, for the range of wavelengths containing the sharpest bands is quite limited. There is, however, no sign of multiplet structure in the corresponding systems of GeS and GeSe, and it therefore seems likely that the interval of 55 cm^{-1} is simply a function of the vibration frequencies, such as $(2\omega_e'' - 4\omega_e')$; this interpretation would require that there should be two Condon parabolae of intensity maxima. It may be remarked that similar analytical difficulties arise for other band-systems in this group, for example PbS (Vago and Barrow 1947).

Table 5. Delandres Scheme for the D – X System of GeTe

14	30598 (0) *3267·3*	318	30280 (0) *3301·6*								
	207		197								
13	30391 (1) *3289·5*	318	30083 (0) *3323·2*								
	178		201								
12	30213 (2) *3308·9*	331	29882 (2) *3345·5*								
	201		199								
11	30012 (3) *3331·1*	329	29683 (3) *3368·0*								
	210		203								
10	29802 (4) *3354·5*	322	29480 (4) *3391·2*								
	205		206								
9	29597 (5) *3377·8*	323	29274 (3) *3415·0*								
	197		203								
8	29400 (6) *3400·4*	329	29071 (3) *3438·9*								
	204		203								
7	29196 (7) *3424·2*	328	28868 (2) *3463·1*								
	209		217								
6	28987 (8) *3448·9*	336	28651 (2) *3489·3*								
	212		204								
5	28775·1 (9) *3474·24*	328·1	28447·0 (2) *3514·31*								
	211·1		204·1								
4	28564·0 (10) *3499·91*	321·1	28242·9 (7) *3539·71*								
	212·8		211·6								
3	28351·2 (9) *3526·18*	319·9	28031·3 (7) *3566·42*						27066·7 (0) *3693·53*	321·6	26745·1 (1) *3737·94*
	213·7		214·9						212·1		205·9
2	28137·5 (9) *3552·97*	321·1	27816·4 (8) *3593·98*	320·0	27496·4 (6) *3635·81*	320·6	27175·8 (2) *3678·70*	321·2	26854·6 (2) *3722·8*	315·4	26539·2 (1) *3766·94*
	216·5		216·3		218·5		218·9		220·3		219·1
1	27921·0 (7) *3580·51*	321·1	27600·1 (8) *3622·15*	322·2	27277·9 (7) *3664·94*	321·0	26956·9 (4) *3708·57*	322·6	26634·3 (2) *3753·5*	314·2	26320·1 (0) *3798·30*
	221·4		219·2		219·8		220·5		220·9		210·1
0	27699·6 (5) *3609·14*	318·7	27380·9 (6) *3651·14*	322·8	27058·1 (6) *3694·71*	321·7	26736·4 (5) *3739·16*	323·0	26413·4 (5) *3784·89*	303·4	26110·0 (3) *3828·87*
↑ v'											
$v'' \rightarrow$	0		1		2		3		4		5

Table 6 (*a*). Bands of the E – X System of GeTe

v' ↑ / v'' →	0		1		2		3		4		5
12	33233 *3008·2*										
	132										
11	33101 *3020·2*										
	142										
10	32959 *3033·2*										
	171										
9	32788 *3049·0*										
	134										
8	32654 *3061·5*										
	150										
7	32504 *3075·7*										
	168										
6	32336 *3091·6*										
	151										
5	32185 *3106·1*										
	153										
4	32032 *3121·0*										
	153										
3	31879 *3136·0*										
	167										
2	31712 *3152·5*										
	150										
1	31562 *3167·5*	317	31245 *3199·6*	316	30929 *3232·3*	332	30597 *3267·3*	317	30280 *3301·6*		
	161		162		164		162		170		
0	31401 *3183·7*	318	31083 *3216·2*	318	30765 *3249·5*	330	30435 *3284·7*	325	30110 *3320·2*	307	29803 *3354·5*

v'	$v''=0$
20	34371 *2908·6*
	141
19	34230 *2920·6*
	130
18	34100 *2931·7*
	131
17	33969 *2943·0*
	146
16	33823 *2955·7*
	158
15	33665 *2969·6*
	158
14	33507 *2983·6*
	143
13	33364 *2996·4*
	131
12	33233 *3008·2*

v'	$v''=0$
29	35352 *2827·9*
	95
28	35257 *2835·5*
	118
27	35139 *2845·0*
	89
26	35050 *2852·2*
	104
25	34946 *2860·7*
	123
24	34823 *2870·8*
	98
23	34725 *2878·9*
	132
22	34593 *2889·9*
	113
21	34480 *2899·4*
	129
20	34371 *2908·6*

Table 6 (*b*). Bands of the E – X System of GeTe

v' ↑ / v'' →	0		1		2		3		4
8	32664 *3060·6*								
	114								
7	32550 *3071·3*								
	150								
6	32400 *3085·5*								
	160								
5	32240 *3100·8*								
	151								
4	32089 *3115·4*								
	160								
3	31929 *3131·0*								
	147								
2	31782 *3145·5*								
	165								
1	31617 *3161·9*	319	31298 *3194·2*	319	30979 *3227·1*	330	30649 *3261·8*	326	30323 *3296·9*
	159		161		159		160		179
0	31458 *3177·9*	321	31137 *3210·7*	317	30820 *3243·7*	331	30489 *3278·9*	345	30144 *3316·5*

Table 7. Summary of Constants

State		GeO	GeS	GeSe	GeTe
	ν_e	—	38884·8	35462·6	(31470)
E	ω_e	—	310·3	217·7	(170)
	$x_e\omega_e$	—	1·43*	1·02†	(1·2)
	ν_e	37766·9	32889·5	30845·7	27750·8
D	ω_e	650·4	375·0	269·4	221·0
	$x_e\omega_e$	4·21	1·51	0·89	0·89
	ν_e	0	0	0	0
X	ω_e	985·5	575·8	408·7	323·9
	$x_e\omega_e$	4·29	1·80	1·36	0·75
D_0'' (ev)		$7{\cdot}_0$	$5{\cdot}6_8 \pm 0{\cdot}1_3$	$4{\cdot}9_8 \pm 0{\cdot}2_5$	$4{\cdot}1 \pm 0{\cdot}4$

* Valid to $v' \simeq 17$. † Valid to $v' \simeq 14$.

All the known observations of vibrational intervals have been used in deriving the electronic and vibrational constants given in table 7. The vibrational levels of the ground states can all be represented adequately by two-constant formulae, but this is not so for the E states, in which the higher vibrational levels converge more rapidly than can be indicated by terms simply in $(v+\frac{1}{2})$ and $(v+\frac{1}{2})^2$. There is also some indication that the levels in the D state begin to converge at high values of v' more rapidly than is given by a linear decrease in vibrational interval.

The values given in table 7 call for no particular comment, except perhaps that for $x_e''\omega_e''$ for GeSe. The value found, 1·36, appears to be high in comparison with the other molecules of the group (Vago and Barrow 1948): the figure predicted would have been about 1·0. It seems likely that this is an illustration rather of the difficulty of evaluating anharmonic constants from limited data on bands with complex isotopic patterns than of a breakdown of the empirical rule.

§4. DISSOCIATION ENERGIES

The vibrational intervals for the E state of GeS and GeSe are plotted against vibrational quantum number in fig. 3, and it appears that rather reliable dissociation limits can be deduced for these molecules. We obtain : $D'_0(\mathrm{E}) = 0{\cdot}9_9$ ev for GeS, 0·84 ev for GeSe, leading to dissociation limits above $v''=0$ at $5{\cdot}7_9$ and $5{\cdot}2_3$ ev respectively. These values fit well with the direct observation of limits at 2 140 and 2 360 Å.

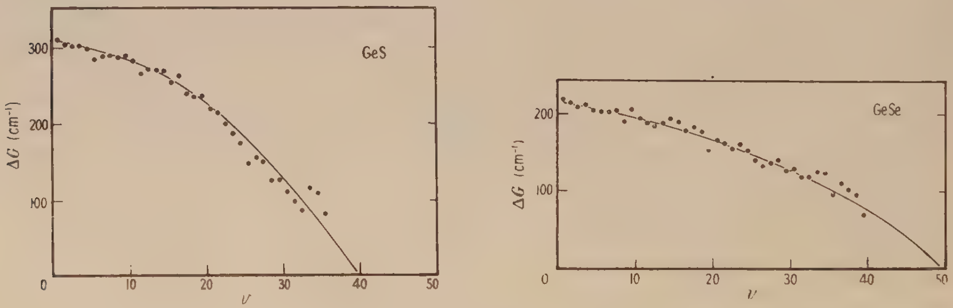

Fig. 3. Course of the vibrational intervals in the E states of GeS and GeSe.

The most plausible view about the dissociation products at these limits is that they are Ge(^{3}P) + X(^{3}P). This view is based on the assumption that the linear Birge–Sponer extrapolations for the ground states of this group of molecules give values of D'' which are approximately correct, and that the E states are singlets. Such combinations of excited atoms as Ge(^{1}D) + S(^{1}D) lie too high for consideration, and only the ground state atomic combination remains. Unfortunately the multiplet separations in these atomic states are far from negligible. The values in electron volts are :

	Ge		O	S	Se	Te
$^3P_2$	0·18	$^3P_0$	0·03	0·07	0·31	0·59
$^3P_1$	0·07	$^3P_1$	0·02	0·05	0·25	0·58
$^3P_0$	0	$^3P_2$	0	0	0	0

It is reasonable to suppose that the ground states dissociate into Ge($^3P_0$) + X($^3P_2$), but it is hardly possible to be certain about the E states. If the products of dissociation of the E states are the excited triplet components, then

$D_0''(\mathrm{GeS}) = 5{\cdot}5_4$ and $D_0''(\mathrm{GeSe}) = 4{\cdot}7_5$ ev. It seems best to leave these results as $D_0''(\mathrm{GeS}) = 5{\cdot}6_6 \pm 0{\cdot}13$; $D_0''(\mathrm{GeSe}) = 4{\cdot}9_8 \pm 0{\cdot}25$ ev.

For GeO the extrapolations are long, and the only reasonable procedure at present seems to be to assume that the linear Birge–Sponer extrapolation holds for the ground state. This gives $D_0'' = 7{\cdot}_0$ ev, a value which one may suspect to be somewhat too high.

For GeTe we know rather little about the E state, but if a $(\Delta G, v)$ curve is drawn of the same general shape as for GeS and GeSe, we obtain $D_0'(\mathrm{GeTe:E}) = 0{\cdot}5_9$ ev. With this $D_0''(\mathrm{GeTe}) = 4{\cdot}_1 \pm 0{\cdot}_4$ ev.

This is as far as the discussion of the dissociation energies of these molecules can be carried in the light of the present information.* It is hoped that work now beginning on the spectroscopy of these molecules in the vacuum ultra-violet region and on their thermochemistry will enable more precise values to be given.

ACKNOWLEDGMENT

One of us (G. D.) thanks the Department of Scientific and Industrial Research for a maintenance grant.

REFERENCES

Barrow, R. F., 1941, *Proc. Phys. Soc.*, **53,** 116.

Barrow, R. F., and Jevons, W., 1940, *Proc. Phys. Soc.*, **52,** 534.

Dennis, L. M., and Hulse, R. E., 1930, *J. Amer. Chem. Soc.*, **52,** 3553.

Foster, L. S., 1946, *Inorganic Syntheses*, II (New York : McGraw-Hill), p. 102.

Jevons, W., Bashford, L. A., and Briscoe, H. V. A., 1937, *Proc. Phys. Soc.*, **49,** 543.

M.I.T. Wavelength Tables, 1939 (London : Chapman and Hall).

Sen Gupta, A. K., 1937, *Z. Phys.*, **105,** 487; 1939, *Proc. Phys. Soc.*, **51,** 62.

Shapiro, C. V., Gibbs, R. C., and Laubengayer, A. W., 1932, *Phys. Rev.*, **40,** 354.

Shaw, R. W., 1937, *Phys. Rev.*, **51,** 12.

Vago, E. E., and Barrow, R. F., 1946 a, *Proc. Phys. Soc.*, **58,** 538; 1946 b, *Ibid.*, **58,** 707; 1947, *Ibid.*, **59,** 449; 1948 *Victor Henri Memorial Volume* (Liège : Desoer), p. 201.

Note added in proof. Recent work on SnO (Drummond and Barrow, 1952, *Proc. Phys. Soc.* A, **65,** 148) suggests that the present E states dissociate into Ge($^3P_2$); which component of the ^3P term of the non-metal is involved is not yet known.

LETTERS TO THE EDITOR

On Mechanical Action in Dielectrics

In a recent communication (Cade 1951) I have criticized the basic equation of Smith-White's theory of force and energy in dielectrics (Smith-White 1949), namely, the Livens force density,

$$f = (P, \operatorname{grad}) E \qquad \ldots\ldots (1)$$

(notation standard), for the reason that this equation does not take account of the fact that the contribution to the field of a volume element of dielectric at the position of E is itself of the same order as E, so that in finding the force on the element this contribution must be subtracted. Smith-White (1951), in reply, has rejected this criticism, principally on the grounds that one is not justified in judging (1) in the light of known electrical principles, but must regard it as a new hypothesis. It is the purpose of this note to consider the points raised in this reply, and it will be shown that they are generally untenable.

Smith-White classifies electrical actions such as are usually contemplated into four types : (i) actions between point charges, (ii) between continuous charge distributions, (iii) between point doublets, and (iv) between continuous doublet distributions. He correctly points out that (i), governed by Coulomb's law, is not so readily generalized to (ii), (iii) and (iv) as is commonly thought. He wrongly states, however, that on account of the non-convergence of an integral the generalization fails when one attempts to apply it to (iv). It is perfectly true that when one tries to write down the electric intensity at a point in a dielectric in terms of an integral over the doublet distribution, the integral, from the strict mathematical standpoint, is non-convergent, but the difficulty is overcome from the physical standpoint by specifying that a cavity surrounding the point, which is in due course allowed to become vanishingly small, shall have a certain shape. One then obtains a finite result depending on the shape. It is well known that for tubular and disc-shaped cavities the integral gives the 'pipe-force' and 'crack-force' respectively (Fowler 1936), and, indeed, by electric intensity in a dielectric we generally mean the pipe-force, as this is the only one which is derivable from a potential, defined in the usual way, and for which the cavity itself has no influence upon a test-particle. The difficulty of non-convergence, therefore, does not prevent us from finding the force on an element of dielectric, but merely demands that we specify the shape of the element. This situation is an interesting one and, except for the analogous one in magnetism, is probably unique in theoretical physics.

Smith-White objects further, however, that it is not permissible to use Poisson's equivalent charge distributions, as I did, for the purpose of calculating the force on an element of dielectric. This is not true, as is immediately evident by use of the principle of action and reaction, which is known to hold for electrostatic forces. Since the force on a point charge, say, due to an element of dielectric is the same as if the element were a certain charge distribution, which is a result of the Poisson–Kelvin theory, then the force on the element due to the point charge is obtainable by replacing the element by the same charge distribution. It is vitally important, of course, to treat an *element of dielectric* and not an *element of equivalent volume charge*, and it was through the tacit appreciation of this point that I stated in my previous communication that an element of dielectric and the rest of the dielectric were to be regarded as 'two polarized bodies'.

The conclusion to be drawn from the above discussion is that it is possible to treat the force on an element of dielectric as a generalization from Coulomb's law, and that it is allowable to use Poisson's equivalent charge distributions. The objection against (1) therefore follows as in my previous note, except that it requires a modified enunciation, since Smith-White's belief that the force density is not derivable from Coulomb's law has led him to the standpoint of proposing (1) as a new hypothesis. We now state that a calculation of the force density by known methods leads to (1) together with an extra term, so that (1), regarded as a hypothesis, is incompatible with established electrical principles.

Finally, Smith-White implies that any difficulties which may be encountered through the treatment of continuous doublet distributions, but which do not occur with discrete doublets, cannot be realistic, since use of continuous distributions is merely a mathematical method of dealing with phenomena which should ideally be treated from the point of view of discrete distributions. This argument, correct in itself, is not relevant, because the difficulty with which we are concerned occurs in whichever way we regard a dielectric. The situation would be different if we were disputing the *form* of (1), but actually we are merely questioning the value of the field strength which has been inserted. If we treat a dielectric as an assembly of doublets for the purpose of finding the mechanical action on part of it, we obtain statistical equations which have the same meaning as those derived by use of a continuous polarization. Any difficulty arising in the latter method is also present in the former, although in the former it may be somewhat disguised by the mathematical formalism. In fact, the use of discrete distributions would not prove the difficulty only apparent, as Smith-White seems to suggest, but would merely make its solution mathematically more difficult, which, as generally agreed, is basically the very reason why continuous distributions are used at all.

University College of the West Indies,
Jamaica.
23rd November 1951.

R. CADE.

CADE, R., 1951, *Proc. Phys. Soc.* A, **64**, 665.
FOWLER, R. H., 1936, *Statistical Mechanics* (Cambridge : University Press), pp. 437–439.
SMITH-WHITE, W. B., 1949, *Phil. Mag.*, **40**, 466; 1951, *Proc. Phys. Soc.* A, **64**, 945.

In the case of action of mechanical force on a material body we usually regard one or other of two ideal situations. The force may act at a *single point* in the body or it may be *distributed* throughout the volume of the body. Though it would be possible to contemplate more general kinds of force distributions, it is usually sufficient to consider only distributions which can be specified by a force density function. This function is then defined throughout the region occupied by the body. Such a specification of a continuously distributed force is possible only if the force acting on an element of the body is proportional to its volume being *independent of the shape of the element*. The notion of force density is meaningless in any other case. Cade asserts that the force acting on an element of a dielectric body depends on its shape; but he also speaks of the " calculation of the force density by known methods ". If the distribution of mechanical force acting in a dielectric is the unique thing in theoretical physics which Cade claims it to be, then this distribution cannot be specified by a force density function.

In spite of the remarks in his note above, Cade does not calculate explicitly the mechanical force on any dielectric element (of whatever shape). He merely refers to the Poisson distributions to make some observations on the problem. There is a sense in which the distribution of mechanical force acting on a dielectric is peculiar—it is distributed partly throughout the *volume* of the body and partly over the *surface* of the body. For this reason the problem of the distribution of the force remains essentially the same however small the dielectric body is taken to be. The crude application by Cade of the principle of action and reaction is wholly inadequate for the discussion of this problem, for it gives merely the *total* force acting on the element.

To conclude, the point at issue is simply this—what is the distribution of the mechanical force which acts on a dielectric body under electrical influence ? I regard this question as a fundamental one, for it affects our whole construction of the mathematical theory of electricity (Smith-White 1951). Cade prefers the established theory due to Korteweg and Helmholtz which I have examined before. I have, in fact, shown that some notions 'generally agreed on' are erroneous, that some 'established electrical principles' are false, and that some 'known methods' are fundamentally unsound.

Department of Mathematics, W. B. SMITH-WHITE.
University of Sydney.
3rd January 1952.

SMITH-WHITE, W. B., 1951, *Proc. Roy. Soc. N.S.W.*, **85**, 15 and 79.

Anomalous Dielectric Loss in some of the Alums

While making measurements on paramagnetic resonance in salts such as the chromic alums, it was noticeable that the dielectric loss in salts of very similar structure was sometimes widely different. It was therefore decided to investigate the dielectric behaviour of these and similar salts at microwave frequencies, and this letter gives a brief outline of the results obtained.

The most interesting result is the way in which the dielectric loss varies with temperature between 80° K and 300° K. In some of the alums there is a marked peak in the loss, which is frequency dependent and which is well described by a Debye type of curve. The results for these alums are given in the table.

	Temperature T_m (°K)				
Alum	$\lambda=3{\cdot}0$	$\lambda=1{\cdot}18$	$\lambda=0{\cdot}85$	a	$b\times10^{-3}$
$AlCH_3NH_3(SO_4)_212H_2O$	262	>300	>300	−30	1·3
$CrCH_3NH_3(SO_4)_212H_2O$	237	>300	>300	−30	1·2
$AlNH_4(SO_4)_212H_2O$	173	200	210	−32	1·2
$FeNH_4(SO_4)_212H_2O$	177	203	213	−32	1·3
$CrNH_4(SO_4)_212H_2O$	175	202	212	−32	1·2
$AlNH_4(SeO_4)_212H_2O$	155	193	—	−30	0·75
$CrNH_4(SeO_4)_212H_2O$	—	193	—	−30	0·75
$CrK(SO_4)_212H_2O$	185	210	215	−33	1·5
$AlK(SO_4)_212H_2O$	188	209	—		
$CrRb(SO_4)_212H_2O$	182	—	—		

λ is in centimetres.

Here λ is the wavelength at which measurements were made and T_m is the temperature at which the maximum loss occurs. At this temperature a relaxation time τ can be defined such that $\omega\tau = 2\pi c\tau/\lambda = 1$, and the variation of τ with temperature can be represented by $\ln \tau = a + b/T$. Several runs were made with each salt and the spread of values of T_m was about 2° at 3 cm wavelength, 3° at 1·18 cm and 5° at 0·85 cm.

As a test that the anomalous absorption can be represented by the Debye expression, a curve was constructed for the case of $AlNH_4(SO_4)_2 12H_2O$ by using the values of a and b to give τ at each temperature and then the Debye expression $\epsilon'' \propto \omega\tau/(1+\omega^2\tau^2)$ to give a quantity proportional to the loss. This curve fitted the experimental points very well in the region where the anomalous absorption was high.

That the variation of τ with temperature is well represented by the above relation over a considerable range is shown, for the case of $AlNH_4(SO_4)_2 12H_2O$, by the results of Guillien (1943), who measured the dielectric loss at frequencies between 50 c/s and $1{\cdot}3 \times 10^7$ c/s. He also found a Debye-like absorption and gave values of a and b which agree with our values within the experimental errors.

The values of a and b given in the table were obtained either from the variation of T_m with frequency or, in cases where this could not be done, from the value of T_m and the width of the absorption curve at one frequency, assuming the Debye expression.

It seems likely that this effect is due to the monovalent ion or possibly to the water molecules surrounding it. The following are the main results on which this view is based.

(i) The effect of replacing Al by Cr or Fe as the trivalent ion is very small, both as regards the position and the magnitude of the absorption maximum.

(ii) The effect of replacing S by Se in $AlNH_4(SO_4)_2 12H_2O$ and $CrNH_4(SO_4)_2 12H_2O$ is to make a small reduction in the temperature at which the maximum occurs, but the magnitude of the absorption is not changed very greatly.

(iii) The univalent ion has a very great influence on the magnitude of the absorption. Thus the maximum absorption in the ammonium and methylamine alums is very large. This may be due to relaxation processes in the molecular ions themselves. However, the potassium alums also show an effect, although much smaller than in the ammonium alums, and there is a just detectable effect in one of the rubidium alums. No effect could be found in $CrCs(SO_4)_2 12H_2O$ or $AlNa(SO_4)_2 12H_2O$.

No absolute measurements of the dielectric loss were made, and therefore the above comparisons of the magnitudes are qualitative only.

Apart from this Debye-like absorption, the following alums show abrupt transitions in both the real and imaginary parts of their dielectric constant at a temperature which is independent of frequency: $AlCH_3NH_3(SO_4)_2 12H_2O$ at 170° ± 2° K, $Cr_3CH_3NH_3(SO_4)_2 12H_2O$ at 160° ± 2° K, $FeNH_4(SO_4)_2 12H_2O$ at 83° ± 2° K, $CrNH_4(SO_4)_2 12H_2O$ at 80° ± 2° K and $CrNH_4(SeO_4)_2 12H_2O$ at 108 ± 2° K. These last two alums are observed to shatter and become opaque, and the transition temperature on warming is a few degrees higher than on cooling.

The transition in $CrNH_4(SO_4)_2 12H_2O$ is clearly the same as that found by Bleaney and Penrose (1948) in paramagnetic resonance experiments and by Kraus and Nutting (1941) in optical experiments. The latter authors also report the transition in $CrNH_4(SeO_4)_2 12H_2O$.

No anomalous effects were found in the following Tutton salts: $Cu(NH_4)_2(SO_4)_2 6H_2O$, $Zn(NH_4)_2(SO_4)_2 6H_2O$, $CuK_2(SO_4)_2 6H_2O$ and $ZnK_2(SO_4)_2 6H_2O$.

A full account of this work is in course of preparation.

The Clarendon Laboratory,
Oxford.
17th January 1952.

J. H. E. Griffiths.
J. A. Powell.

Bleaney, B., and Penrose, R. P., 1948, *Proc. Phys. Soc.*, **60,** 395.
Guillien, R., 1943, *C. R. Acad. Sci., Paris*, **217,** 443.
Kraus, D. L., and Nutting, G. C., 1941, *J. Chem. Phys.*, **9,** 133.

Further Evidence for the Lord–Rees–Wise Theory of Luminescence Decay of ZnS.Ag*

The investigations of Lord, Rees and Wise (1947) on luminescence have been justly criticized (for example by Garlick and Gibson 1948) on the grounds that they were confined to one phosphor. However, recent discussions with Rees and Wise on their subsequent luminescence researches have encouraged the author to publish some old work on the application of the Lord–Rees–Wise theory to the results of other workers.

The results analysed by the method of Lord, Rees and Wise were those of Johnson and Davis (1939) and of Nelson, Nottingham and Johnson (1939). These were the only available observations, of suitable time range, for ZnS.Ag. Both groups of workers used the same phosphor (exact composition not stated) and carried out all observations at room temperature. Johnson and Davis used ultra-violet (λ2537 Å) excitation at two different exciting intensities. Nelson, Nottingham and Johnson irradiated the phosphor with 10 000 v electrons at four different current densities.

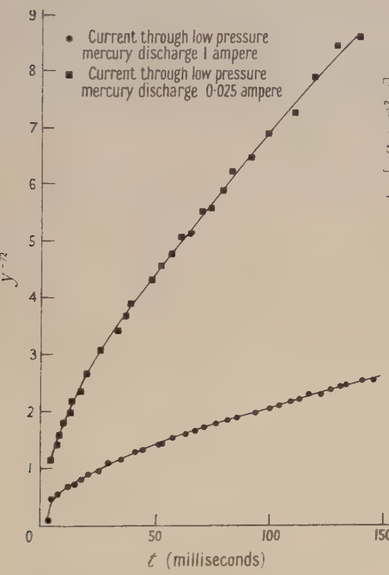

Fig. 1. $y^{-1/2}$ plotted against t for observations of Johnson and Davis.

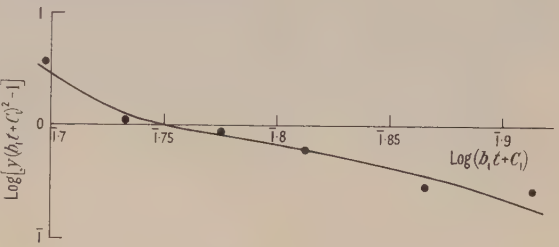

Fig. 2. Representative plot of $\log[y(b_1t+C_1)^2-1]$ against $\log(b_1t+C_1)$.

Exciting intensity	$b_1 \times 10^3$	ρ
Current through mercury lamp		
1 amp	11·75	8·6
0·025 amp	50	8·2
Electron current density		
1180 μA/cm²	190	4·5
74 μA/cm²	240	7·7
1·8 μA/cm²	330	12·7

Lord, Rees and Wise have shown that if two activating centres (silver and interstitial zinc) are present, the decay, if bimolecular, will eventually satisfy $y^{-1/2}=b_1t+C_1$, where y is the recorded luminescent intensity at time t, and b_1 and C_1 are constants; b_1 is proportional to the square root of the recombination coefficient for zinc centres. They further showed that, at shorter times, $\log[y(b_1t+C_1)^2-1]=\log B+(1-\rho)\log(b_1t+C_1)$ would be satisfied. In this expression B and ρ are constants; ρ is the ratio of the recombination coefficients of silver and zinc centres.

The reciprocal of the square root of the recorded luminescent intensity was therefore plotted against time for all observations except those for the smallest electronic current density, which were very scattered: curves for the observations of Johnson and Davis are shown in fig. 1. In every case there is a fair time range over which $y^{-1/2}vt$ is linear. b_1 and C_1 were deduced from the curves. $\operatorname{Log}[y(b_1t+C_1)^2-1]$ was then plotted against $\log(b_1t+C_1)$ for the observations: a representative plot, that for 1 180μA/cm² electronic excitation, is shown in fig. 2. ρ and $\log B^{1/(\rho-1)}$ were derived from the slope and intercept respectively of the linear part of these curves; the b_1 and ρ values are given in the table.

In order to evaluate the theoretical expression for the luminescent intensity at very short times, values of a further parameter ζ, the initial ratio of concentrations of ionized silver and zinc centres, are required. These could not be obtained as they depended on the unknown spectral response curve of the photocell used to record the observations.

---

* This investigation was included in work approved by the University of London for the degree of Ph.D.

It thus appears that the observations of Johnson and Davis and of Nelson, Nottingham and Johnson also correspond quantitatively to a bimolecular decay law with two types of activating centre. Moreover, as found by Lord, Rees and Wise, the values of the derived constants differ in some respects from those expected on the simple theory. Since electron bombardment raises the temperature of a phosphor appreciably (Fonda 1945), ρ again decreases with increasing temperature: this was explained by Lord, Rees and Wise on the basis of traps associated with ionized activating centres. That the lowest electron current density ρ value is greater than the ultra-violet value may arise from the different kinds of excitation. Since Lord, Rees and Wise used $\lambda 3650$ Å excitation, a similar explanation may also apply to the difference between their value of ρ at room temperature and that of Johnson and Davis; on the other hand, this difference might arise from different preparative conditions of the phosphors. The b_1 values of both groups of American workers increase with decreasing exciting intensity, as did those of Lord, Rees and Wise: it may be that copper centres are again responsible. Although the Americans do not mention the presence of copper, it is unlikely to be absent from a ZnS.Ag phosphor (Rees 1942). There are insufficient observations to determine whether the curves deviate from $y^{-1/2}=b_1t+C_1$ at long times, as would be expected if copper is present.

The results of Johnson and Davis and of Nelson, Nottingham and Johnson would seem to lend support to the Lord–Rees–Wise theory of luminescence of ZnS.Ag phosphors.

Chelsea Polytechnic,
London.
7th January 1952.

MARY P. LORD.

FONDA, G. R., 1945, *Trans. Electrochem. Soc.*, **87**, 339.
GARLICK, G. F. J., and GIBSON, A. F., 1948, *Proc. Phys. Soc.*, **61**, 102.
JOHNSON, R. P., and DAVIS, W. L., 1939, *J. Opt. Soc. Amer.*, **29**, 283.
LORD, M. P., REES, A. L. G., and WISE, M. E., 1947, *Proc. Phys. Soc.*, **59**, 473.
NELSON, R. B., NOTTINGHAM, W. B., and JOHNSON, R. P., 1939, *J. Appl. Phys.*, **10**, 335.
REES, A. L. G., 1942, *Chem. Soc. Ann. Rep.*, **39**, 76.

The Use of Gold Leaf as a Reference Material in the Determination of Lattice Constants by Electron Diffraction

In a recent issue of this journal Boswell (1951) has reported measurements by the electron diffraction method of the lattice constants of several alkali halides of small crystal sizes. He used an evaporated film of TlCl as the standard reference material. In contradistinction to Finch and Fordham (1936), who used beaten gold leaf as a reference, Boswell found no significant increase in lattice dimensions as compared with the x-ray values for the alkali halides for crystal sizes greater than 150 Å; with smaller crystal sizes a progressive *reduction* in lattice constants was found.

A series of electron diffraction experiments carried out several years ago by the present writer at the suggestion of Professor G. I. Finch in an effort to determine the reasons for the discrepancies found by Finch and Fordham has been described in full elsewhere (Garrod 1947), but, as the results were not submitted for general publication, it may be of interest to state them briefly here.

The investigation was restricted to specimens of high-purity NaCl prepared by evaporation from a heated platinum or tungsten filament *in vacuo* on to either a graphite (from 'Aquadag') or a gold substrate. With one exception the gold films were prepared by thinning beaten gold leaf in N/100 KCN solution. After evaporation of the NaCl, the composite specimens were left in air for periods ranging from approximately one minute to several days before being transferred to the electron diffraction camera, in which the gold and sodium chloride diffraction patterns were recorded simultaneously. The mean crystal sizes for the NaCl films (when examined in the camera) ranged from 80–150 Å. Composite graphite–gold specimens were also made and examined. In addition, two graphite–gold–sodium chloride specimens were prepared; one of these was a composite specimen in which the three diffraction patterns were recorded simultaneously, in the other a modified 'split-shutter' technique was used by which gold and NaCl rings were first recorded together on one half of the plate and the other half then exposed to record the graphite pattern.

The results were as follows :

(i) From five composite graphite–sodium chloride specimens the lattice constant of NaCl referred to the C–C spacing in graphite ($a=2\cdot4563$ A) was found to agree with the x-ray value (5·627 Å) to within ±0·05%, which was the estimated probable error in measurement.

(ii) From ten gold leaf–sodium chloride specimens, however, a (NaCl) referred to a value of 4·070 Å for the lattice constant of gold ranged from 5·630 to 5·642 Å, an increase of 0·05 to 0·27% over the x-ray value. (Similar anomalies have recently been observed by Uyeda and Kato (private communication) for KCl films referred to gold.) There was no evidence of any correlation between the mean crystal size of an NaCl film and the value obtained for its lattice parameter.

(iii) From the two Au–C–NaCl specimens the values found for a (NaCl) referred to a value for a (Au) of 4·070 Å were 5·635 and 5·637 Å, but when referred to graphite the values were 5·630 Å in each case for a (NaCl) and 4·067, 4·065 Å for a (Au).

(iv) One composite Au–NaCl specimen was prepared in which the gold reference film was produced by evaporating gold *in vacuo*. In this case the value for a (NaCl) was found to be 5·629 Å.

It therefore appeared from these results that for a crystal size larger than about 100 Å the lattice parameter obtained for NaCl films agreed within experimental error with the accepted x-ray value, and these conclusions are confirmed by Boswell's experiments. Furthermore, they pointed to the unreliability of beaten gold leaf as a reference material in accurate electron diffraction work, a result that was suggested by the previous observations of Riedmiller (1936), Boochs (1939) and Chia-Si Lu and Malmberg (1943). It is also interesting to note that whereas a recalculation by Finch and Wilman (1937) of the previous results of Finch and Fordham (1936) gave a *mean* value for a (Au) of 4·067 Å referred to precision x-ray measurements for the C–C spacing in graphite, the spread in values for nine 'split-shutter' graphite–gold patterns ranged from 4·053 to 4·081 Å.

The origin of the anomalously low values of lattice parameter that sometimes occur in thin gold films prepared from beaten leaf is still rather obscure. It might be expected that, as a result of the severe compressive stresses operative during rolling and beating of the gold in manufacture of the leaf, a residual system of internal stresses would be produced which would cause a contraction in lattice spacing in those (hkl) planes that are approximately normal to the plane of the leaf and that are responsible for the diffraction process in transmission-type photographs in electron diffraction work. However, complementary back-reflection x-ray measurements carried out on samples of gold leaf similar to those used for the electron diffraction experiments outlined above indicated that the contraction in interplanar spacing for (420) planes making an angle of 72° with the plane of the leaf was only 0·04 to 0·06%. This is much too small to account completely for some of the electron diffraction results. Very different crystal sizes are responsible for the diffraction process in the two cases, and it may be that the change in lattice spacing due to cold work is greater for the surface layers than for the material in bulk, but there does not at present appear to be any direct evidence in support of this suggestion. It is also possible that surface tension forces in the thin gold films may play an important part (Rymer and Butler 1947), but it is difficult to see why such an effect should be more pronounced in beaten leaf than in evaporated films of the same crystal size.

Defence Research Laboratories,
Victoria, Australia.
10th January 1952.

R. I. Garrod.

Boochs, H., 1939, *Ann. Phys., Lpz.*, **35**, 333.
Boswell, F. W. C., 1951, *Proc. Phys. Soc.* A, **64**, 465.
Chia-Si Lu, and Malmberg, E. W., 1943, *Rev. Sci. Instrum.*, **14**, 271.
Finch, G. I., and Fordham, S., 1936, *Proc. Phys. Soc.*, **48**, 85.
Finch, G. I., and Wilman H., 1937, *Ergebn. exakt. Naturw.*, **16**, 353.
Garrod, R. I., 1947, *Thesis* (University of London).
Riedmiller, R., 1936, *Z. Phys.*, **102**, 408.
Rymer, T. B., and Butler, C. C., 1947, *Proc. Phys. Soc.*, **59**, 541.

The Crystal Parameters of Beryllium

Several values of the crystal parameters of beryllium have appeared in the literature since 1921, and on first glance there would appear to be disagreement between the results of different workers. On closer examination the differences are more apparent than real because the values have been expressed in different units and at different temperatures, and the purity of the material sometimes is not definitely stated. The purpose of this note is to bring the different published values together, and to present them all in terms of the same unit, the true Ångström, at the same temperature.

The first two determinations were made by Meier in 1921 and by McKeehan in 1922. The values at room temperature were

Meier : $a=2{\cdot}286$ KX $\;2{\cdot}291$ Å $\;c=3{\cdot}619$ KX $\;3{\cdot}626$ Å $\;c/a=1{\cdot}583$

McKeehan : $a=2{\cdot}283$ KX $\;2{\cdot}288$ Å $\;c=3{\cdot}607$ KX $\;3{\cdot}614$ Å $\;c/a=1{\cdot}580$

The crystal Ångström (KX unit) is multipled by 1·00202 to convert it into the true or absolute Ångström (Å) of 10^{-8} cm. These early values are in fair agreement considering the accuracy of measurement at the time the determinations were made and the uncertain purity of the material employed. They were the accepted crystal parameters of beryllium until 1932 when Neuburger determined the lattice constants of material containing traces of iron, barium and carbon; at 20°C they were found to be :

$a=2{\cdot}2680$ KX $\;2{\cdot}2726$ Å $\;c=3{\cdot}5941$ KX $\;3{\cdot}6014$ Å $\;c/a=1{\cdot}5847$

The axial ratio agreed closely with that found by Meier, but the individual values of the parameters differed materially from those of the previous workers.

Measurements were made in this laboratory in 1935 and 1936 with powder material of 99·8% purity, containing as impurities 0·01% iron, 0·05% carbon, 0·005% nitrogen and traces of silicon and aluminium. The following summary of the parameter values at 20°C was published by Owen and Richards in 1936 :

a (KX)	c (KX)	c/a	References
$2{\cdot}2812_6$	$3{\cdot}5780_0$	$1{\cdot}5684_3$	Owen, Pickup and Roberts (1935)
$2{\cdot}2811_1$	$3{\cdot}5770_8$	$1{\cdot}5681_3$	Owen and Pickup (1935)
$2{\cdot}2813_4$	$3{\cdot}5773_2$	$1{\cdot}5680_3$	Owen and Richards (1936)

Mean values :

	a	c	c/a	
	$2{\cdot}2812_4$ KX	$3{\cdot}5774_7$ KX	$1{\cdot}5682_1$	at 20°C
or	$2{\cdot}2858_5$ Å	$3{\cdot}5847_0$ Å	$1{\cdot}5682_1$	

In 1949 Gordon, using powder material of 99·4% purity, gave the following mean values at 25°C : $a=2{\cdot}2858_7$ Å; $c=3{\cdot}5843_2$ Å; $c/a=1{\cdot}5680_3$. Reduced to 20°C, using the thermal expansion curves of Owen and Richards (1936), these figures become $a=2{\cdot}2857_2$ Å; $c=3{\cdot}5841_2$ Å ; $c/a=1{\cdot}5680_5$. These values are in much closer agreement with the values found in this laboratory (1935, 1936) than with those found by Neuburger (1932).

Further determinations of the lattice constants of beryllium are to be found in a paper by Kaufmann, Gordon and Lillie (1950), who used beryllium in different forms : powder, lump, distilled and flake. They find slight differences between the values of the constants according to the state of the material ; the maximum difference, amounting to about 1 in 2 500, was observed in the c-parameter.

Gordon (1949) also measured the thermal expansion of beryllium in powder form at temperatures up to 1 000°C. This range of temperature exceeds that employed by Owen and Richards (1936), the highest temperature reached by whom was 550°C. It is of interest to examine the two sets of values over this restricted range. The results are shown graphically in the figure. There is close agreement between the two sets of results except over the range 0° to 250°C for the c-parameter, but even over this range the divergence is not pronounced, and one is justified in stating that, although the purities of the materials used in the two investigations differ slightly, the results obtained between room temperature and 550°C in 1949 agree closely with those obtained in 1936.

At 20° c the values of the lattice parameters of beryllium in powder form may be taken as follows :

99·4% purity (Gordon 1949) $a=2{\cdot}2857_2$ Å; $c=3{\cdot}5841_2$ Å; $c/a=1{\cdot}5680_5$.
99·8% purity (Owen and Richards 1936) $a=2{\cdot}2858_5$ Å; $c=3{\cdot}5847_0$ Å; $c/a=1{\cdot}5682_1$.

The *a*-parameters agree within the limits of experimental error. The difference between the values of the *c*-parameters may be due to the difference in the purities of the materials. Without further investigation it is impossible to make a more definite statement concerning the value of this parameter. The above determinations of the crystal parameters of beryllium do not confirm the measurements of Neuburger (1932).

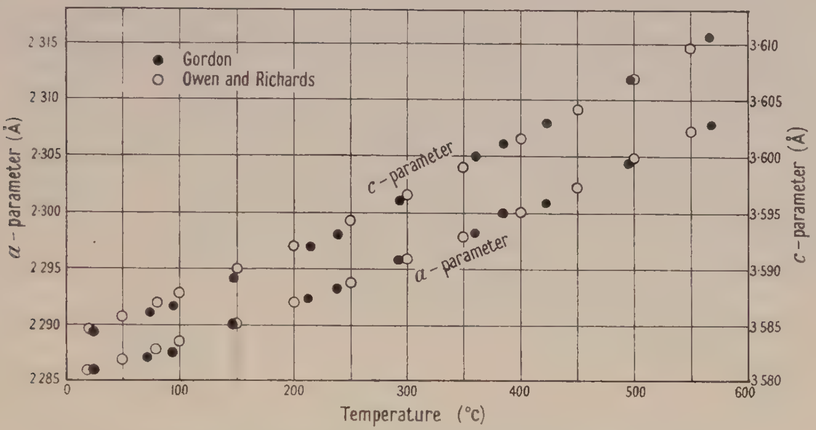

Variation, with temperature, of the crystal parameters of beryllium.

University College of North Wales,
Bangor.
1st February 1952.

E. A. Owen.

Gordon, P., 1949, *J. Appl. Phys.*, **20**, 908.
Kaufmann, A. R., Gordon, P., and Lillie, D. W., 1950, *Trans. Amer. Soc. Mech. Engrs.*, **42**, 785.
McKeehan, L. W., 1922, *Proc. Nat. Acad. Sci., Wash.*, **8**, 270.
Meier, G., 1921, *Diss.*, Göttingen.
Neuburger, M. C., 1932, *Z. phys. Chem.*, **17**, 285.
Owen, E. A., and Pickup, L., 1935, *Phil. Mag.*, **20**, 1155.
Owen, E. A., Pickup, L., and Roberts, I. O., 1935, *Z. Kristallogr.*, **91**, 70.
Owen, E. A., and Richards, T. L., 1936, *Phil. Mag.*, **22**, 310.

Response of Organic Scintillators to d–d Neutrons

Because of their high proton density, organic scintillation crystals have proved very useful in the detection of fast neutrons by proton recoil. To estimate the neutron energy or flux it is necessary to know the pulse height distribution of the recoil protons.

We have investigated the recoil pulse height spectra in anthracene, trans-stilbene, and diphenyl-acetylene of neutrons produced by the d–d reaction; an occluded target was used with deuterons of 150 kev energy. To minimize inelastic scattering in the vicinity of the target, this was made of thin aluminium, and not more than 4 gamma quanta/1000 neutrons originated from it (Beghian *et al.* 1950).

The crystals, supplied by National Radiac Inc., were disc shaped, 1·5 cm in diameter, 5 mm thick, and surrounded by aluminium reflectors. These were used in conjunction with a 14-stage E.M.I. photomultiplier, Type 6262, followed by a linear amplifier, and single channel kicksorter.

The pulse height distributions are shown in figs. 1 and 2. Since various amplifier gains were used, the voltage scale does not represent the same scale of pulse height in each case. The ratio of maximum pulse heights for anthracene, stilbene, and diphenyl-acetylene is 1 : 0·6 : 0·2.

In the case of stilbene, the form of the distribution shows that pulse height is closely proportional to scintillation energy. For anthracene, however, the rise at low energies indicates that the pulse height is a more rapidly increasing function of energy.

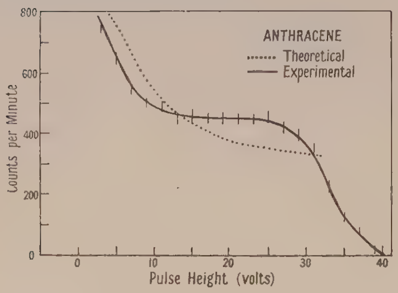

Fig 1.

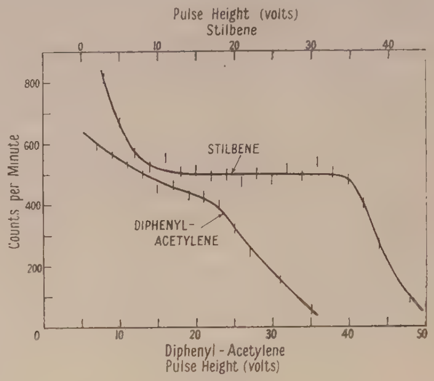

Fig. 2.

Taylor *et al.* (1951) have measured the light output of anthracene as a function of energy for deuterons, alpha-particles, molecular hydrogen ions and protons. Using their data, it is possible to calculate the expected recoil pulse height distribution and this is shown in fig. 1. Taylor's data for protons do not extend below 1 MeV, and for lower energies the calculations are based on extrapolation from the alpha-particle measurements. This may be the reason for the lack of close agreement between the calculated and experimental curves.

We wish to thank Lord Cherwell and Dr. H. Halban for their interest, and the Paul Foundation of the Royal Society for a grant which made this work possible.

The Clarendon Laboratory,
Oxford.
22nd January 1952.

R. A. Allen.
L. E. Beghian.
J. M. Calvert.

Beghian, L. E., Grace, M. A., Preston, G., and Halban, H., 1950, *Phys. Rev.*, **77**, 286.
Taylor, C. J., Jentschke, W. K., Remley, M. E., Eby, F. S., and Kruger, P. G., 1951, *Phys. Rev.*, **84**, 1034.

New Energy Level in ^{7}Li

A new energy level in ^{7}Li at 4·77 ± 0·10 MeV has recently been discovered by Gove and Harvey (1951) in experiments on the inelastic scattering of protons, deuterons and α-particles from ^{7}Li and the reaction ^{9}Be(d, α)^{7}Li, using deuterons with 14 MeV energy. The level has also been observed by Gelinas, Class and Hanna (1951) from measurements on the energies of the α-particles emitted from a beryllium target bombarded with 0·5 MeV deuterons. These workers obtained a value of 4·62 ± 0·02 MeV for the excitation energy.

In investigations of (d, α) reactions in light elements using a magnetic analyser, we have observed a group of α-particles from a beryllium target whose energy would correspond to a transition to this level in ^{7}Li. A short account of the experimental method has been given by Ashmore and Raffle (1951), and the existence of the level in ^{7}Li reported by Raffle (1951).

When a target of beryllium 0·2 mg/cm^2 thick, evaporated on to a gold backing foil, was bombarded with 5·31 ± 0·07 MeV deuterons from the Liverpool 37-inch cyclotron, the α-particle spectrum shown in the figure was obtained by magnetic analysis in a direction at 90 degrees to the incident beam. The peak at a magnetic field of 786 ± 4 is due partly to α-particles from oxygen contamination, and partly to $^7Li^{3+}$ recoils from transitions to the ground and 0·48 Mev levels of ^7Li. These recoil atoms, which have an energy of about 3·5 Mev, could be identified by the height of the pulse that they produced in the proportional counter used as a detector.

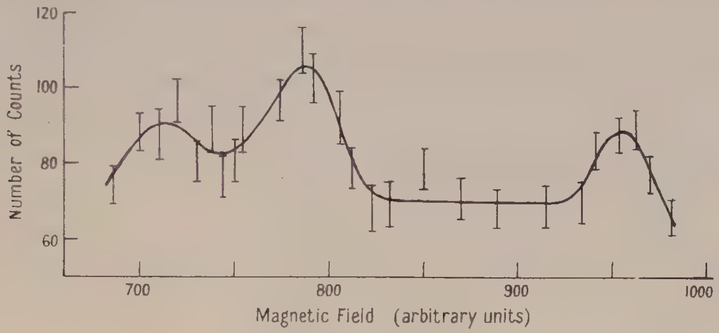

Spectrum from $^9Be(d, \alpha)\,^7Li$.

The peak at a magnetic field of 956 ± 4 corresponds to an α-particle energy of 4·04 ± 0·04 Mev, corrected for absorption in the target. This gives a Q value for the reaction $^9Be(d, \alpha)^7Li$ of 2·56 ± 0·10 Mev compared with the value of 2·53 ± 0·02 Mev obtained by Gelinas, Class and Hanna. Using a Q value of 7·15 Mev for the transition to the ground level of ^7Li we obtain a value of 4·59 ± 0·10 Mev for the excitation energy of the new level.

Nuclear Physics Research Laboratory,
University of Liverpool.
28th January 1951.

A. Ashmore.
J. F. Raffle.

Ashmore, A., and Raffle, J. F., 1951, *Proc. Phys. Soc.*, **64**, 754.
Gelinas, R. W., Class, C. M., and Hanna, S. S., 1951, *Phys. Rev.*, **83**, 1260.
Gove, H. E., and Harvey, J. A., 1951, *Phys. Rev.*, **82**, 658.
Raffle, J. F., 1951, *Ph.D. Thesis*, University of Liverpool.

The Photo-disintegration of Nitrogen-14 Nuclei

In the course of recent experiments on the multiple disintegration stars found in Ilford nuclear emulsions irradiated by bremsstrahlung of maximum energy 29 Mev we have been able to ascribe two small groups of stars to the photo-disintegration of nitrogen-14 nuclei. The first group consists of four-particle stars in which one track is considerably longer than any of the other three, and these are supposed to be due to the reaction reported by Goward and Wilkins (1951), namely $^{14}N + h\nu \rightarrow {}^2H + 3\,{}^4He - 17{\cdot}6$ Mev.

A second group of ^{14}N stars has been observed in two different plates—a beryllium-loaded E1 plate exposed to 80 röntgens of x-rays with a maximum energy of 26 Mev, and an ordinary C2 plate exposed to 100 röntgens at a maximum energy of 29 Mev. Each star consists of three tracks, the longest one being identified as a proton track by comparison with known proton tracks nearby; a second track is of greater density and of moderate length, and the third track is very short (fig. 1). In the first plate two of these events were observed in an area which contained 32 triple stars caused by the reaction $^{12}C(\gamma, 3\alpha)$. In the second plate three of the events were recorded together with 27 ^{12}C stars. In this energy range, therefore, the ratio of the numbers of ^{12}C stars and presumed ^{14}N triple stars is approximately 12 : 1.

The five stars mentioned above were investigated by applying the condition of conservation of momentum to the process, while it was assumed that no neutrons were emitted. By resolving the momentum of the proton emitted in a direction perpendicular to that of the very short track, we calculated the momentum of the particle carrying the track of intermediate length. The momenta (in mass-Mev units) in three cases were 3·8, 5·2, 4·9 and the corresponding ranges (in microns) 5·5, 10·4, 16·6.

Allowing for experimental errors, due chiefly to the difficulty of carrying out accurate measurements on tracks which dip steeply in the emulsion, it is found that these results agree closely with the range–momentum curve for α-particles.

The momentum of the very short track in each star was found by a similar method, and the values obtained in four cases are plotted against the observed ranges in fig. 2.

On the same graph are drawn the range–momentum curves for ^{10}B and ^{12}C ions, derived from the data of Millar and Cameron (1950), the range–momentum curve for α-particles at low energies, and two points for ^{8}Li ions observed in the beryllium-loaded plate as products in the reaction $^{9}Be+h\nu \rightarrow {}^{1}H+{}^{8}Li$. It is evident from fig. 2 that the very short tracks correspond to those produced by ions of mass number between 8 and 10. We are therefore led to ascribe these stars to the reaction $^{14}N+h\nu \rightarrow {}^{1}H+{}^{4}He+{}^{9}Be-18{\cdot}4$ Mev.

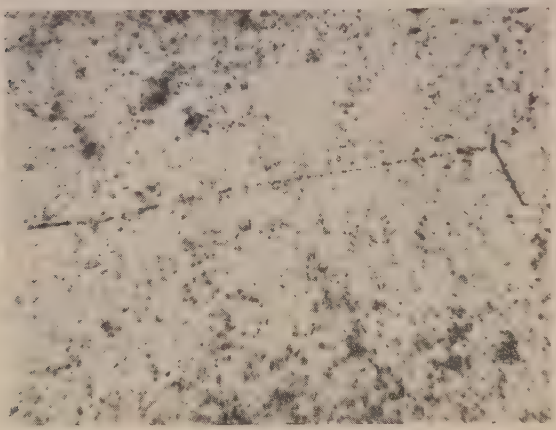

Fig. 1. Triple star. $^{14}N \rightarrow {}^{1}H+{}^{4}He+{}^{9}Be$.

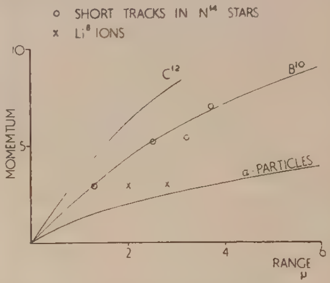

Fig. 2. Range–momentum relations for α-particles, ^{10}B and ^{12}C ions.

The total energies of the product particles were found in four cases to be 4·5, 7·4, 8·7 and 10·8 Mev, corresponding to γ-ray energies of 22·9, 25·8, 27·1 and 29·3 Mev respectively. Efforts have been made to find out whether the reaction proceeds in two stages, e.g. via ^{5}Li or via excited states of ^{10}B or ^{13}C. No conclusions can be drawn from so few data, but three cases out of four agree with a mode of disintegration via an excited level in ^{10}B at about 9 Mev above the ground state.

We should like to thank Professor Mitchell for the use of the synchrotron and facilities in the Department of Radiotherapeutics at Cambridge.

Oundle School,
Northants.
Department of Radiotherapeutics,
The University, Cambridge.
5th February 1952.

D. L. Livesey.
C. L. Smith.

Goward, P. K., and Wilkins, J. J., 1951, *Proc. Phys. Soc.* A, **64**, 312.
Millar, C. H., and Cameron, G. W., 1950, *Phys. Rev.*, **78**, 78.

Long Wavelength Absorption Band of Thiophene

The ultra-violet absorption spectrum of thiophene has been investigated theoretically by Longuet-Higgins (1949), experimentally by Price and Walsh (1941), Menczel (1927) and more recently by Millazzo (1947, 1948). Similar chemical properties of the two isosters, benzene and thiophene have been recorded in the literature. Recent investigations also show that there is similarity in the spectroscopic character of these two molecules (Walsh 1948).

Thiophene shows selective absorption below about 2600 Å down to the vacuum ultra-violet. An absorption spectrum in the region 2600–2000 Å has been assigned by Millazzo (1948) to two or possibly three electronic transitions in thiophene. In view of the similarity between these two molecules, it was thought of interest to investigate the possibility of obtaining a longer wavelength absorption corresponding to 3400 Å singlet–triplet transition of benzene, which has been recorded in absorption by Sklar (1937) and Pitts (1950) and in emission by Shull (1949).

Concentrated solutions (2N and 4N) of carefully purified thiophene were measured in n-hexane on a calibrated Beckman Quartz Spectrophotometer Model DU using an optical path of 5 cm. An absorption band with two maxima at 3180 Å and 3130 Å with $\epsilon_{\max}=0\cdot048$ was recorded. The low intensity of the band suggests that it represents a forbidden transition and perhaps corresponds to the singlet–triplet transition of thiophene.

Singlet–triplet transitions of a large number of molecules have been investigated recently by Kasha (1950), Reid (1950) and others. The various criteria described by Kasha for identifying the types of triplet transitions ($\Pi-\Pi$ or $n-\Pi$), considering both theory and experiment, have been applied in the present case.

Assuming that the long wavelength transition here recorded represents a single singlet–triplet transition analogous to 3 400 Å absorption of benzene, the mean life and oscillator strength are found to be of the order of $\tau=4\times10^{-3}$ sec and $f=0\cdot5\times10^{-6}$. The ratio f_{11}/f_{31} (where f_{11} is the oscillator strength of the first allowed singlet–singlet transition, and f_{31} that of the singlet–triplet one) in the present case is of the order of 10^6. These quantities fall within the range to assign the transition in question to a multiplicity forbidden singlet–triplet one. It is much stronger than the corresponding absorption of benzene ($f=1\cdot2\times10^{-8}$), since the transition in thiophene is no longer symmetry-forbidden due to the reduction of symmetry from D_{6h} in benzene to C_{2v} in thiophene.* The bands persist even in an acid medium though with a slight change of intensity. This perhaps proves that the absorption is a $\Pi-\Pi$ type singlet–triplet absorption of thiophene. There is a certain amount of uncertainty as to whether the upper state is a single triplet level or two triplet levels separated by 500 cm^{-1} corresponding to two observed maxima. The vibrational analysis of the long column vapour absorption spectrum and the corresponding phosphorescence may give a unique assignment and is likely to throw some light on the corresponding transition in benzene.

Department of Chemical Technology,
Bombay University, Bombay.
5th February 1952.

M. R. Padhye.
S. R. Desai.

Kasha, M., 1950, *Discussions of the Faraday Society*, **9**, 14.
Longuet-Higgins, H. C., 1949, *Trans. Faraday Soc.*, **45**, 173.
Menczel, S., 1927, *Z. phys. Chem.*, **125**, 161.
Millazzo, G., 1947, *Experientia*, **3**, 370; 1948, *Rend. Ist. Super Sanità*, **11**, 372.
Pitts, A. C., 1950, *J. Chem. Phys.*, **18**, 1416.
Price, W. C., and Walsh, A. D., 1941, *Proc. Roy. Soc.* A, **179**, 201,
Reid, C., 1950, *J. Chem. Phys.*, **18**, 1673.
Shull, H., 1949, *J. Chem. Phys.*, **17**, 295.
Sklar, A. L., 1937, *J. Chem. Phys.*, **5**, 669.
Walsh, A. D., 1948, *Quart. Rev.*, **2**, 85.

* Either $^3B_{1u}$ or $^3B_{2u}$ to $^3A_1$ or $^3B_1$, both allowed.

Report of the Copenhagen Meeting of the General Assembly of the International Union of Pure and Applied Physics

The General Assembly of the Union met at Copenhagen on the 11th, 12th and 13th July 1951 on the occasion of a conference organized by Professors N. Bohr and S. Rozental under the auspices of the Union.

The Assembly sent a message to the Director-General of UNESCO expressing its gratitude for the very effective help which that organization extends to the Union. The Assembly also expressed its gratitude to all members of the former Executive Committee, to such Vice-Presidents as are not eligible for re-election and in particular to the President, Professor H. A. Kramers.

The following elections were made unanimously :

Executive Committee

President : N. F. Mott (Bristol).

Vice-Presidents : E. Amaldi (Rome), G. Borelius (Stockholm), A. Heyrowsky (Prague), P. Huber (Bâle), K. S. Krishnan (New Delhi), M. L. Oliphant (Canberra), J. C. Slater (Cambridge, Mass.), and J. A. Wheeler (Princeton, N.J.).

Secretary-General : P. Fleury (Paris).

Specialized Committees

1. *Finance* : E. Bauer (Paris), C. J. Gorter (Leiden).
2. *Symbols, Units and Nomenclature* : A. Pérard, President (until the end of 1951), H. König, President (Berne), J. de Boer, Secretary (Amsterdam), J. Cabannes (Paris), E. Guggenheim (Reading), E. Perucca (Turin), J. H. Van Vleck (Cambridge, Mass.).
3. *Thermodynamics and Statistical Mechanics* : J. Mayer, President (Chicago), I. Prigogine, Secretary (Brussels), E. Bauer (Paris), J. A. Beattie (Cambridge, Mass.), S. R. de Groot (Utrecht), E. Rushbrooke (Newcastle, U.K.).
4. *Cosmic Rays* : P. M. S. Blackett, President (Manchester), L. Leprince-Ringuet, Secretary (Paris), C. D. Anderson (Pasadena, California), G. Bernardini (Rome), H. J. Bhabha (Bombay), M. S. Vallarta (Mexico).
5. *Very Low Temperatures* : F. E. Simon, President (Oxford), C. J. Gorter, Secretary (Leiden), F. C. Brickwedde (Washington, D.C.), K. Clusius (Zürich), A. van Itterbeek (Louvain), C. E. Lane (Newhaven, Conn.).
6. *Publications* : J. H. Awbery, President (London), G. A. Boutry, Secretary (Paris), M. Fierz (Bâle), A. D. Fokker (Amsterdam), E. Hutchisson (Cleveland, Ohio), E. Perucca (Turin).
7. In addition the General Assembly has decided to form a new specialized committee for *Acoustics*. It has named the following to join in this Committee :

   R. H. Bolt, President (Cambridge, Mass.), C. W. Kosten, Secretary (Delft), F. Canac (Marseille), F. Ingerslev (Copenhagen), A. Giacomini (Rome), E. Mayer (Göttingen), W. P. Wilson (Tadworth, U.K.).

   Mr. Wilson having been unable to accept, his name was replaced by that of Mr. W. West (London).

The following proposed conferences were discussed and were considered favourably, though it was agreed that the list was provisional, and could be changed by the Executive Committee according to the funds available and in consequence of suggestions of local organizing Committees).

1952. Structure and properties of solid surfaces (Chicago : September or October 1952).
Spectroscopy of β and γ rays (Amsterdam : the dates were fixed later as 1st 7th September 1952).
Thermodynamics of phase transitions (Paris : the dates were fixed later as 3rd–7th June 1952).
The relation between optics and the study of short waves, or some other subject in optics (Milan in April or May 1952).

1953, Nuclear physics (Italy).

1954. Physiological optics and its connection with instrumental optics (Spain ?).
Fundamental problems of theoretical physics (Kyoto).
Thin films (Bristol).
Acoustics (at a place to be fixed).
Spectroscopy (at a place to be fixed).

The various specialized Committees reported on their work. The summary printed here includes only the report of the Committee for Symbols, Units and Nomenclature (S.U.N.), which was adopted by the General Assembly. Their recommendations are as follows :

1. It was recommended that the use of the word 'billion' should be avoided in scientific literature. The use was recommended, for example, of either 10^9 ev or GeV (as agreed by IUPAP in 1948).

2. After prolonged discussion, the S.U.N. Committee decided, so as not to take any steps which would increase the cost of printing, that the recommendations adopted in 1948 concerning the indices affixed to the symbols for the chemical elements should not be changed.

3. IUPAP recommended to physicists who wish to confine the word 'isotope' to different atoms having the same atomic number, the use of the word 'nuclide' to describe atoms which are identical both as regards their atomic number and their mass number. This recommendation is only to take effect after agreement with the Union of Chemistry.

4. The practical system of units, which will be called the Giorgi's system or the m.k.s.a. system, is to be based on the following units : metre, kilogram-mass, second, ampere ; in certain cases a different choice of four independent units could be made.

5. Since, in the near future, the c.g.s. system and the m.k.s.a. system may both be employed at the same time in pure and applied physics, and in order to facilitate the conversion of one of these units into the other, the introduction is recommended, with a view to defining the secondary units, of the following c.g.s. systems founded on the *four* principal units : (*a*) the c.g.s. electrostatic system, or c.g.s.e. system, based on the centimetre, the gramme, the second and the electrostatic unit of charge; (*b*) the electromagnetic c.g.s. system, or c.g.s.m. system, based on the centimetre, the gramme, the second and the deca-ampere.

6. (*a*) It was recommended that IUPAP suggest to the International Commission of Electrotechnics that a joint Committee should be set up to formulate recommendations on all questions concerning rationalization of units. (*b*) It is not desirable to recommend to physicists that only rationalized equations should be used or only non-rationalized equations. (*c*) The General Assembly of the Union of Physics considers that, in the case of rationalized equations, the rationalization should be obtained by the introduction of new measures.

7. The International Union of Physics authorizes the publication of the list of symbols of which the adoption is recommended by the S.U.N. Committee.

REVIEWS OF BOOKS

Experimental Spectroscopy, by R. A. Sawyer. Pp. x + 358. 2nd Edition. (London : Chapman and Hall, 1951.) 30*s*.

This is the second edition of a deservedly popular work. The thirteen chapters are headed as follows : History of spectroscopy, Light sources, Spectroscopic apparatus—general principles, Prism spectroscopes and spectrographs—theory and construction, Prism spectrographs—types and uses, The diffraction grating—theory and production, The diffraction grating—mountings and use, The photographic process, The determination of wavelength, The determination of spectral intensity, Apparatus and methods of infra-red spectroscopy, The spectroscopy of the vacuum ultra-violet, Spectrochemical analysis.

None of these subjects is treated exhaustively, but each chapter is admirably supplied with a bibliography and with references to original papers. The writing and production of the book both deserve praise.

Occasionally one finds a slip in the text. For example, on page 81, the author speaks of astigmatism in terms of horizontal and vertical lines, whereas he really means radial lines and concentric circles. Again, on page 57, the author errs in thinking that a meniscus-shaped lens with a stop spaced from it is necessary for the removal of coma from a single lens.

The expression for the resolving power of a prism may be written down almost at sight for the optical path difference between the basal and apical rays has an increment $t\,dn$ due to an index change dn arising from a change in wavelength $d\lambda$. Setting $t\,dn=\lambda$, the required result follows. The proof used by the author is too long, and it obscures the underlying physical basis of the resolving power formula. This is in marked contrast to his treatment of diffraction, which eschews any extended analysis and obtains results by almost physical reasoning.

In describing the so-called *incoherent* and *coherent* modes of illumination, the author treads cautiously. It is hinted that the experimentalists find little to choose between the two methods. Indeed, it would be surprising if they did, for the coherence of the light illuminating the slit is exactly the same in the two cases, provided the source is sufficiently broad compared with the Airy diffraction pattern of the condenser in the ' incoherent ' case; and provided, in the ' coherent ' case, the angle subtended by the source at the slit equals that subtended by the condenser aperture in ' incoherent ' illumination.

These slight weaknesses of the book undoubtedly exist because the author is primarily an experimentalist. One shudders, however, to think what the experimental parts of a theoretician's book would be like.

This book will find a welcome place, not only among spectroscopists, but among those who, while not specialists in the field, require to know its methods and instruments.

H. H. HOPKINS.

CONTENTS FOR SECTION B

PAGE

Prof. L. Bru, Dr. M. P. Rodriguez and Miss R. Vega. Analogies between the Diffraction of Light and Electron Diffraction by Gas Molecules . . 249

Prof. L. Bru, Dr. M. Cubero and Dr. J. Garrido. Homometric Diffraction Gratings 255

Dr. J. C. E. Jennings. The Virtual Optics of the Median Plane of Axially Symmetric Magnetic Prisms 256

Dr. W. Ehrenberg and Dr. J. C. E. Jennings. Measurements of the Electron-Optical Properties of Solenoid Prisms 265

Mr. G. W. Gordon-Smith. The Spectral Reflection Characteristics of a Smoked Magnesium Oxide Surface 275

Mr. H. Martin and Mr. H. A. Woods. Low-frequency Noise Spectra of Hot-filament Low-pressure Discharge Tubes 281

Mr. B. H. Flowers, Mr. J. D. Lawson and Mr. E. B. Fossey. A Thick-walled Ionization Chamber for Measuring the Intensity of X-Radiation of Energy up to 25 MeV 286

Mr. A. Cownie and Prof. L. S. Palmer. The Effect of Moisture on the Electrical Properties of Soil 295

Letters to the Editor:

- Mr. J. H. Calderwood, Dr. R. Cooper and Mr. A. A. Wallace. The Electric Breakdown of Alkali Halide Crystals 301
- Dr. R. Cooper and Miss J. Harrington. Positive Current Creep in Selenium Rectifiers 303
- Mr. A. K. Saha and Miss M. Ghosh. The Mechanism of the Low-frequency Electrodeless Discharge in Chlorine and the Influence of Irradiation . 304
- Dr. J. W. Menter, Dr. J. Nutting and Mrs. A. L. Tsou. Austenite in Low Carbon Iron 305
- Report of the Copenhagen Meeting of the General Assembly of the International Union of Pure and Applied Physics 306

Reviews of Books 308

Contents for Section A 310

Abstracts for Section A 311

ABSTRACTS FOR SECTION B

Analogies Between the Diffraction of Light and Electron Diffraction by Gas Molecules, by L. BRU, M. P. RODRIGUEZ AND R. VEGA.

ABSTRACT. Monochromatic light has been diffracted by a unit formed by an ensemble of slits with a common axis, in which all periodicities which a molecule can exhibit are represented. By a suitable choice of the slit areas we can, moreover, take account of the contribution to the expression of the intensity of each of these periodicities. Analysis leads to expressions similar to those used in the interpretation of the pattern obtained in electron diffraction by gases. These have been applied to the cases of benzene and carbon tetrachloride. The positions of the diffraction maxima and minima agree to within little more than one per cent with those of the corresponding electron diffraction patterns. Values found for interatomic distances (starting from the relative formula of radial distribution) also agree with the real ones within the foregoing limit.

Homometric Diffraction Gratings, by L. BRU, M. CUBERO and J. GARRIDO.

ABSTRACT. Diffraction by homometric gratings is examined by the ‘ fly’s eye ’ device. The patterns obtained confirm the theoretical conclusions.

Geometrical Electron Optics of the Median Plane of Axially Symmetric Magnetic Prisms: The Virtual Optics of the General Field, by J. C. E. JENNINGS.

ABSTRACT. The angle between the asymptotes of a ray is developed as a power series in its impact parameter about some value which characterizes the ‘ principal ray ’. When this value is zero, the principal points of the equivalent lens coincide at the axis of symmetry; in all other cases it is ‘ thick ’. The focal length is here associated with the coefficient of the linear term, the transverse aberrations with those of the higher terms. The quadratic aberration vanishes for a wide range of relative $H\rho$ if the principal ray is suitably chosen. Foci with quadratic aberration are intercepts of the caustic curve, whose cusp lies at the cubic focus. The dependence of aberration upon magnification and the conditions in which the cubic as well as the quadratic aberration vanish are discussed.

Measurements of the Electron-Optical Properties of Solenoid Prisms, by W. EHRENBERG and J. C. E. JENNINGS.

ABSTRACT. Cathode rays were deflected and focused in the median plane between a pair of similar coaxial solenoids. Foci free of quadratic aberration were found at all pole separations and ratios of electron momentum to field strength, when the impact parameters of the electrons were suitably selected. This property would enable a spectrum to be photographed with fairly uniform quality over a considerable range of $H\rho$. The loci of these foci were found. Values of the aberration coefficients and of the dispersion are given.

The Spectral Reflection Characteristics of a Smoked Magnesium Oxide Surface, by G. W. GORDON-SMITH.

ABSTRACT. This paper describes an absolute determination of the spectral luminance factors of a flat smoked magnesium oxide surface, in the wavelength range 0·4–0·72 micron, for normal incidence and 45° view. The results give an almost constant luminance factor of 1·005 over the middle of this range, with an increase to about 1·01 at the ends of the spectrum.

The selectivity of a similar oxide coating on the interior of a small spherical integrator was also studied by a comparison with the flat surface. In these conditions the reflection factor was found to be 0·975 in the middle of the spectrum, falling to 0·962 at 0·4 micron and 0·972 at 0·72 micron.

The coatings were fresh, of thickness just over 1 mm, and made from the smoke of burning magnesium ribbon. A photoelectric method was used, and problems connected with the linearity of the photocell characteristic and with the spectral transmission of the monochromator used were examined and are discussed. Adequate references are given to various earlier investigations.

Low-frequency Noise Spectra of Hot-filament Low-pressure Discharge Tubes, by H. Martin and H. A. Woods.

ABSTRACT. Measurements have been made of the low-frequency noise spectrum of a number of hot-cathode discharges in mercury vapour saturated at room temperature. As previously reported by Cobine and Gallagher, the spectrum is continuous, with superposed peaks. The latter can be partly attributed to harmonic components of ionic relaxation oscillations. The upper frequency limit of the continuum exceeds 10 Mc/s in some instances. Most of the noise from the tubes studied originated near the cathode. Some relations have been traced between the noise and oscillations and position on the current–voltage characteristic curve for the tube, but there is variation from one tube to another.

A Thick-walled Ionization Chamber for Measuring the Intensity of X-Radiation of Energy up to 25 *mev*, by B. H. Flowers, J. D. Lawson and E. B. Fossey.

ABSTRACT. A thick-walled ionization chamber suitable for measuring the radiation intensity from synchrotrons and betatrons operating at energies up to 25 Mev is described. Calibration curves giving the current in the chamber per incident photon as a function of photon energy are given. The effect of wall thickness and secondary x-rays produced in the wall have been considered and included in the calculations. Experimental results consistent with the theory are described.

The Effect of Moisture on the Electrical Properties of Soil, by A. Cownie and L. S. Palmer.

ABSTRACT. Measurements of the dielectric constant of soil containing different known percentages of moisture were made at a fixed frequency of 430 Mc/s. The method adopted involved the use of a coaxial transmission line terminated with a sample of the soil under test. The line consisted of a central rod with a concentric tube about 2½ metres in length. Measurements were made with soil samples containing from 4·1% to 47·7% moisture. The dielectric constant was found to vary from 4·0 to 31·4. The values are shown graphically and compared with those obtained by nine other authors. The conductivity could not be measured accurately with the method used, but it was estimated to vary from about $1{\cdot}5\times10^{9}$ e.s.u. with 4% moisture to 4×10^{10} e.s.u. with 50% moisture.

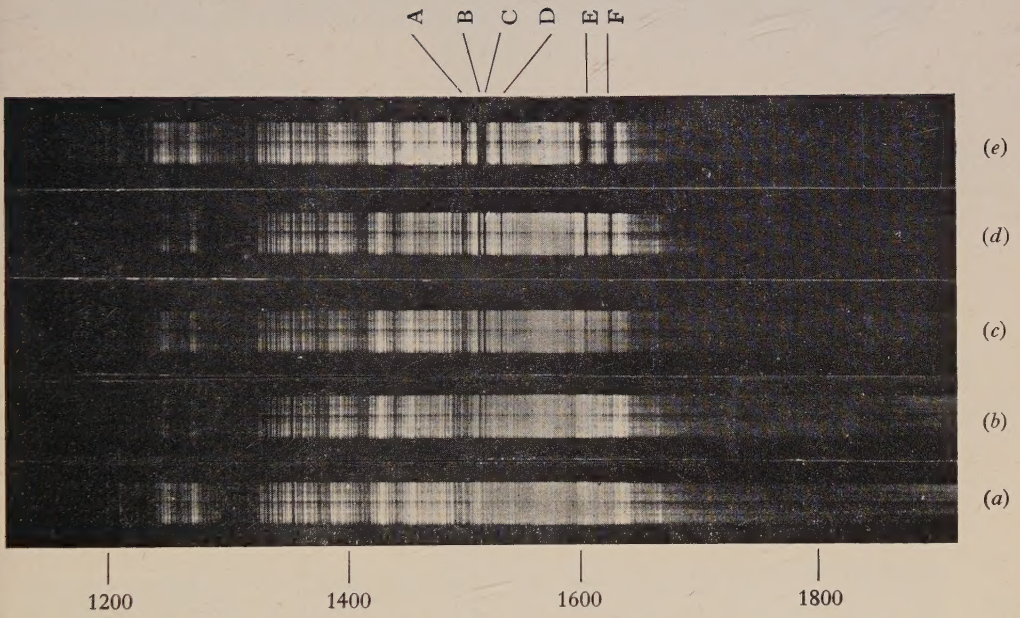

Schumann region absorption spectrum of Ga vapour.
(*a*) 20° ; (*b*) 1100° ; (*c*) 1250° ; (*d*) 1440° ; (*e*) 1610°c.

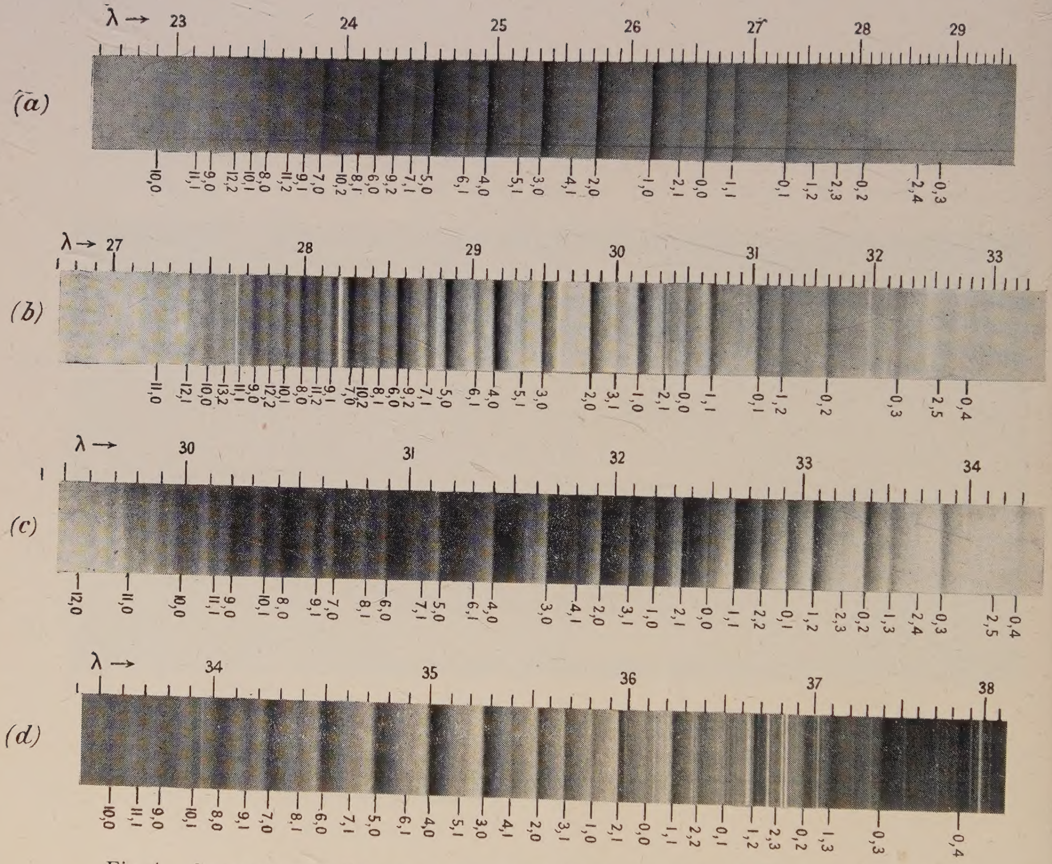

Fig. 1. Spectrograms of the D – X systems: (*a*) GeO; (*b*) GeS; (*c*) GeSe; (*d*) GeTe.

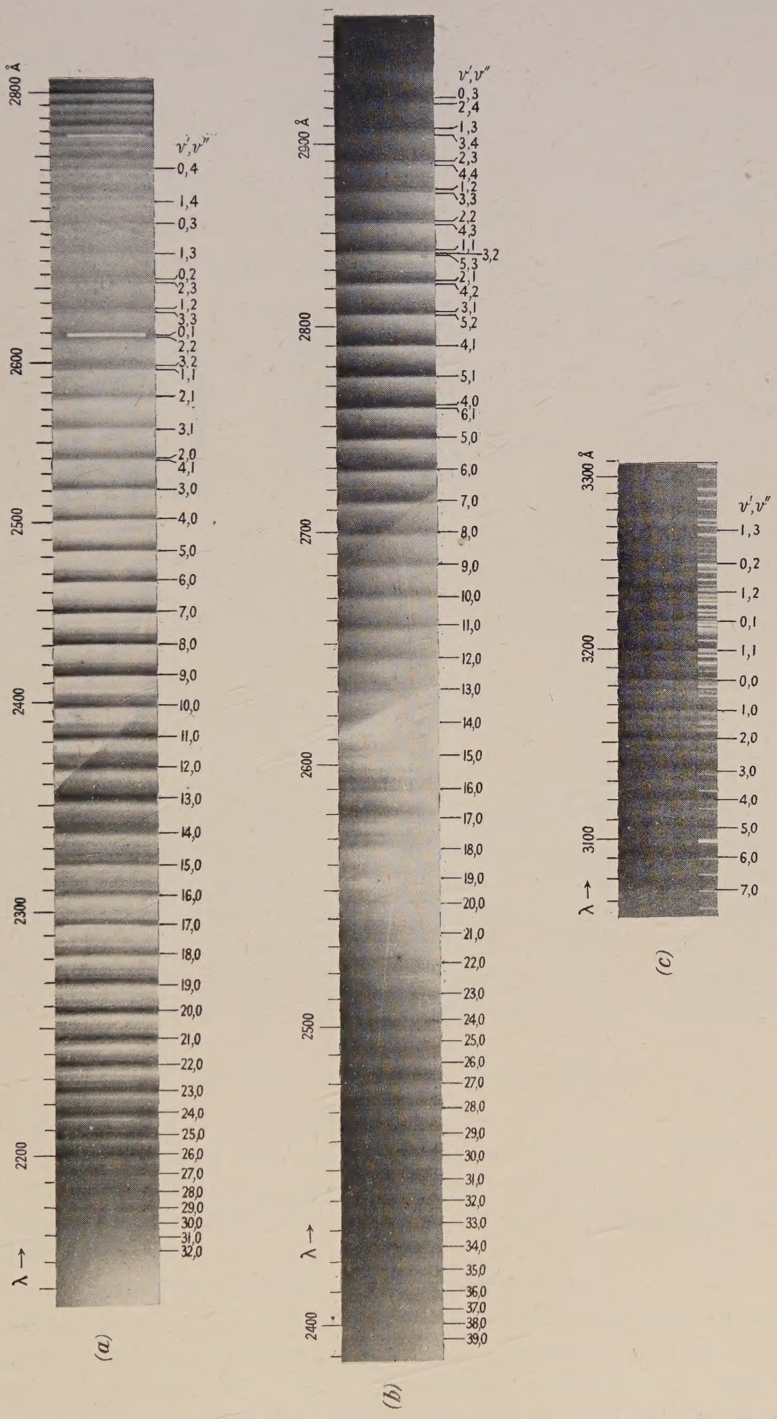

Fig. 2. Spectrograms of the E − X systems: (*a*) GeS; (*b*) GeSe; (*c*) GeTe.